A Thesis for the Degree of Ph.D. in Engineering

A Study on Stochastic Geometry Based Modeling and Analysis of Cellular Networks

August 2016

Graduate School of Science and Technology
Keio University

He Zhuang

Acknowledgments

I would like to express my special appreciation and thanks to my supervisor, Prof. Tomoaki Ohtsuki. He gave me a lot of chances to be a full-fledged scientist. His advice was crucial to undertake new research challengs and keep persevering even when results were solw to come. I am deeply grateful for all the empowerment I received under his supervision that let me define my own pace. These experiences will help my carrier as a researcher.

The committee members Prof. Iwaso Sasase, Prof. Hiroshi Shigeno, Prof. Yukitoshi Sanada, Prof. Pooi-Yuen Kam deserve a special mention. They gave me a lot advice that helped improve the quality of this dissertaion.

My family and friends were a great support from both mental and financial aspects.

Contents

List of Figures

Chapter 1

Introduction

1.1 Background

As 4G technique has been widely applied, and more and more researchers are focusing on the techniques for realizing 5G. However, as mobile service providers, they even more concern how to deploy and maintain the wireless networks. For example, how many base stations (BSs) should be implemented in an area? How to set the transmit power? How to optimize the coverage probability or throughput? How to allocate the resource block? A general and tractable model of the modern cellular networks is necessary to answer these questions. Using the model, we can simulate the cellular networks performance under different parameters, and verify the effectiveness of new techniques. The model is not only used to characterize the operation, and also helpful for designing and optimizing the cellular networks.

In the era of information explosion, the demand for fast and convenient communication is constantly increasing. To meet the demand, mobile communication gets fast development. Benefiting from mobile terminals, such as mobile phone, laptop, tablet, even vehicles, people around the world can communicate with each other without the limitation of movement. The mobile communication service is rendered by the wireless cellular networks deployed by the mobile communication provider. A typical cellular networks consist of BSs deployed in some areas. The BSs and the mobile terminals can in turn be transmitters or receivers. Each transmitter-receiver pair

requires its own wireless link. At a given time, the link that several BSs transmit simultaneously toward its own mobile users is called downlink. The opposite direction link that from mobile users to BSs is called uplink.

Recent years, with the population of the terminals, the large number of mobile terminals results in the great demand of high communication traffic (network capacity). The multiple-input multiple-output (MIMO) technique, benefiting from the multiple transmit and receive antennas, can significantly increase the capacity of wireless networks, and reduce transmit power. MIMO has become a key technique of wireless communication standards including IEEE 802.11n (Wi-Fi), IEEE 802.11ac (Wi-Fi), HSPA+ (3G), WiMAX (4G), and Long Term Evolution (4G). The massive MIMO is also an essential elementary of 5G [1–3].

To increase spatial frequency efficiency and transmit capacity, the modern cellular network deployments are increasingly transforming from homogeneous deployments to heterogeneous networks (HetNets). HetNets play a key role in the next-generation wireless systems, such as the Third Generation Partnership Project (3GPP) Long-Term Evolution Advanced (LTE-A) [4] and the IEEE 802.16m Worldwide Interoperability for Microwave Access (WiMAX) [5]. The concept of HetNets is to bring transmitters closer to users in order to enhance the system capacity, provide coverage, and save power [6]. Comparing to the homogeneous networks (one tier) [7], the HetNets consist of different tiers, which differ in terms of transmit power, deployment density, and even transmission technique. Usually, each tier is comprised of one kind of BSs, such as operator-deployed macro BSs, Pico BSs [8] [9], and user-deployed Femto BSs [10]. Due to the coexistence of different tiers, the HetNets introduce the problem of cross-tier interference. Furthermore, BSs in every tier, particularly user-deployed femto BSs, obviously increase the randomness of the BSs locations, which undoubtedly makes analysis of HetNets a challenge. In this case, traditional analysis of the HetNets based on deterministic models of BSs' locations is no longer applicable, even intractable. As a result, there is a strong demand for a new model for analysis of HetNets.

1.2 Related Works

The work that applying Stochastic Geometry (SG) to analysis of wireless networks can be traced back to the late 70's. To author's best knowledge, [11] firstly analyzes the capacity of packet radio networks in which the nodes' locations are considered randomly rather than deterministic. Following [11], some researchers make determined efforts, however their works are confined to apply SG to only the analysis of ad hoc networks [12] [13]. At beginning of the development of wireless cellular networks, the BSs are deployed almost as hexagonal grid. However, inorder to increase the capacity of cellular networks, the cellular networks transform to HetNets. It means that BSs in HetNets, particularly user-deployed femto BSs, obviously increase the randomness of the BSs' locations. In this case, using SG to characterize the BSs can naturally capture the randomness of the BSs' locations. Furthermore, due to powerful mathematic tool, using SG can also get tractable results. Motivated by these advantages, researchers attempt to apply SG to model cellular networks.

Downlink

The first related important paper on the topic was published in 2011 [14], which uses Poisson point process (PPP) to model one tier networks and gets a tractable result of coverage probability and average rate of users. Although just modeling one-tier network, the paper contributes to the topic greatly, since it gives a very good sample of analyzing networks with PPP. Following [14], many cellular networks models are proposed based on PPP. The authors in [15] [16] not only extended the result of [14] to K tiers, but also considered the both open and closed access cases. It should be noted that [14–16] provided the base of the analysis of the HetNets with PPP. The authors of [17] developed a general and tractable model that consists of multi cellular networks, each deploying up to K different tiers of access points (APs), each class of APs is modeled as an independent PPP, with mobile user locations modeled as another independent PPP, all channels further consisting of Rayleigh fading.

Most models typically assumes that all BSs from each tier always transmit data

to its user pair, however, practically some BSs might be idle and hence would not contribute to the load and aggregate interference. It results in the diversity in the loads served by different ties and low accuracy of signal-to-Interference plus Noise Ratio (SINR). In [18], authors overcame the drawback above by assuming transmit independently with a given probability. Due to the high transmission power gap with the macro BSs, small cell BSs, such as Pico and Femto BSs, could provide higher received signal strength (RSS) than macro BSs only in very near area. It results in the overload of macro BSs and light of small cell BSs, since a user associates with BS based on the RSS. In [19] [20], the authors investigated the above issue and introduced a biasing factor to control the network load of each network tier. The biasing factor can be thought as a virtual increase of transmit power of a given network tier. Usually, it is used to virtually increase the RSS provided by small cells and then lighten the load of macro BSs

The relationship between BS density and energy-efficient is investigated in [21]. The authors in [21] proposed a general PPP model of HetNets, and derived the upper and lower bounds of the optimal BS density for homogeneous scenarios. Based on the bounds, they obtained the optimal macro/micro BS (base station) density for energy-efficient heterogeneous cellular networks with quality of service (QoS) constraints. In [22], authors introduce a new analytical methodology to evaluate the average rate, which avoids the computation of the coverage probability and needs only the moment generating function (MGF) of the aggregate interference at the probe mobile terminal. Authors of [23] develop a sequence of equivalence relations for HetNets and use them to derive semi-analytical expressions for the coverage probability at the mobile station when the transmissions from each BS may be affected by random fading with arbitrary distributions as well as attenuation following arbitrary path loss models. More works on coverage probability analysis for PPP based HetNets model can be found in [24–27].

The access mechanism can be classified to be open access, closed access, and hybrid access. In hybrid access small cells, the available spectrum is partitioned into two groups. One group is assigned to the closed subscriber group to guarantee their QoS,

while the other group is assigned to the non-subscribers to enhance their coverage and reduce the interference experienced from them [28]. In [29], authors proposed a two tiers PPP model considering hybrid access. They derived the distributions of SINR, and mean achievable rates of nonsubscribers and subscribers, and thus optimized the hybrid access policy in a two tier HetNets.

Fractional frequency reuse (FFR) is an attractive interference management technique, which can remarkably increase spectral efficiency [30, 31]. The authors in [30, 31] propose an analytical K tiers model for evaluating strict FFR and soft frequency reuse (SFR) deployments based on the spatial PPP. The papers not only derive the cell-edge user coverage probability and average rate, but also propose a new method of partitioning the users. As well known, in order to use FFR technique, we need to know who are the cell-edge users. The traditional method partitions the users by spatial locations, which is effective for the deterministic model. However, because of introducing randomness to the BSs' locations, the traditional method is unavailable for the PPP model. [30, 31] partition the users into the cell-edge users and cell-interior users by the SINR threshold, thus solve the problem very well [28]. Early work on MIMO networks with FFR is also found in [32]. The paper considers both MIMO networks and FFR with the deterministic model, and demonstrates that the proposed trisector frequency partition can not only effectively overcome the intergroup interference, but can avoid executing the complex multi base-station joint processing for a huge number of cluster of cells at all locations [32]. Although being a great reference for the design and deployment of MIMO HetNets with FFR, their analysis is constrained to the deterministic model and does not consider the SG model, thus the flexibility and applicability of the conclusions are seriously affected.

As far as I know, the authors of [33, 34] firstly apply the PPP model to analyze the MIMO HetNets. [35] concludes that MIMO channel power distribution follows the Gamma distribution. In [33, 34], based on the conclusion of [35], the authors evaluate the upper bound on the coverage probability using a PPP tool, thereby give us a new excellent method to analyze MIMO HetNets. [36, 37] studied MIMO based downlink HetNets with joint transmit–receive diversity using orthogonal space–time

block coding at the BSs and maximal-ratio combining (MRC) at the users. The further works about modeling and analyzing MIMO HetNets based on PPP can be found in [38–44] The authors in [45] applied PPP model to analyze MIMO HetNets utilizing the FFR technique. The downlink performance of a massive MIMO HetNets is studied in [46].

Hardcore point process (HCPP) is a point process where points are forbidden to be closer than a certain minimum distance. Therefore, it is more suitable for modeling BSs' distribution than PPP. Since the more accurate analysis based on HCPP is at the cost of computation complexity, HCPP is not widely used in modeling cellular networks. In [47–49], HCPP is used to model a two–tier cellular network composed of multiple macro BSs, multiple cognitive femto access points, multiple users in a multiple channels environment. The authors investigated the optimization of outage probability in a cellular networks including cognitive networks.

Uplink

Different from downlink analysis, the uplink analysis pays more attention to power control due to the restriction of the transmitters of uplink (mobile terminals). In [50, 51], authors modeled BSs and users by independent PPP and considered Rayleigh fading to evaluate the uplink coverage probability. Although only a simple model is proposed in [50, 51], they gave us a paradigm for analyzing uplink HetNets based on SG. Following it, many more practical and more rigorous models for HetNets were developed. In [52], the authors modeled a multi-tier cellular network where all network tiers were assumed to follow independent homogeneous PPPs. Considering the mobile terminals power control, they derived the expression of outage probability and spectral efficiency. Based on the similar model, the author of [53] derived the expression of the average symbol error probability for different modulation schemes due to aggregate network interference. The more rigorous models for HetNets uplink can be found in [54–58]

1.3 Contributions

In the first part of this thesis, we introduce the background of SG based modeling and analysis of wireless cellular networks in chapter 1. We explain why do we need a general model of cellular networks, and the motivation of applying SG to model cellular networks. We briefly review the history of SG analysis on cellular networks and also summarize the related work of the topic, which is very helpful for understanding and studying the history and development of applying SG to model cellular networks. The basic knowledge of SG are introduced then. The three most frequently used classical point process (PP) are presented in Section 2.1. Meanwhile, we also introduce the related properties and Voronoi tessellation of PP. They are the necessary knowledge before beginning the study of modeling cellular networks.

In second part, we use PPP to model BSs' locations and propose a framework to analyze the downlink coverage probability of HetNets utilizing the FFR technique. Based on this model, the tractable expressions of typical users' coverage probability under both closed and open access cases are obtained. Then, we propose a tractable and flexible model for K–tier MIMO HetNets, with the FFR technique, based on the spatial PPP. In this work, we show the numerical coverage probabilities of different FFR and access cases under the full Space division multiple access (SDMA) and single-user beamforming (SU-BF), and discuss the effects of main parameters on the coverage probability. We also illustrate how to use the coverage probability results to derive the average rate expressions. These analyses can assist system designers in designing networks, and evaluating new algorithm related to MIMO HetNets. To author's best knowledge, this work applies SG to model MIMO HetNets with the FFR technique.

So far all the analyze based on PPP need to utilize the mathematical tool, the probability generating functional (PGFL) [59] of the PPP, which contributes significantly on simplifying computations, the resulting expressions usually only involve computable integrals, even the closed form expressions in some special cases. However, it restricts the channel of networks to exponential distribution, which greatly

limits the application of the PPP model. To break through the channel limitation, in this paper, we develop a novel way of analyzing cellular networks based on PPP, which maintains the generality of the PPP model, and derives the closed form expressions of coverage probability at a given distance of the serving BS.

In one word, the main contributions of this thesis are as follows:

- We introduce the basic knowledge of the SG: the classical point process, and the related properties.
- Based on SG we model and analysis the of HetNets and MIMO HetNets utilizing FFR technique.
- We develop a novel way of analyzing cellular networks based on PPP, which successfully breaks through the channel limitation, maintains the generality of the PPP model.

1.4 Outline of Dissertation

The outline of this dissertation is shown in Fig. 1-1. Chapter 1 firstly introduces the background, objective of the SG based model of cellular networks. The related works and contributions of this dissertation are presented. The fundamentals of SG and necessary related content are presented in Chapter 2. Chapters 3 and 4 are two studies on modeling and analysis of HetNets and MIMO HetNets utilizing FFR technique, respectively. The results of these two chapters are derived using probability generating functional (PGFL) of PPP, which results in restrictions of modeling cellular networks. To break through the restrictions, A new approach to utilize PPP is proposed. Chapter 5 depicts how to apply the new approach to analysis of cellular networks. The dissertation conclusion and future works are discussed in Chapter 6.

The detailed relationship between chapters and techniques is illustrated in fig. 1-2. Chapter 2 introduces the elementary knowledge of SG. In the study of modeling and analysis on cellular networks, there are two types of models: stochastic model

and deterministic model. Deterministic model assumes the BSs distributed regularly, commonly used are hexagonal and square models. Stochastic model applies stochastic geometry to model cellular networks, which uses PPs to characterize the BSs' locations. Commonly used are PPP, HCPP and Poisson point process (PCP). Based on the powerful mathematic tool PGFL, stochastic model is widely applied to model wireless networks, e.g., Ad Hoc, cognitive, cellular networks. This dissertation focuses on modeling cellular networks. After many years development, the stochastic model is successfully used to model one tier cellular networks and HetNets. This dissertation further widen the application of stochastic model. Chapter 3 models and analyzes HetNets and MIMO HetNets utilizing FFR technique based on the stochastic model. By introducing MIMO to the framework of Chapter 3, a tractable and flexible model for K tiers MIMO HetNets, with FFR technique is proposed in this Chapter 4. The different access mechanism, open access and closed access, are considered in both 3 and 4. Chapters 3 and 4 analyzes cellular networks based on PGFL, which is only valid to Rayleigh channel. Therefore, the channel of stochastic model restricts to fast fading, which greatly limits the application of the PPP model. which greatly limits the application of the PPP model. In Chapter 5, utilizing the conclusion of deterministic model, we develop a probabilistic approach of analyzing cellular networks based on PPP, which successfully breaks through the channel limitation, maintains the generality of the PPP model.

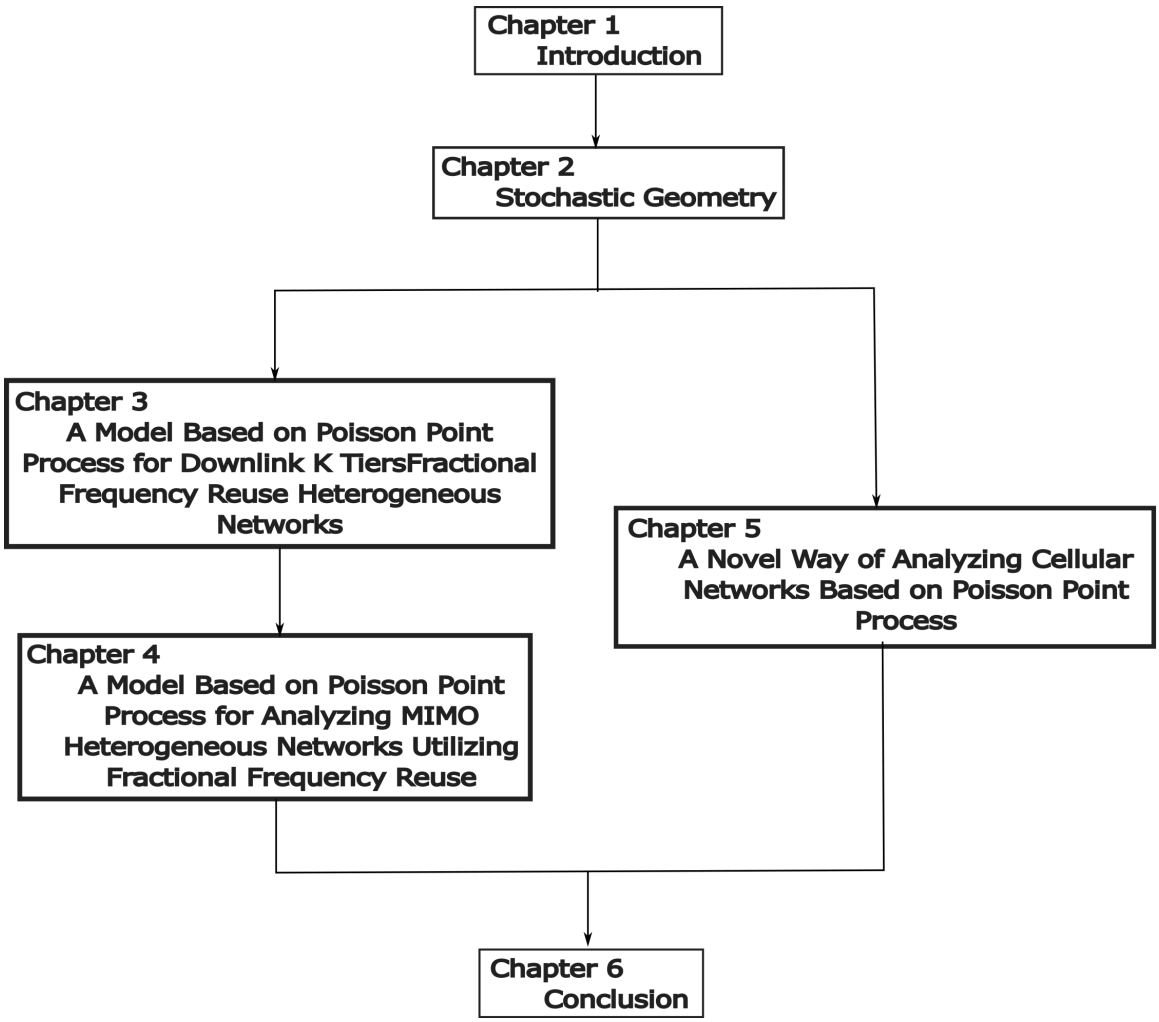

Figure 1-1: Outline of this dissertation

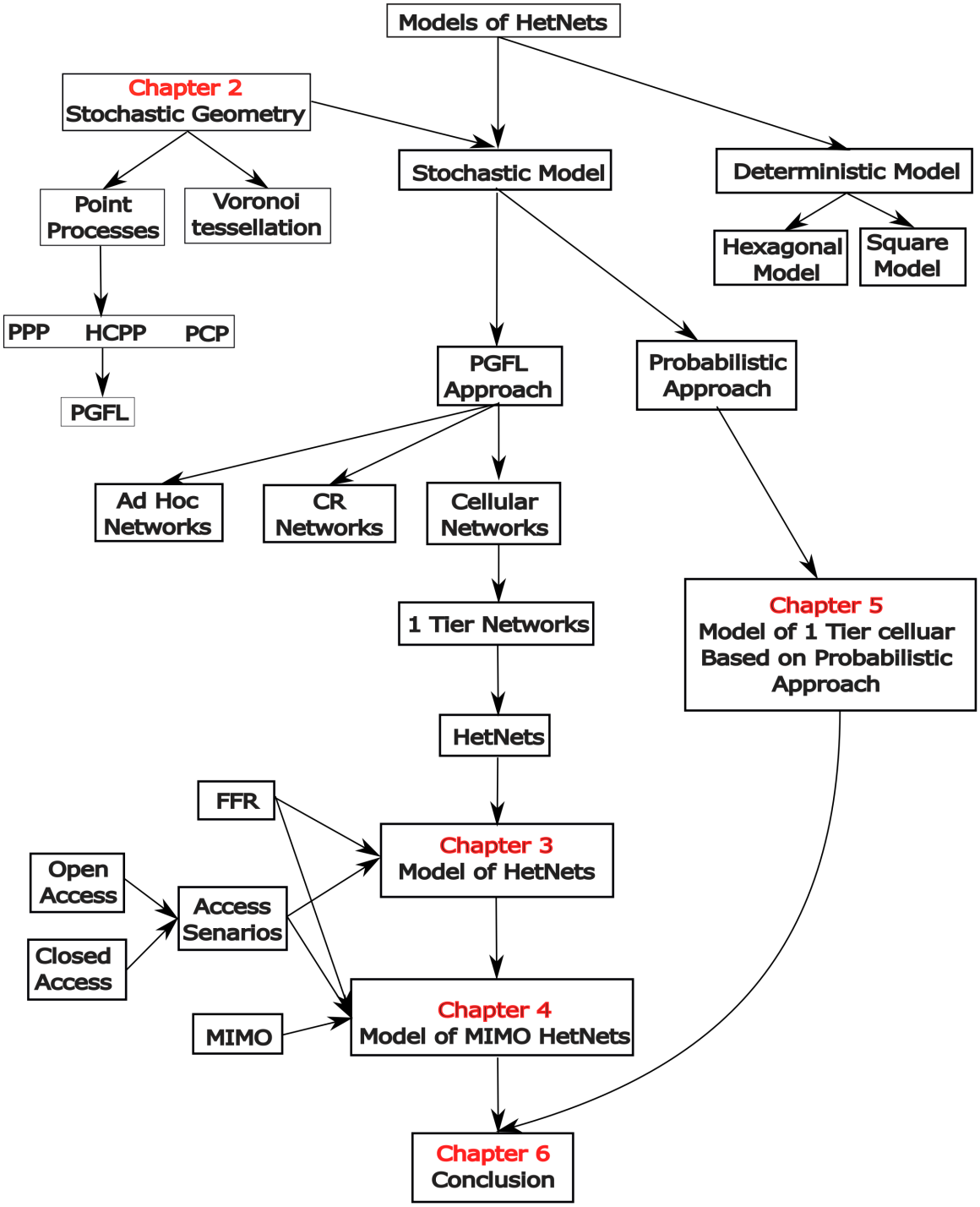

Figure 1-2: Relationship between chapters and techniques

Chapter 2

Stochastic Geometry

A wireless cellular network can be viewed as a collection of BSs, located in a plane. Considering downlink, each BS transmits to a corresponding receiver thought as a user, simultaneously. The interference seen by a receiver is the sum of the signal powers received from all transmitters, except its own transmitter. In a simple model, the geometry of the locations of the BSs plays a key role since it determines SINR [60]. SG is the study of random spatial patterns. It provides a natural way of characterizing the locations of the BSs, and thus modeling and analyzing the cellular networks from a macroscopic view. Compared with traditional model (deterministic model), modeling scale cellular networks in terms of SG model is more suitable and general. SG, which we use as a mathematic tool, is intrinsically related to the theory of point processes. Therefore, in this chapter, I present the elementary knowledge of SG and necessary related content are presented, which is the basic of SG for modeling cellular networks.

2.1 Classical Stochastic Geometry

Point process (PP) is the most basic object studied in SG. Visually and loosely speaking, a PP is a random collection of points residing in some space. This space can be considered as the d–dimensional Euclidean space $\mathbb{R}^d$. In the applications of modeling wireless networks, each point represents the locations of a BS.

2.1.1 Poisson Point Process (PPP)

One of the simplest and important PP is the so called PPP. It is also the most frequently used one on modeling and analyzing wireless networks.

Definition of PPP

Definition 2.1.1 (PPP). *The PPP Φ of intensity measure Λ is defined by means of its finite dimensional distributions:*

$$P\{\Phi(A_1) = n_1, \ldots, \Phi(A_k) = n_k\} = \prod_{i=1}^{k} \left(e^{\Lambda(A_i)} \frac{\Lambda(A_i)^{n_i}}{n_i!} \right)$$

for every $k = 1, 2, \ldots$ and all bounded, mutually disjoint sets A_i for $i = 1, \ldots, k$. If $\Lambda(d_x) = \lambda d_x$ is a multiple of Lebesgue measure (volume) in $\mathbb{R}^d$, we call Φ a homogeneous PPP and λ is its intensity parameter [60].

This definition is very abstract and difficult to understand. For readers' convenience, an alternative definition is given as:

Definition 2.1.2 (PPP). *A PP $\Phi = \{x_i; i = 1, 2, 3, ...\} \in \mathbb{R}^d$ with intensity λ is a PPP if and only if the number of points inside any compact set $A \subset \mathbb{R}^d$ is a Poisson random variable, and the numbers of points in disjoint sets are independent [61].*

Definition 2.1.3 (PPP). *A PP $\Phi = \{x_i; i = 1, 2, 3, ...\} \in \mathbb{R}^d$ with intensity λ is a random point set such that*

- *The number of points $\mathcal{N}(A)$ for any bounded $A \subset \mathbb{R}^d$ follows a Poisson distribution with*

$$\mathbb{E}(\mathcal{N}(A)) = \lambda \times |A|, \text{ where } |A| \text{ denotes the area of } A.$$

- *$\mathcal{N}(A)$ and $\mathcal{N}(B)$ are independent if A and B are independent (disjoint sets)*

It is not evident that such a point process exists. Although the definition is very clear, how to get a realization of PPP is unknown.

Realization of PPP

We take a 2 dimensional spacial PPP as an example to illustrate how to simulate it. Considering to get a PPP realization with intensity λ on $A = [-L, L]$. There are two steps as follow:

1. Getting a number of points in the set A, which is a Poisson random variable with mean $\lambda|A|$.

2. Conditioned on the number of points, and distribute the points within the A.

The corresponding matlab code is as:

- N=poissrnd($\lambda|A|$);

- Points = unifrnd(-L,L,N,2);

Fig. 2-1 illustrates one realization of PPP with $\lambda = 2$, generated by the codes above.

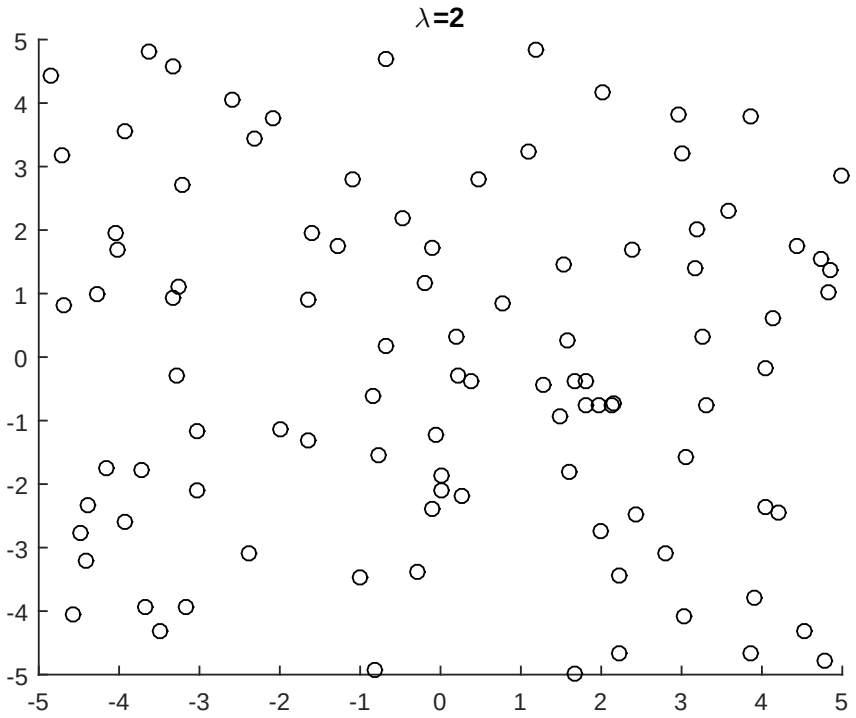

Figure 2-1: One realization of PPP with $\lambda = 2$

Distance to nearest point

Usually, the analysis is conducted on a user locating on origin, and the users in the cellular networks are assumed to connect to the nearest BS. Therefore, the probability density function (PDF) of the distance r that from the nearest BS to the user is an important and necessary for analyzing the cellular networks. The nearest distance r means all points must be farther than r. Considering 2 dimensional space, one simple fact is that the null probability of a PPP in a set A is $\exp(-\lambda|A|)$. Therefore,

$$\mathbb{P}[r > R] = \mathbb{P}[\text{No point nearer than } R] = e^{-\lambda\pi R^2}.$$

Then, the cumulative distribution function (CDF) of r is

$$F_r(R) = \mathbb{P}[r < R] = 1 - e^{-\lambda\pi R^2}.$$

Finally, the PDF of r can be obtained as

$$f_r(r) = \frac{dF_r(r)}{d_r} = e^{-\lambda\pi r^2} 2\pi\lambda r \text{ [14]}.$$

Probability Generating Functional (PGFL) of PPP

In the process of analysis of cellular networks, PGFL, as a mathematic tool, plays a key role on dealing with the interference of the cellular networks. The PGFL of PPP is

Theorem 2.1.1. *Let $f : \mathbb{R}^d \to \mathbb{R}$ be a measurable function and $\Phi\{x_i; i = 1, 2, 3, ...\} \in \mathbb{R}^d$ a PPP, then*

$$\mathbb{E}\Big[\prod_{x_i \in \Phi} f(x_i)\Big] = exp\Big\{-\int_{\mathbb{R}^d} \big(1 - f(x)\big)\Lambda(dx),\Big\} \tag{2.1}$$

where Λ is a locally finite non-null intensity measure on $\mathbb{R}^d$ [60]

Considering 2 dimensional space, the intensity measure of PPP is a constant $\Lambda = \lambda$. Therefore, the theorem 2.1.1 can be depicted as

Lemma 2.1.2. *Let $f : \mathbb{R}^2 \to \mathbb{R}$ be a measurable function and $\Phi\{x_i; i = 1, 2, 3, ...\} \in \mathbb{R}^2$ denotes a PPP with intensity λ, then*

$$\mathbb{E}\Big[\prod_{x_i \in \Phi} f(x_i)\Big] = exp\Big\{-\int_{\mathbb{R}^2} \big(1 - f(x)\big)\lambda dx\Big\}. \tag{2.2}$$

It should be noted that the x in formula (2.2) is a variable denoting points coordinate rather than scalar variables. In the study of signal process, the signal attenuation depends on distance from transmitter to receiver. Therefore, utilizing the PGFL of PPP for analyzing cellular networks requires transforming the variable x in formula (2.2) to the distance. To achieve the purpose, we resort to polar coordinates, then $dx = rdrd\theta$, here r and θ denote distance and angle, respectively. Then formula (2.2) can be written in terms of polar coordinates as

$$\begin{aligned}
\mathbb{E}\Big[\prod_{x_i \in \Phi} f(x_i)\Big] &= \exp\Big\{-\int_{\mathbb{R}^2} \big(1 - f(x)\big)\lambda dx,\Big\} \\
&= \exp\Big\{-\lambda \int_0^{2\pi} d\theta \int_0^{\infty} \big(1 - f(r)\big) dr,\Big\} \\
&= \exp\Big\{-2\pi\lambda \int_0^{\infty} \big(1 - f(r)\big) dr,\Big\}
\end{aligned} \tag{2.3}$$

The detail of PGFL application on analyzing cellular works will be introduced in Chapters 3, 4.

2.1.2 Other Point Processes

PPP is the most frequently used PP, however, there are some other point processes. The study of PP is beyond of this thesis, here only two other PPs are briefly introduced, for details please refer to [59] and [60].

Hardcore Point Process (HCPP)

From the method of realization of PPP, we can know PPP uniformly distributes in the space, therefore, the points may be very near to each other. However, in the practical cellular networks, the BSs are exclusive to each other in order to mit-

igate interference and increase the capacity. To increase the model accuracy, some researchers resort to hardcore point process (HCPP) to model HetNets.

Definition 2.1.4 (HCPP). *An HCPP is a repulsive point process where no two points of the process coexist with a separating distance less than a predefined hard core parameter r_h. A PP $\Phi = \{x_i; i = 1, 2, 3, ...\} \in \mathbb{R}^d$ is an HCPP if and only if $\|x_i - x_j\| \geq r_h, \forall x_i \subset \Phi, i \neq j$, where $r_h \geq 0$ is a predefined hard core parameter, $\|\cdot\|$ is the Euclidean norm [28].*

Form the definition, we can know that HCPP is a point process where points are forbidden to be closer than a certain minimum r_h distance, it is closer to practical cellular networks. Therefore, using HCPP to characterize the locations of BSs can get more accurate results than using PPP. However, since HCPP is more complex than PPP, the more accurate results derived by HCPP model are at the cost of high computation complexity.

Poisson Cluster Process (PCP)

In daily life, people usually assemble in some special places, such as stations, mall, which means the users of cellular networks are not distributed as uniformly. To model this phenomenon better, many researchers resort to Poisson cluster process.

Definition 2.1.5 (PCP). *The PCP models the random patterns produced by random clusters. The Poisson cluster process is constructed from a parent PPP $\Phi = \{x_i; i = 1, 2, 3, ...\} \in \mathbb{R}^d$ by replacing each point $x_i \in \Phi$ with a cluster of point M_i are independently and identically distributed in the spatial domain [28].*

The PCP is suitable to model BSs or users if they are clustered according to certain social behavior.

2.2 Models of BSs

There are two types of models used to analyze cellular networks: deterministic and stochastic models. Deterministic model uses regular shape and points to characterize

the cell and BSs, respectively. The typical examples are hexagonal and square grid models. Stochastic model uses Voronoi tessellation and point process to characterize the cell and BSs, respectively. A simple and typical sample of stochastic model and deterministic model are shown in Fig. 2-2 2-3, respectively. In Fig. 2-2, the triangles are one realization of a PPP. They are randomly distributed in the area, and used to characterize the BSs' locations. The tessellation shown is called Voronoi tessellation, which is used to depict the cell borders of PPP model. In Fig. 2-3, each cell borders are shown by a regular hexagon. The point in the central of each hexagon denotes the BSs. The two models represent opposite poles of BSs' distribution, random and regular. Therefore, in theory the results derived by them denote upper and lower bounds.

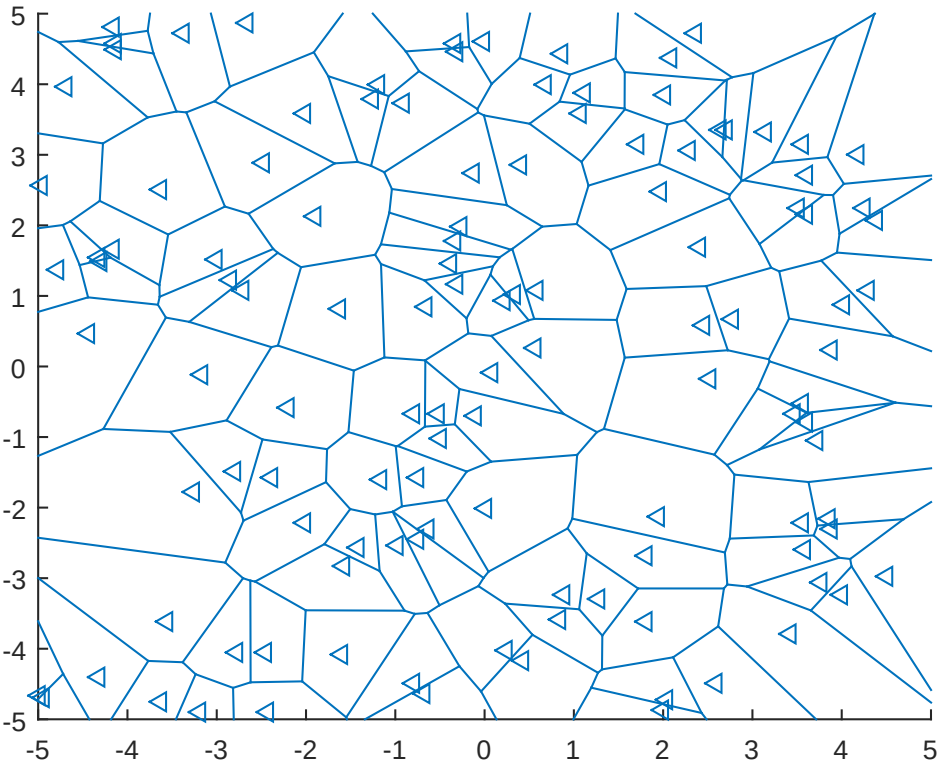

Figure 2-2: One realization of PPP with the Voronoi tessellation

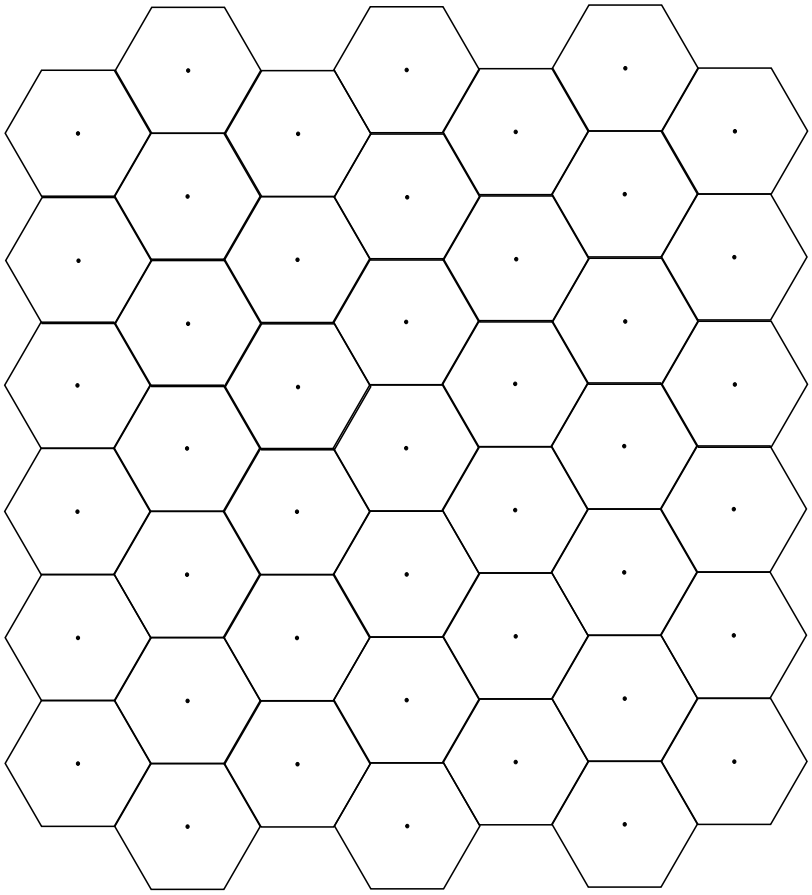

Figure 2-3: Hexagonal model

Chapter 3

A Model Based on Poisson Point Process for Downlink K Tiers Fractional Frequency Reuse Heterogeneous Networks

Chapters 3-5 are the applications of PPP on modeling cellular networks. In this chapter, PPP is used to model downlink HetNets utilizing FFR. We derive tractable expressions of coverage probability under both open and closed access schemes, which even can be simplified to a simple closed form for interference-limited HetNets (neglect noise).

3.1 System Model

3.1.1 Fractional Frequency Reuse (FFR)

As an attractive interference management technique, fractional frequency reuse (FFR) has been included in fourth generation (4G) wireless standards including WiMAX 2 (802.16m) and 3rd Generation Partnership Projectlong term evolution (3GPP-LTE) since release 8 [30] [62]. This will undoubtedly promote employing FFR

in different wireless applications. FFR can remarkably improve the rate, coverage, and spectral efficiency (SE) of cell edge users, with low complexity of implementation.

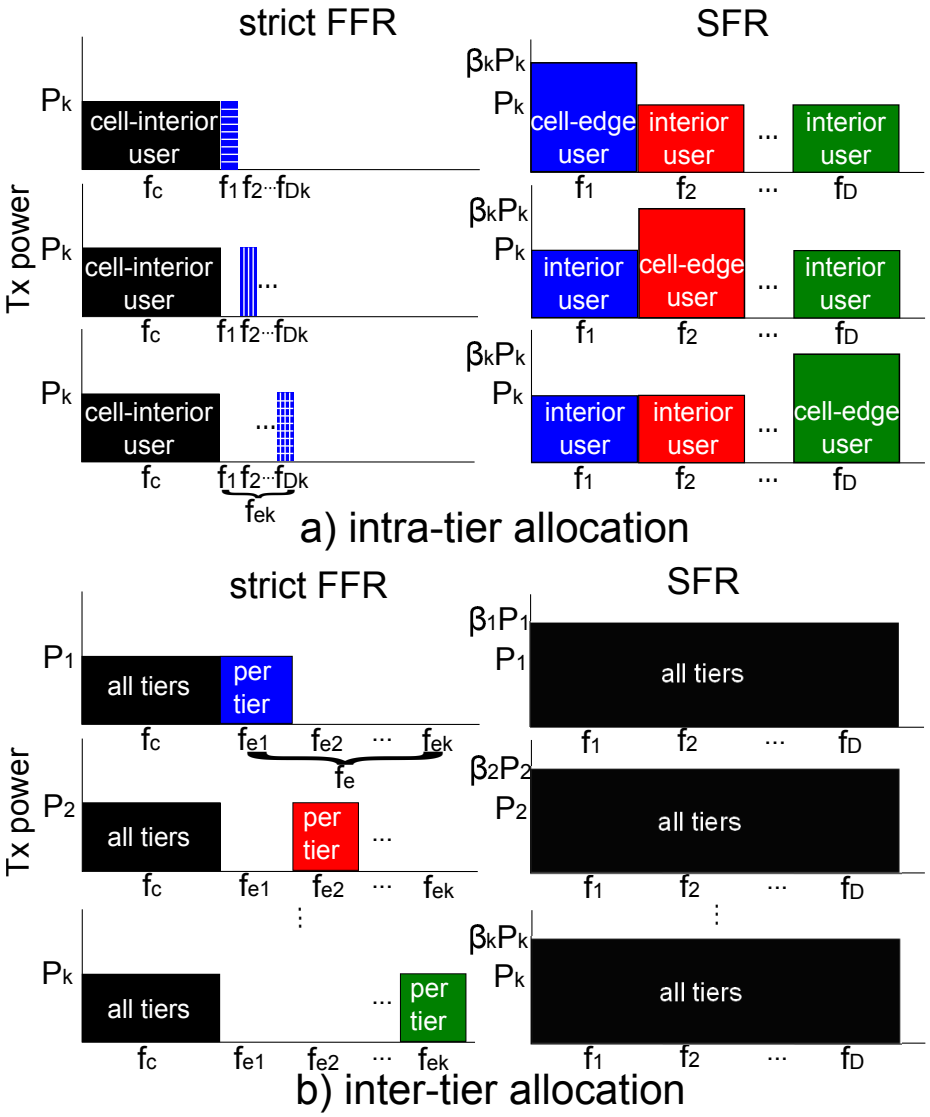

Figure 3-1: Strict FFR and SFR frequency and transmit power allocation.

There are two main types of FFR: strict FFR and SFR. Fig. 3-1 (a) and (b) illustrate strict FFR and SFR frequency and transmit power allocation from inter-tier and intra-tier point of views, respectively.

Under strict FFR, from inter-tier view, the whole frequency resource is partitioned to $f_c + f_e$ subbands, where f_c is the common subband, which is shared by the interior users of each tier, f_e is used as edge users' subbands. f_e is further divided into $\sum_{k=1}^{K} f_{ek}$, where K is the number of tiers and f_{ek} is allocated to the k_{th} tier as total

edge users' subbands. Because each f_{ek} is used by just k_{th} tier, the k_{th} tier edge users only receive interference from k_{th} tier.

From intra-tier view, f_{ek} is further divided to D_k subbands f_j, where D_k is reuse factor of k_{th} tier. These subbands will be chosen uniformly to transmit to the k_{th} tier edge users. That means the intra-tier interference received by the edge user of the k_{th} tier is further thinned with D_k. In general strict FFR removes cross-tier interference and significantly thins intra-tier interference for edge user at the cost of low spectral efficiency [30] [63].

Under SFR, the whole frequency resource is equally partitioned to D subbands, these subbands can be shared by all cells of all tiers. From intra-tier view, each cell chooses one subband for edge user transmission. Correspondingly interior users are allocated the rest $D-1$ subbands. That means SFR does not have the reserved subbands, so the edge users of SFR will experience interference from all cells of all tiers, which result in low SINR. To improve the SINR, SFR increases edge users' transmit power to $\beta_k P_k$ where P_k is the interior user's transmit power, and $\beta_k > 1$ power control factor, which ranges typically from 0 to 20 dB [64] [65]. Thus, comparing to strict FFR, SFR gets great spectral utilization at the cost of experiencing much more interference [30] [64].

It should be noted that the total transmit power at each BS may differ from each other for SFR, and there should be power constraint in the practical application. The main purposal in this chapter is providing a simple model for analyzing HetNets. To theorize our model clearly, we simplify the parameters without considering the power constraint. However, the total transmit power of each BS can be constrained by setting the upper limit of β_k. Furthermore, if there are some BSs using different transmission powers in one tier, we can divide the original tier into two tiers with appropriate densities, which is enabled by the fact that independently thinning a PPP leads to two independent PPPs [33].

3.1.2 HetNets Model

We consider a cellular downlink K tiers HetNets utilizing FFR, and use different independent PPP Φ_k with density λ_k to model the BSs of each tier. Without loss of generality, we conduct analysis on a typical user located at the origin. The typical user can connect to any tier without any restriction under open access case, however is allowed to access to only a subset of tiers under closed access case. We assume the typical user can access to just one tier at a time and to the nearest BS of the tier. We also assume each tier has the same transmit power P_k and the same threshold of SINR T_k. The locations of k_{th} tier serving BSs are denoted as x_k, and those of the other BSs are denoted as y. The distances from the typical user to the nearest BS of k_{th} tier is denoted as r_k. Referring to [59], since the k_{th} tier BSs are distributed as PPP with density λ_k, r_k will follow the Rayleigh distribution, furthermore its probability density function (PDF) is $f_{r_k}(r_k) = e^{\lambda_k \pi r_k^2} 2\pi\lambda_k r_k$ [14]. This model is applicable both to non-orthogonal (CDMA) and orthogonal (TDMA, OFDMA) HetNets.

3.1.3 Channel Model

We consider the Rayleigh fading, and more complex channel distributions can be considered in the model [14] [66]. The direct link from the serving BS to the typical user and interference links from the other BS to the typical user are i.i.d. exponentially distributed with mean μ, which are denoted by $g_{kx_k} \sim \exp(\mu)$ and $G_{kx_k} \sim \exp(\mu)$, respectively. Define the received power of the typical user at the origin from the nearest serving BS as $P_r = P_k g_{kx_k} r_k^{-\alpha}$, where α is the path loss exponent. The received SINR of the typical user is defined as

$$SINR(x_k) = \frac{P_k g_{kx_k} r_k^{-\alpha}}{\sum_{j=1}^{K} I_j + \sigma^2},$$

where $I_j = \sum_{y \in \Phi_j} P_j G_{jy} R_{jy}^{-\alpha}$, R_{jy} are the distances from the j_{th} tier's interference BSs to the typical user, and σ^2 is the constant additive noise.

With FFR, we need to define who the edge users are. For the deterministic

model, we can partition the users by spatial locations. However, for PPP model, it is ineffective due to the randomness of BSs' locations. Thus, we partition the users into edge users or interior users by SINR threshold [30] [31]. We compute a mobile user's SINR to the nearest BS of the k_{th} tier and check if it is less than the tier's FFR threshold T_k. If so, then the user is classified as an edge user, otherwise interior user.

3.2 Coverage Probability

In this section, we will derive the coverage probability of edge user for SFR and strict FFR. We assume that a typical user is covered by k_{th} tier if its downlink SINR from the nearest BS of k_{th} tier is greater than the threshold T_k. In other words, the coverage probability equals the complementary cumulative distribution function (CCDF) of the SINR. The coverage probability of edge user is conditional one, because it depends on the coverage probability of interior user. With FFR, when a mobile user is classified as an edge user, BSs transmit to it on the reserved FFR band. Thereby, the edge user will experience new direct interference channel, denoted as $\hat{g}_{kx_k} \sim \exp(\mu)$ and $\hat{G}_{kx_k} \sim \exp(\mu)$, respectively, which also follow exponential distribution, but are independent of g_{kx_k} and G_{kx_k}. Correspondingly, the interference of the edge users from k_{th} tier changes to $\hat{I}_j = \sum_{y \in \Phi_j} P_j \hat{G}_{jy} R_{jy}^{-\alpha}$ and the SINR of the k_{th} tier edge users is denoted as $\hat{S}INR_k$, that describes the next subsections.

3.2.1 Open Access Case

In open access case, a typical user can connect to any tier without any restriction [67]. Because the BSs' locations of each tier are modeled by independent PPP, the coverage probabilities of each tier are also independent. Thus, under open access scheme the coverage probability can be thought as the sum of the coverage probability of each tier. Considering FFR technique, the coverage probability of open access can be expressed as

$$\mathbb{P}\Big(\bigcup_{k=1}^{K} \hat{S}INR_k > \hat{T}_k \mid \bigcap_{j=1}^{K} SINR_j < T_j \Big), \tag{3.1}$$

where $\hat{T}_k$ means the thresholds of the k_{th} tier edge users, and T_j means the SINR threshold of j_{th} tier interior users. Due to the independence between each tier, (3.1) can be evaluated as

$$\begin{aligned}
&\mathbb{P}\Big(\bigcup_{k=1}^{K} \hat{SINR}_k > \hat{T}_k \mid \bigcap_{j=1}^{K} SINR_j < T_j\Big) \\
&\sum_{k=1}^{K} \mathbb{P}\big(\hat{SINR}_k > \hat{T}_k \mid \bigcap_{j=1}^{K} SINR_j < T_j\big) \\
&\overset{a}{=} \sum_{k=1}^{K} \frac{\mathbb{P}\big(\hat{SINR}_k > \hat{T}_k\,,\ \bigcap_{j=1}^{K} SINR_j < T_j\big)}{\mathbb{P}\big(\bigcap_{j=1}^{K} SINR_j < T_j\big)} \\
&= \sum_{k=1}^{K} \frac{\mathbb{P}\big(\hat{SINR}_k > \hat{T}_k\,,\ \prod_{j=1}^{K} SINR_j < T_j\big)}{\mathbb{P}\big(\prod_{j=1}^{K} SINR_j < T_j\big)},
\end{aligned} \tag{3.2}$$

where a means conditioning on r_k, and using conditional probability formula $\mathbb{P}(A|B) = \frac{\mathbb{P}(AB)}{\mathbb{P}(B)}$.

SFR Case

As mentioned previously, SFR improves the SINR of the edge users by increasing transmit power, rather than allocating reserved subbands. That means the edge users experience both cross-tier and inter-cell interference. Under SFR, the SINR of k_{th} edge and interior user can be denoted as $\hat{SINR}_k = \frac{\beta_k P_k \hat{g}_k r_k^{-\alpha}}{\sum_{n=1}^{K} \eta_n \hat{I}_n + \sigma^2}$, $SINR_j = \frac{P_j g_j r_j^{-\alpha}}{\sum_{m=1}^{K} \eta_m I_m + \sigma^2}$, respectively, where $\eta_k = (D_k - 1 + \beta_k)/D_k$. Because increasing the edge users' transmit power will correspondingly impact on interference, so we introduce η_k to consolidate the influence of the edge and interior users form k_{th} tier. Now for SFR, eq. (3.2) can

be further expressed as

$$P_{SFR}(\hat{T}_k) = \sum_{k=1}^{K} \frac{\mathbb{P}\left(\frac{\beta_k P_k \hat{g}_k r_k^{-\alpha}}{\sum_{n=1}^{K} \eta_n \hat{I}_n + \sigma^2} > \hat{T}_k \,,\, \prod_{j=1}^{K} \frac{P_j g_j r_j^{-\alpha}}{\sum_{m=1}^{K} \eta_m I_m + \sigma^2} < T_j \right)}{\mathbb{P}\left(\prod_{j=1}^{K} \frac{P_j g_j r_j^{-\alpha}}{\sum_{m=1}^{K} \eta_m I_m + \sigma^2} < T_j \right)}. \tag{3.3}$$

After evaluating (3.3), we can get the coverage probability as theorem 3.2.1.

Theorem 3.2.1. *(SFR, open access, edge user, HetNets): The coverage probability of edge user with SFR and open access scheme is*

$$P_{SFR,op}(\hat{T}_k) = \sum_{k=1}^{K} \frac{\int_0^\infty \rho(k,\lambda) \mathrm{e}^{-\hat{s}_k \sigma^2} f_{SFR}(\hat{s}_k) \cdot \left(1 - \mathrm{e}^{-s_k \sigma^2} f_{SFR}(s_k) \right) \mathrm{d}r_k}{\int_0^\infty \rho(k,\lambda) \left(1 - \mathrm{e}^{-s_k \sigma^2} f_{SFR}(s_k) \right) \mathrm{d}r_k}, \tag{3.4}$$

where $\rho(k,\lambda) = 2\pi r_k \lambda_k e^{-\pi r_k^2 \lambda_k}$, $\hat{s}_k = \frac{\mu \hat{T}_k r_k^\alpha}{P_k \beta_k}$, $s_j = \frac{\mu T_j r_j^\alpha}{P_j}$ *and*

$$f_{SFR}(s) = \exp\left(-(s\mu^{-1})^{\frac{2}{\alpha}} C(\alpha) \sum_{m=1}^{K} \lambda_m (\eta_m P_m)^{\frac{2}{\alpha}} \right), \tag{3.5}$$

where $C(\alpha) = 2\pi^2 \mathrm{csc}(\frac{2\pi}{\alpha}) \alpha^{-1}$.

Proof: see the A.1.

We can observe from theorem 3.2.1 that the coverage probability is only a function of the relevant SFR and HetNets' parameters, and very tractable, just containing single integral. The reason for introducing integral is that evaluating (3.3) needs to condition on and decondition on r_k. The terms $f_{SFR}(\hat{s}_k^{\frac{2}{\alpha}})$ and $f_{SFR}(s_k^{\frac{2}{\alpha}})$ come from $\hat{SINR}_k$ and $SINR_k$ terms of (3.3), respectively. In (3.3), the edge and interior users have the same SINR pattern, they are in the same situation, besides transmit power, thus we can express the results of them by the same function.

Comparing to the conventional derivations of [30] [31], the expressions of theorem 3.2.1 are simple and general, which contain only single integral and consider K tiers HetNets. There are two reasons of that. Firstly, the different tiers BSs' locations are

modeled by independent PPP, which means the BSs from different tiers are totally independent. This independence is used in (3.1), which plays a key role in simplifying the expressions. Secondly, [15] provides a simple method of evaluating the Laplace transform under PPP model. Based on this conclusion, the simple expression of (A.4) can be derived.

The expressions of theorem 3.2.1 can be further simplified for interference-limited case to a simple closed form expression.

Lemma 3.2.2. *(No noise, SFR, open access, HetNets). In interference-limited network, the coverage probability of edge user with SFR and open access scheme is*

$$P_{SFR,op,IL} = \sum_{k=1}^{K} \frac{\pi\left(\pi + T_k^{\frac{2}{\alpha}}\theta\right)}{\left(\pi + (\frac{\hat{T}_k}{\beta_k})^{\frac{2}{\alpha}}\theta\right)\left(\pi + (\frac{\hat{T}_k}{\beta_k})^{\frac{2}{\alpha}}\theta + T_k^{\frac{2}{\alpha}}\theta\right)}, \tag{3.6}$$

where $\theta = \lambda_k^{-1} P_k^{-\frac{2}{\alpha}} C(\alpha) \sum_{m=1}^{K} \lambda_m (\eta_m P_m)^{\frac{2}{\alpha}}$.

Proof: see the A.2.

This conclusion is not only helpful for system design of the HetNets with SFR, but also gives us some important observations. For $T_k = \hat{T}_k \beta_k^{-1}$, (3.6) can be further simplified to

$$P_{SFR,op,IL} = \sum_{k=1}^{K} \frac{\pi}{\left(\pi + 2T_k^{\frac{2}{\alpha}}\theta\right)}. \tag{3.7}$$

Considering only one tier network ($K = 1$), (3.6) changes to

$$P_{SFR,op,IL} = \frac{\pi\left(\pi + T_k^{\frac{2}{\alpha}}\theta_1\right)}{\left(\pi + (\frac{\hat{T}_k}{\beta_k})^{\frac{2}{\alpha}}\theta_1\right)\left(\pi + (\frac{\hat{T}_k}{\beta_k})^{\frac{2}{\alpha}}\theta_1 + T_k^{\frac{2}{\alpha}}\theta_1\right)}, \tag{3.8}$$

where $\theta_1 = C(\alpha)\eta_1$. From (3.8), we note that the coverage probability of edge user in interference-limited one tier network with SFR is independent of density and transmit power of BSs, and only depends on the thresholds of edge and interior user and transmit power control factor β_k. We can find the similar observation in [14] and

[15]: in one tier network interference-limited network the coverage probability of interior user is independent of density and transmit power of BSs. Including above observations, we can conclude that neglecting noise, density and transmit power do not affect coverage probability of both edge and interior users.

Strict FFR

For Strict FFR case, the interior users use common subband f_c, thereby, it will be interfered by both inter-cell and cross-tier BSs. However, the edge user is allocated reserved subbands to reduce cross-interference, that means the edge users of strict FFR just experience one tier's interference, furthermore, thinned with D_k. The SINR of k_{th} edge and interior user can be denoted as $\hat{SINR}_k = \frac{D_k P_k \hat{g}_k r_k^{-\alpha}}{\hat{I}_k+\sigma^2}$, $SINR_k = \frac{P_j g_j r_j^{-\alpha}}{\sum_{m=1}^{K} I_m+\sigma^2}$, respectively. Now for strict FFR, (3.2) can be further expressed as

$$P_{sFFR}(\hat{T}_k) = \sum_{k=1}^{K} \frac{\mathbb{P}\left(\frac{D_k P_k \hat{g}_k r_k^{-\alpha}}{\hat{I}_k+\sigma^2} > \hat{T}_k\,,\ \prod_{j=1}^{K} \frac{P_j g_j r_j^{-\alpha}}{\sum_{m=1}^{K} I_m+\sigma^2} < T_j\right)}{\mathbb{P}\left(\prod_{j=1}^{K} \frac{P_j g_j r_j^{-\alpha}}{\sum_{m=1}^{K} I_m+\sigma^2} < T_j\right)}. \tag{3.9}$$

Comparing eqs. (3.9) and (3.3), they are similar and (3.9) is much easier, because its edge user's SINR does not contain cross-tier interference. So referring to the method of SFR, after evaluating it, we can derive

Theorem 3.2.3. *(strict FFR, open access, edge user, HetNets): The coverage probability of edge user with strict FFR and open access scheme is*

$$P_{sFFR,op} = \sum_{k=1}^{K} \frac{\int_0^\infty \rho(k,\lambda) \mathrm{e}^{-\hat{s}_k \sigma^2} f_{edge}(\hat{s}_k) \cdot \left(1-\mathrm{e}^{-s_k \sigma^2} f_{sFFR}(s_k)\right) \mathrm{d}r_k}{\int_0^\infty \rho(k,\lambda) \left(1-\mathrm{e}^{-s_k \sigma^2} f_{sFFR}(s_k)\right) \mathrm{d}r_k} \tag{3.10}$$

where $s_j = \frac{\mu T_j r_j^{\alpha}}{P_j}$, $\hat{s}_k = \frac{\mu \hat{T}_k r_k^{\alpha}}{P_k D_k}$,

$$f_{sFFR}(s) = \exp\left(- (s\mu^{-1})^{\frac{2}{\alpha}} C(\alpha) \sum_{m=1}^{K} \lambda_m P_m^{\frac{2}{\alpha}} \right), \tag{3.11}$$

$$f_{egde}(s) = \exp\Bigg(- (s\mu^{-1})^{\frac{2}{\alpha}} C(\alpha)\lambda_k P_k^{\frac{2}{\alpha}} \Bigg). \tag{3.12}$$

Proof: see the A.3.

The expressions of theorem 3.2.3 are similar to that of theorem 3.2.1. We can see from (3.10), which also contains only single integral, and the interference term of edge and interior user are included in $f_{sFFR}(s)$ and $f_{egde}(s)$, respectively.

These expressions also can be further simplified for interference-limited network to a simple closed form expression.

Lemma 3.2.4. *(No noise, strict FFR, HetNets). In interference-limited network, the coverage probability of edge user with strict FFR and open access scheme is*

$$P_{SFR,op,IL} = \sum_{k=1}^{K} \frac{\pi\Bigg(\pi + T_k^{\frac{2}{\alpha}}\theta'\Bigg)}{\Bigg(\pi + (\frac{\hat{T}_k}{D_k})^{\frac{2}{\alpha}} C(\alpha)\Bigg)\Bigg(\pi + (\frac{\hat{T}_k}{D_k})^{\frac{2}{\alpha}} C(\alpha) + T_k^{\frac{2}{\alpha}}\theta'\Bigg)}, \tag{3.13}$$

where $\theta' = \lambda_k^{-1} P_k^{-\frac{2}{\alpha}} C(\alpha) \sum_{m=1}^{K} \lambda_m P_m^{\frac{2}{\alpha}}$.

Proof: refer to the proof of corollary 3.2.2.

The conclusion of corollary 3.2.4 is similar to that of SFR, and more simple, this is because the k_{th} tier edge user of strict FFR just experiences inter-cell interference from k_{th} tier.

Considering only one tier network ($K = 1$), Eq. (3.13) changes to

$$P_{SFR,op,IL} = \frac{\theta_1'\Bigg(\theta_1' + T_k^{\frac{2}{\alpha}}\Bigg)}{\Bigg(\theta_1' + (\frac{\hat{T}_k}{D_k})^{\frac{2}{\alpha}}\Bigg)\Bigg(\theta_1' + (\frac{\hat{T}_k}{D_k})^{\frac{2}{\alpha}} + T_k^{\frac{2}{\alpha}}\Bigg)}, \tag{3.14}$$

where $\theta_1' = \pi C(\alpha)^{-1}$.

Eq. (3.14) shows the coverage probability of edge user in interference-limited one tier network with strict FFR is independent of density and transmit power of BSs, and only depends on the thresholds of edge and interior user and reuse factor D_k.

Furthermore, if let $T_k = \hat{T}_k D_k^{-1}$, the coverage probability of edge user just depends on T_k, which is as

$$\sum_{k=1}^{K} \frac{\theta_1'}{\left(\theta_1' + 2T_k^{\frac{2}{\alpha}}\right)}. \tag{3.15}$$

Now considering (3.8) and (3.14), we can conclude that neglecting noise, in one tier network, for both SFR and strict FFR, density of BSs and transmit power do not affect coverage probability of both edge and interior users.

3.2.2 Closed Access

Under closed access scheme, a mobile user accesses to only a subset of tiers and the rest of the tiers act purely as interference [68]. This access scheme is applied extensively in private owned infrastructure, such as user-deployed femto BSs or company-deployed pico BSs, which is used to improve service to their staffs. In this work, we assume the typical user can access to a subset $B \subset \{1, 2, \cdots, K\}$, and due to the independence between each tier, the coverage probability under closed access case can be thought as the sum of those of the each subset tier under closed access case. With FFR, the coverage probability can be expressed as

$$\mathbb{P}\Big(\bigcup_{k\in B} \hat{SINR}_k > \hat{T}_k \mid \bigcap_{j\in B} SINR_j < T_j\Big). \tag{3.16}$$

Referring to (3.2), (3.16) equals

$$\sum_{j\in B} \frac{\mathbb{P}\big(\hat{SINR}_k > \hat{T}_k\,,\, \prod_{j\in B} SINR_j < T_j\big)}{\mathbb{P}\big(\prod_{j\in B} SINR_j < T_j\big)}. \tag{3.17}$$

SFR

In section 3.2.1, we have already introduced the SINR of k_{th} edge and interior users, now plug them into (3.17), we can derive

Theorem 3.2.5. *(SFR, closed access, edge user, HetNets): The coverage probability of edge user with SFR and closed access scheme is*

$$P_{SFR,cl} = \sum_{k\in B} \frac{\int_0^\infty \rho(k,\lambda) \mathrm{e}^{-\hat{s}_k \sigma^2} f_{SFR}(\hat{s}_k) \cdot \left(1 - \mathrm{e}^{-s_k \sigma^2} f_{SFR}(s_k)\right) \mathrm{d}r_k}{\int_0^\infty \rho(k,\lambda) \left(1 - \mathrm{e}^{-s_k \sigma^2} f_{SFR}(s_k)\right) \mathrm{d}r_k}, \tag{3.18}$$

where $\hat{s}_k = \frac{\mu \hat{T}_k r_k^\alpha}{P_k \beta_k}$, $s_j = \frac{\mu T_j r_j^\alpha}{P_j}$, $\rho(k,\lambda)$ *and* $f_{SFR}(s_k)$ *are given in theorem 3.2.1.*

Proof: refer to the proof of theorem 3.2.1. The process of theorem 3.2.5 proof is almost same as that of theorem 3.2.1, only the tiers calculated are different, theorem 3.2.5 considers a subset $B \subset \{1, 2, \cdots, K\}$ *rather than all tiers* K*.*

Similar to corollary 3.2.2, the following corollary specializes from theorem 3.2.5, to interference-limited (no noise) HetNets.

Lemma 3.2.6. *(No noise, SFR, closed access, HetNets). In interference-limited netxwork, the coverage probability of edge user with SFR and closed access scheme is*

$$P_{SFR,cl,IL} = \sum_{k\in B} \frac{\pi\left(\pi + T_k^{\frac{2}{\alpha}}\theta\right)}{\left(\pi + (\frac{\hat{T}_k}{\beta_k})^{\frac{2}{\alpha}}\theta\right)\left(\pi + (\frac{\hat{T}_k}{\beta_k})^{\frac{2}{\alpha}}\theta + T_k^{\frac{2}{\alpha}}\theta\right)}, \tag{3.19}$$

where θ *is given in corollary 3.2.2.*

Proof: refer to the proof of corollary 3.2.2. The difference from corollary 3.2.2 is only the tiers calculated, corollary 3.2.6 considers a subset $B \subset \{1, 2, \cdots, K\}$ *rather than all tiers* K*.*

Let $T_k = \hat{T}_k \beta_k^{-1}$, (3.19) can be further simplified to

$$\sum_{k\in B} \frac{\pi}{\left(\pi + 2T_k^{\frac{2}{\alpha}}\theta\right)}. \tag{3.20}$$

The analysis of one tier ($K = 1$) network in closed access scheme, please refer to that of open access case, which is given in the analysis part after corollary 3.2.2. This

is because for one tier network, there is no difference between open access and closed access cases.

strict FFR

For strict FFR, we also consider users are allowed to connect to a subset tiers $B \subset \{1, 2, \cdots, K\}$. Plugging the SINR of k_{th} edge and interior users, which are introduced in 3.2.1, into (3.17), we can derive

Theorem 3.2.7. *(strict FFR, closed access, edge user, HetNets): The coverage probability of edge user with strict FFR and closed access scheme is*

$$P_{sFFR,cl} = \sum_{k \in B} \frac{\int_0^\infty \rho(k,\lambda) \mathrm{e}^{-\hat{s}_k \sigma^2} f_{edge}(\hat{s}_k) \cdot \left(1 - \mathrm{e}^{-s_k \sigma^2} f_{sFFR}(s_k)\right) \mathrm{d}r_k}{\int_0^\infty \rho(k,\lambda) \left(1 - \mathrm{e}^{-s_k \sigma^2} f_{sFFR}(s_k)\right) \mathrm{d}r_k} \tag{3.21}$$

where $s_j = \frac{\mu T_j r_j^\alpha}{P_j}$, $\hat{s}_k = \frac{\mu \hat{T}_k r_k^\alpha}{P_k D_k}$, $f_{sFFR}(s)$ *and* $f_{egde}(s)$ *are given in (3.11) and (3.12), respectively.*

Proof: refer to the proof of theorem 3.2.1.

Similar to corollary 3.2.4, the following corollary specializes from theorem 3.2.7, to interference-limited (no noise) HetNets.

Lemma 3.2.8. *(No noise, strict FFR, closed access, HetNets). In interference-limited network, the coverage probability of edge user with strict FFR and closed access scheme is*

$$P_{sFFR,cl,IL} = \sum_{k \in B} \frac{\pi \left(\pi + T_k^{\frac{2}{\alpha}} \theta'\right)}{\left(\pi + (\frac{\hat{T}_k}{D_k})^{\frac{2}{\alpha}} C(\alpha)\right) \left(\pi + (\frac{\hat{T}_k}{D_k})^{\frac{2}{\alpha}} C(\alpha) + T_k^{\frac{2}{\alpha}} \theta'\right)}, \tag{3.22}$$

where θ' *is given in corollary 3.2.4.*

Proof: refer to the proof of corollary 3.2.2.

Let $T_k = \hat{T}_k D_k^{-1}$, (3.22) can be further simplified to

$$\sum_{k \in B} \frac{\pi}{\left(\pi + 2T_k^{\frac{2}{\alpha}}\theta\right)}. \tag{3.23}$$

The analysis of one tier ($K = 1$) network in the closed access scheme, please refer to the that of open access case, which is give in the analysis part after corollary 3.2.4.

3.2.3 Propositions

Observe theorems and corollaries above carefully, we can further give some propositions. First, the expressions of corollary 3.2.2-3.2.8 do not contain the mean μ of exponential distribution followed by channel. Not only that, in the procedure of proving corollary 3.2.2-3.2.8, for example in A.2, (A.7) is the outage probability of interior user, which also does not contain μ. Thus, this conclusion can be seen as derived in the interference-limited HetNets without FFR. Thereby, we can give one proposition as

Proposition 1. *No matter with or without FFR, in interference-limited HetNets, the coverage probability of edge or interior is independent of channel parameter μ.*

Comparing (3.4), (3.10) to (3.18), (3.21), respectively, we will easily observe that the difference between them is just the sum of tiers, if we let subset B contain all tiers, then they are the same, and if we assume the subset just contains one tier, $B = \{k\}$, then (3.18), (3.21) become the coverage probabilities of k_{th} tier under SFR and strict FFR, respectively. Furthermore, they equal with that of open access case. Thereby, we can give

Proposition 2. *The coverage probability of k_{th} tier with FFR under open access case is the same as that of single tier under closed access case.*

$$\mathbb{P}\big(\hat{SINR}_k > \hat{T}_k \,|\, \bigcap_{j=1}^{K} SINR_j < T_j\big) = \mathbb{P}\big(\hat{SINR}_k > \hat{T}_k \,|\, SINR_k < T_k\big) \tag{3.24}$$

Referring to (3.2), the term $\mathbb{P}\big(\bigcap_{j\neq K} SINR_j < T_j\big)$ contained by the left formula of (3.24) will be simplified out, due to the independence between each tier, thereby we can get proposition 4.2.2.

Based on proposition 4.2.2, we can derive easily

Proposition 3. *The coverage probability of edge user with FFR under open access scheme equals the sum of the coverage probability of each single tier under closed access scheme.*

$$P_{FFR,op} = \sum_{k=1}^{K} \mathbb{P}\big(\hat{S}INR_k > \hat{T}_k \,|\, SINR_k < T_k\big). \tag{3.25}$$

3.3 Numerical Result and System Design Implication

In this section we show the numerical results of coverage probability and discuss the influence of main parameters on it. For clearly illustrating HetNets performance analysis, we consider limited-interference and two tiers ($K = 2$) networks. The related simulation parameters are as: $D_k = [3, 3]$, $T_k = [1, 1]$dB, $\hat{T}_k = [1, 1]$dB, $P_k = [20, 1]$W, $\beta_k = [8, 8]$, $\alpha = 2.8$, $\lambda_k = [24, 96]$ BSs per 10km^2.

3.3.1 Coverage Probability

Fig. 3-2 and Fig. 3-3 show the coverage probabilities of edge user for both open and closed access cases.

For open access, we can see from Fig. 3-2, the coverage probability of strict FFR is much higher than that of SFR. This is because strict FFR can reduce the inter-tier interference, furthermore thin intra-tier interference with D_k. However, instead of reducing inter-tier interference, SFR improves the SINR of edge user by increasing their transmit power, which simultaneously also increases the interference of the whole HetNets and decreases the coverage probability. Thus, in coverage probability respect, Strict FFR is better than SFR.

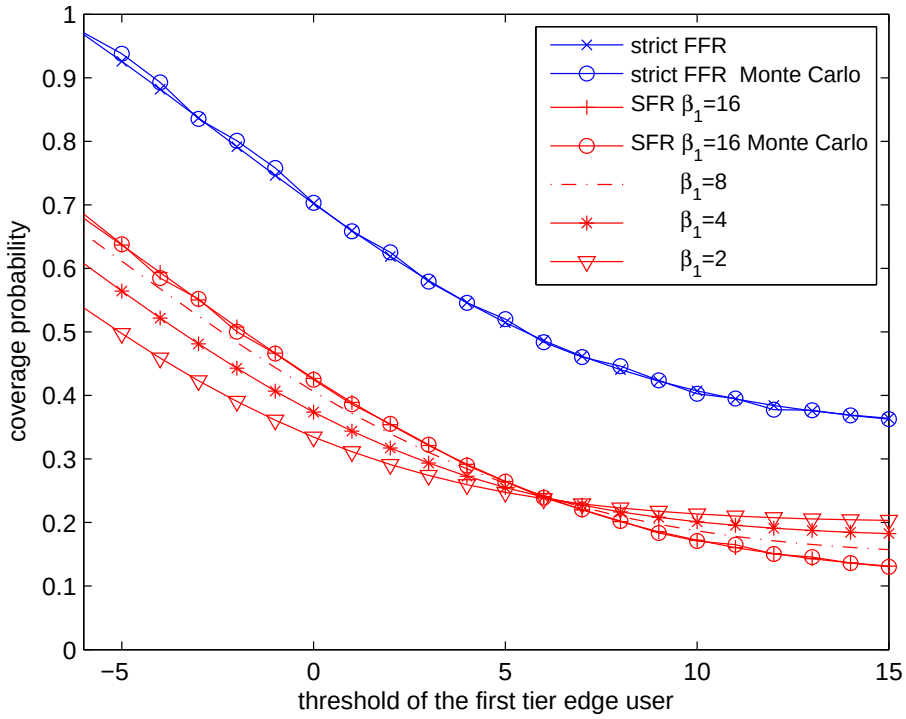

Figure 3-2: Downlink edge user coverage probability for open access with FFR

We can also see from Fig. 3-2, for the low threshold of first edge user $\hat{T}_1$, the coverage probability of SFR increases with the increase of β_1. However, for the high threshold, the situation is gradually reversed. This is because in the simulation we just increase the β_1, which increases the coverage probability of first tier and decreases that of second tier, simultaneously. For low $\hat{T}_1$, the improvement of the first tier coverage probability is dominant, however with the increase of $\hat{T}_1$, situation changes gradually, and finally the improvement can not offset the loss of second tier coverage probability.

For the closed access, we can see from Fig. 3-3, increasing β_k can increase the coverage probability of first tier edge user, which is consistent with SFR theory, and the performance of strict FFR is also better than that of SFR.

It should be noted that for both access cases, the bigger β_k is, the higher the coverage probability of k_{th} tier edge user is. However the improvement becomes smaller and smaller, and finally approaches a limited value rather than 1, even in the

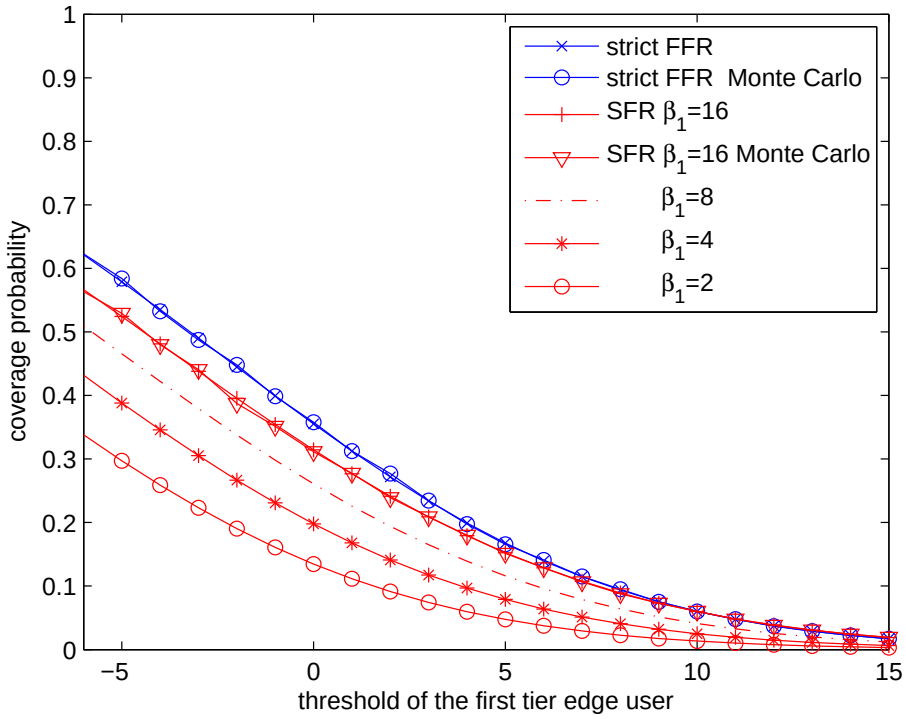

Figure 3-3: Downlink first tier edge user coverage probability for closed access with FFR

case of $\beta_k = \infty$.

Fig. 3-3 just shows the coverage probabilities of first tier under closed access case, according to proposition 4.3.1, which can be also seen as the first tier coverage probability of open access case.

3.3.2 System Design Implication

Now we discuss the influence of main HetNets' parameters on the coverage probability of edge user.

BSs' Density

We first discuss the effects of the density of BSs on the coverage probability of edge user. For the sake of convenience, we define $\kappa = \lambda_2/\lambda_1$, and change κ only by changing λ_2.

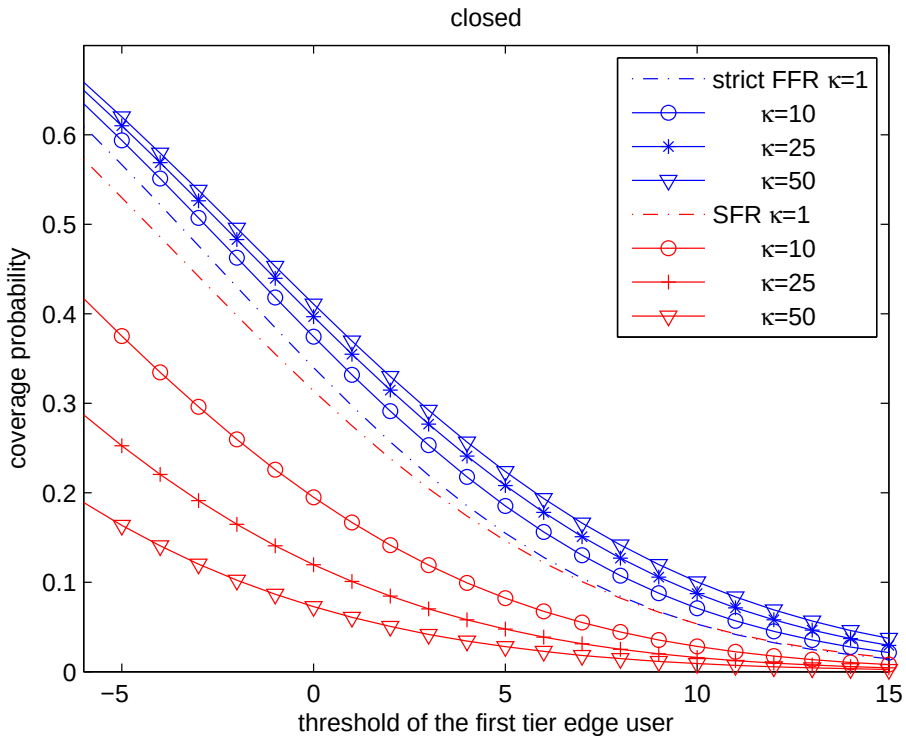

Figure 3-4: Relation between κ and first tier edge user coverage probability under closed access case

Fig. 3-4 shows the relationship between the coverage probability of first edge user and κ under closed access case. For strict FFR, increasing λ_2 increases the coverage probability of first tier cell-edge user. This is because increasing λ_2 will reduce the SINR of first tier users, due to the closed access restriction, which makes more and more first tier users become edge users. These edge users can get reserved subbands, thus whose coverage probability is increased.

For SFR, the results are contrary to those of strict FFR. This is because SFR does not reduce the interference of edge users, thus the increase of interference directly impacts on the first cell-edge users, thereby decreases their coverage probability.

Threshold T_2

We know that only changing the threshold of second interior user T_2 does not change HetNets situation at all, thus under the closed access case, T_2 can not impact on the coverage probability of first tier user.

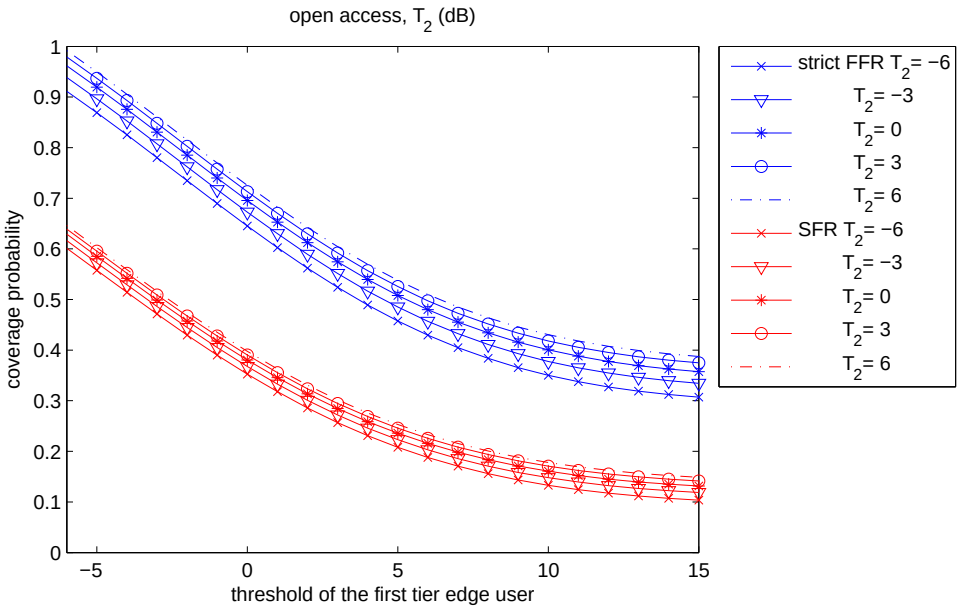

Figure 3-5: Relation between κ and first tier edge user coverage probability under closed access case

Fig. 3-5 shows the effects of T_2 on the coverage probability of edge user under open access scheme. For both strict FFR and SFR, increasing T_2 will increase the coverage probability of edge user. The reason is that increasing T_2 makes more and more users become cell-edge users, thereby increases the coverage probability.

3.4 Conclusion

We use PPP to model BSs' locations, and propose a framework to analyze the downlink coverage probability of HetNets utilizing the FFR technique. We give tractable expressions of typical users' coverage probability under both closed and open access cases, which can be furthermore simplified to a close form in interference-limited networks. Through analysis, some useful propositions and interesting observations are proposed: the coverage probability of edge user is independent of channel parameter μ; The coverage probability of edge user with FFR under open access scheme equals the sum of the coverage probability of each single tier under closed access scheme; In one tier network with FFR, both for SFR and strict FFR, density of BSs and transmit power do not affect coverage probability of both edge and interior

users. We give the numerical results of coverage probability, and discuss the effects of main parameters on it. These analysis can assist system designers in designing networks, and evaluating new algorithm about HetNets utilizing FFR.

Chapter 4

A Model Based on Poisson Point Process for Analyzing MIMO Heterogeneous Networks Utilizing Fractional Frequency Reuse

MIMO is a key technique of wireless communication standards including IEEE 802.11n (Wi-Fi), IEEE 802.11ac (Wi-Fi), HSPA+ (3G), WiMAX (4G), and Long Term Evolution (4G). Therefore, the modeling and analysis of MIMO cellular networks appear to be of essence. By introducing MIMO to the framework of Chapter 3, a tractable and flexible model for K tiers MIMO HetNets, with FFR technique is proposed in this chapter.

4.1 System Model

4.1.1 BS Location Model

In this section, we consider an orthogonal frequency-division multiple access (OFDMA) cellular downlink MIMO HetNets consisting of K tiers of BSs. The BSs' locations of the k_{th} tier are modeled as independent PPP Φ_k [59] with the density λ_k. First we

get the number of the points in a bounded area, which follows a Poisson distribution. Secondly, we distribute the points within the area uniformly, then the points are a realization of PPP. Without loss of generality, we conduct analysis on a typical single antenna user located at the origin. According to [69], the modern networks are typical interference-limited networks, that means the noise of the network can be ignored. Therefore we will compute the SIR instead of SINR for the typical user at the origin. We assume the typical user can access just one tier at a time and connect to the nearest BS of the tier. Which location is set as x_k. Since the BSs are distributed as PPP, the distance between the user and the nearest BS $\|x_k\|$ will follow the exponential distribution, furthermore its PDF is $f_{\|x_k\|}(\|x_k\|) = e^{\lambda_k \pi \|x_k\|^2} 2\pi\lambda_k \|x_k\|$ [59]. We assume the BSs of the k_{th} tier have the same transmit power P_k and the same target SIR T_k.

4.1.2 MIMO Channel

Before going into the technical details, it is necessary to point out that MIMO channel is quite different from the single antenna channel. For classical single antenna channel, both direct and interfering links are exponentially distributed. However, for MIMO channel, the direct and interfering links follow different distributions (mainly in terms of parameters). In our considered scope, that means the channel distribution of the link from a multi antenna BS to a typical single antenna user differs in terms of the MIMO technique and what kind of BS (serving or interfering) it is. This is because if it is a serving BS, it will precode its data for a typical user, which may lead to a different channel distribution from the case when it simply acts as an interferer. We assume that the channel for the direct link from the nearest BS of k_{th} tier, which located at x_k, to a typical user is denoted by h_{kx_k}, and the other links, which are from the BSs located at y_j, are considered as interfering links. The channel of the interfering links is denoted by g_{jy_j}.

The appendix A of [34] has proved in detail that for linear precoding, both direct and interference links follow the Gamma distribution, denoted by $h_{kx_k} \sim \Gamma(\Delta_k, 1)$ and $g_{kx_k} \sim \Gamma(\Psi_k, 1)$, where Δ_k and Ψ_k depend on the multi-antenna technique adopted.

For zero-forcing pre-coding, $\Delta_k = M_k - \Psi_k + 1$ and M_k is the number of antennas. According to [34], if consider the channel vector multiplying linear precoding vector as the direct link h_{kx_k}, then after deriving, we can get that h_{kx_k} follows Gamma distribution. The interference link is as well. Furthermore, [34] also proves and gives other instances following three specific transmission techniques:

- Space-division multiple-access (SDMA): in this case, the BS of k_{th} tier, which is with M_k antennas, serves $\Psi_k > 1$ users. When $\Psi_k = M_k$, we term it as full SDMA, for which $\Delta_k = 1$.

- Single-user beamforming (SU-BF): in this case, $\Delta_k = M_k$ and $\Psi_k = 1$, which models MISO eigen-beamforming or SU-BF with perfect channel state information (CSI) and the BS serves $\Psi_k = 1$ users.

- $\Delta_k = \Psi_k = 1$: this case models the special case of single-input single-output (SISO). It should be noted that this case is just a special case of SISO and is not our key point. For more information of this case, please refer to [30].

Because the proof of MIMO channel listed is beyond the scope of this paper, interested readers are recommended to refer to [7] for more details.

We define the received power of the typical user at the origin from the serving BS as $P_r = P_k h_{kx_k} \|x_k\|^{-\alpha}$, where α is the path loss exponent. Denoting the set of interfering BSs in the k_{th} tier as Z_k, i.e., BSs that use the same subband as the typical user, the received SIR of the typical user is defined as

$$SIR(x_k) = \frac{P_k h_{kx_k} \|x_k\|^{-\alpha}}{\sum\limits_{j \in K} I_j},$$

where $I_j = \sum_{y \in Z_j} P_j g_{jy_j} \|y_j\|^{-\alpha}$.

To use the FFR, the user should be first classified . We compute the typical user's SIR from the nearest BS of the k_{th} tier, and check whether it is smaller than the predetermined threshold T_k. If so, then the user is classified as a cell-edge user, and if not, the user is classified as a cell-interior user.

4.2 Closed Access Coverage Probability Analysis

From this section, we will derive the coverage probability of a typical user. We assume that a typical user is covered by k_{th} tier if its downlink SIR from the nearest BS of k_{th} tier is greater than the threshold T_k, in other words, the coverage probability equals the CCDF of the SIR, and denoted as

$$\mathrm{P}_c = \mathbb{P}(SIR_k > T_k).$$

In the networks without FFR, the cell-interior user with lower SIR than the thresholds is not covered. However, in the networks using FFR, if a cell-interior user is not covered, it becomes a cell-edge user and experiences new direct and interference channels, which not only also follow Gamma distributions, but also are independent of h_k and g_k, and are denoted as $\hat{h}_{kx_k} \sim \Gamma(\Delta_k, 1)$ and $\hat{g}_{ky_k} \sim \Gamma(\Psi_k, 1)$, respectively. Correspondingly, the interference of k_{th} tier of the cell-edge users changes to $\hat{I}_k = \sum_{y_k \in Z_k} P_k \hat{g}_{ky_k} \|y_k\|^{-\alpha}$ and the SIR of the cell-edge users is denoted as SIR_{edge}, which is further introduced later.

4.2.1 Coverage with Strict FFR

Under strict FFR case, the cell-interior users use common subband f_c, thereby, it will be interfered by both inter-cell and cross tier BSs. However, the cell-edge user only experiences the inter-cell interference, furthermore, the interference will be thinned with a reuse factor of D_k, according to the reserved frequency allocation scheme of cell-edge users. As introduced in the last paragraph of section 4.1.2, we partition the users into the cell-edge users and cell-interior users by SIR threshold. Only if the typical user's SIR as a cell-interior user is smaller than threshold, namely $SIR_k < T_k$, the typical user can become a cell-edge user. Therefore, the cell-edge user's coverage probability is conditioned on its SIR as a cell-interior user, thus is a

conditional probability, denoted as

$$\begin{aligned} & \mathbb{P}(SIR_{edge} > T \,|\, SIR_k < T_k) \\ = \;& \mathbb{P}\Big(\frac{D_k P_k \hat{h}_{kx_k} \|x_k\|^{-\alpha}}{\hat{I}_k} > T \;\Big|\; \frac{P_k h_{kx_k} \|x_k\|^{-\alpha}}{\sum_{k=1}^{K} I_k} < T_k\Big) \end{aligned} \tag{4.1}$$

where T is the new threshold for cell-edge user, and evaluating (4.1), we can get the conclusion as (hereinafter for convenience of notation, we express $\|x_k\|$ as x_k).

Theorem 4.2.1. *(strict FFR, closed access, edge user, MIMO channel): The coverage probability of a k_{th} tier cell-edge user in the MIMO HetNets with strict FFR and closed access is*

$$P_{FFR,cl} = \frac{\int_0^\infty \rho(k,\lambda) \cdot \mathrm{f}_1(\hat{s}_{1x_k}) \cdot \big(1 - \mathrm{f}_1'(s_{1x_k})\big)\mathrm{d}x_k}{\int_0^\infty \rho(k,\lambda) \cdot \big(1 - \mathrm{f}_1'(s_{1x_k})\big)\mathrm{d}x_k} \tag{4.2}$$

where $\hat{s}_{1x_k} = \frac{T x_k^\alpha}{P_k D_k}$, $s_{1x_k} = \frac{T_k x_k^\alpha}{P_k}$,

$$\rho(k,\lambda) = 2\pi x_k \lambda_k e^{-\pi x_k^2 \lambda_k} \tag{4.3}$$

$$\mathrm{f}_1(x) = \sum_{i=0}^{\Delta_k - 1} \frac{1}{i!}\big[\big(-x\big)^i \frac{\delta^i}{\delta\big(x\big)^i} \exp\big(-x^{\frac{2}{\alpha}} \lambda_k P_k^{\frac{2}{\alpha}} \mathrm{C}\big(\alpha, \Psi_k\big)\big)\big]$$

$$\mathrm{f}_1'(x) = \sum_{i=0}^{\Delta_k - 1} \frac{1}{i!}\big[\big(-x\big)^i \frac{\delta^i}{\delta\big(x\big)^i} \exp\big(-x^{\frac{2}{\alpha}} \sum_{j=1}^{K} \lambda_j P_j^{\frac{2}{\alpha}} \mathrm{C}\big(\alpha, \Psi_j\big)\big)\big]$$

and

$$\mathrm{C}(\alpha, \Psi_j) = \frac{2\pi}{\alpha} \sum_{m=1}^{\Psi_j} \binom{\Psi_j}{m} \mathrm{B}\left(\Psi_j - m + \frac{2}{\alpha}, m - \frac{2}{\alpha}\right) \tag{4.4}$$

$$\mathrm{B}(x,y) = \int_0^1 t^{x-1}\big(1-t\big)^{y-1}\mathrm{d}t$$

Proof: see the appendix B.1.

The coverage probability is only a function of the relevant FFR, MIMO and HetNets' parameters. The reason for introducing an integral is that (4.1) is a conditional probability, evaluating it first needs to condition on the typical BS's location x_k, and

deconditioning on it will introduce the integral. The similar method is also applied by the following theorems. $\mathrm{f}_1(\hat{s}_{1x_k})$ and $\mathrm{f}_1'(s_{1x_k})$ express the probability (conditioning on x_k) of cell-edge users with new subband and cell-interior users, respectively. Comparing them, we can find that the main difference is a sum term from 1 to K in f_1'. It means before being allocated a new reserved subband, typical users experience the cross tier interference, but after being allocated a new reserved subband, the user just experiences the same tier interference thinned with D_k. We can also observe that the influence of different MIMO techniques is shown in the sum term about Δ_k and Ψ_k, furthermore Δ_k introduces the $\Delta_k - 1$ order derivative.

4.2.2 Coverage with SFR

Now we focus on the coverage probability of SFR case. In this case, every BS uses all of the D subbands, and uniformly picks up one of the subbands to transmit to cell-edge user. The SIR of the cell-edge user is increased by increasing the transmit power by the β parameter. As introduced in strict FFR case, the cell-edge user's coverage probability is also conditioned on its SIR as a cell-interior user, thus is a conditional probability, expressed as

$$\mathbb{P}\left(\frac{\beta_k P_k \hat{h}_{kx_k}\|x_k\|^{-\alpha}}{\sum_{k=1}^{K}\eta_k \hat{I}_k} > T \,\middle|\, \frac{P_k h_{kx_k}\|x_k\|^{-\alpha}}{\sum_{k=1}^{K}\eta_k I_k} < T_k\right) \tag{4.5}$$

evaluating above formula, we can get

Theorem 4.2.2. *(SFR, closed access, edge user, MIMO channel): The coverage probability of the k_{th} tier cell-edge user in the MIMO HetNets with SFR and closed access is*

$$P_{SFR,cl} = \frac{\int_0^\infty \rho(k,\lambda)\cdot \mathrm{f}_2(\hat{s}_{2x_k})\cdot\big(1-\mathrm{f}_2(s_{2x_k})\big)\mathrm{d}x_k}{\int_0^\infty \rho(k,\lambda)\cdot\big(1-\mathrm{f}_2(s_{2x_k})\big)\mathrm{d}x_k} \tag{4.6}$$

where $\rho(k,\lambda)$ *is given by (4.3),* $\hat{s}_{2x_k} = \frac{Tx_k^{\alpha}}{\beta_k P_k}$, $s_{2x_k} = \frac{T_k x_k^{\alpha}}{P_k}$, $f_2(x) =$

$$\sum_{i=0}^{\Delta_k - 1} \frac{1}{i!}\Big[\big(-x\big)^i \frac{\delta^i}{\delta\big(x\big)^i} \exp\big(-x^{\frac{2}{\alpha}} \sum_{j=1}^{K} \lambda_j \big(\eta_j P_j\big)^{\frac{2}{\alpha}} \mathrm{C}\big(\alpha, \Psi_j\big)\big)\Big]$$

and $\mathrm{C}\big(\alpha, \Psi_j\big)$ *is given by (4.4).*

Proof: see the appendix B.2.

In fact, different from the strict FFR, under SFR case, both cell-edge and cell-interior users are in the same situation, exception for transmit power. Thus, the coverage probabilities (conditioning on x_k) can be expressed by the same function $\mathrm{f}_2(\hat{s}_{2x_k})$ and $\mathrm{f}_2(s_{2x_k})$, respectively.

4.2.3 Numerical Result of Closed Access

For closed access case, we also consider the interference-limited network. The related simulation parameters are as: $D_k = [3,3,3]$, $T_k = [3,3,3]$dB, $P_k = [20,5,1]$W, $\alpha = 4$, $\lambda_k = [24,72,216]$ BSs per 10km^2. We give a curve of $\Delta_k = 1$ and $\Psi_k = 1$ special case, which is considered as a limiting form of both SDMA and SU-BF to express the variation trend of them. Under full SDMA case, $\Delta_k = 1$ and $\Psi_k = M_k$, and under SU-BF, $\Delta_k = M_k$ and $\Psi_k = 1$, which reduces the expression of coverage probability significantly. It should be noted that to theorize our model clearly, all tiers are assumed to adopt same MIMO technique. However, our model is not restricted to uniform MIMO technique across different tiers. Substituting Δ_k and Ψ_j of each tier with different values as introduced in Section 4.1.2, we can get the result of MIMO HetNets using different MIMO techniques.

Fig. 4-1 shows the derived coverage probability of the first tier strict FFR cell-edge users for the three tier interference-limited networks. For SDMA, we can see that the coverage probability decreases with the increase of Ψ_k, here we consider full SDMA, that means $\Psi_k = M_k$. For SU-BF, the probability increases with the increase of Δ_k. The results of both SDMA and SU-BF accord with the MIMO channel theorem.

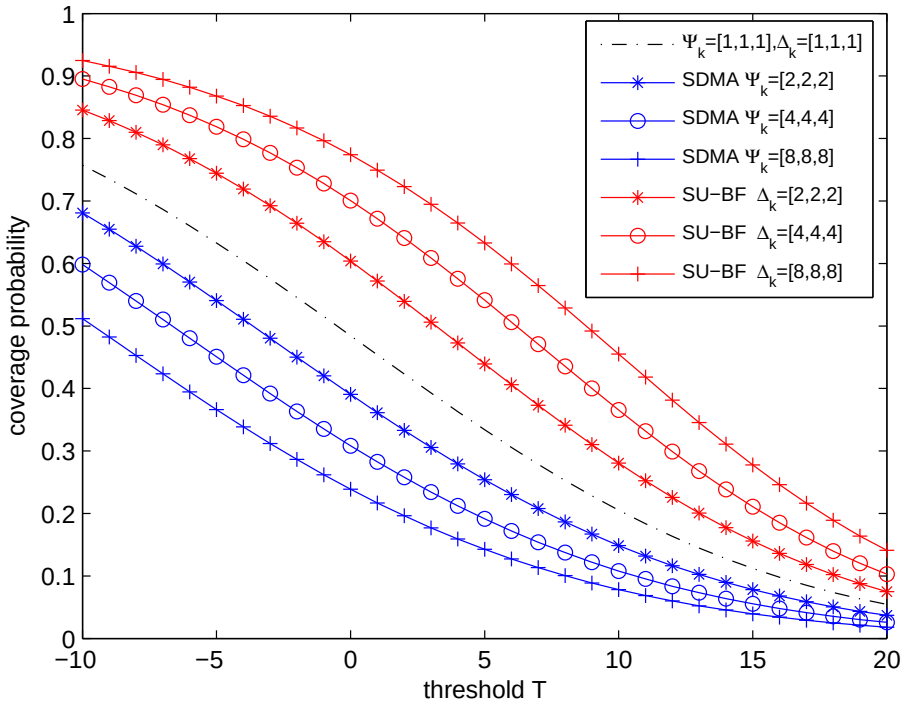

Figure 4-1: Downlink first tier cell-edge user coverage probability for strict FFR with closed access

Fig. 4-2 shows the derived coverage probability of the first tier SFR cell-edge users. Comparing to Fig. 4-1, we can see that the coverage probability is similar to that in Fig. 4-1 but lower. This is because SFR increases the coverage probability by increasing the transmit power, which increases the interference of the whole networks, and strict FFR can remove the cross-tier interference effectively.

4.3 Open Access Coverage Probability Analysis

Due to the complexity of the open access case, we consider two tiers networks in the following analysis. Compared to three tiers, considering two tiers networks greatly reduces the complexity of the expressions, while our conclusion can be easily extended to unlimited number of tiers. Correspondingly we define the SIR of first and second tier users as $SIR_1 = \frac{P_1 h_{1x_1} x_1^{\alpha}}{I_1+I_2+P_2 g_{2y_2} x_2^{\alpha}}$, $SIR_2 = \frac{P_2 h_{2x_2} x_2^{\alpha}}{I_1+I_2+P_1 g_{1y_1} x_1^{\alpha}}$, respectively, where $I_1 = \sum_{y_1 \in Z_1/x_1} P_1 g_{1y_1} y_1^{-\alpha}$, $I_2 = \sum_{y_2 \in Z_2/x_2} P_2 g_{2y_2} y_2^{-\alpha}$. Because open access allows

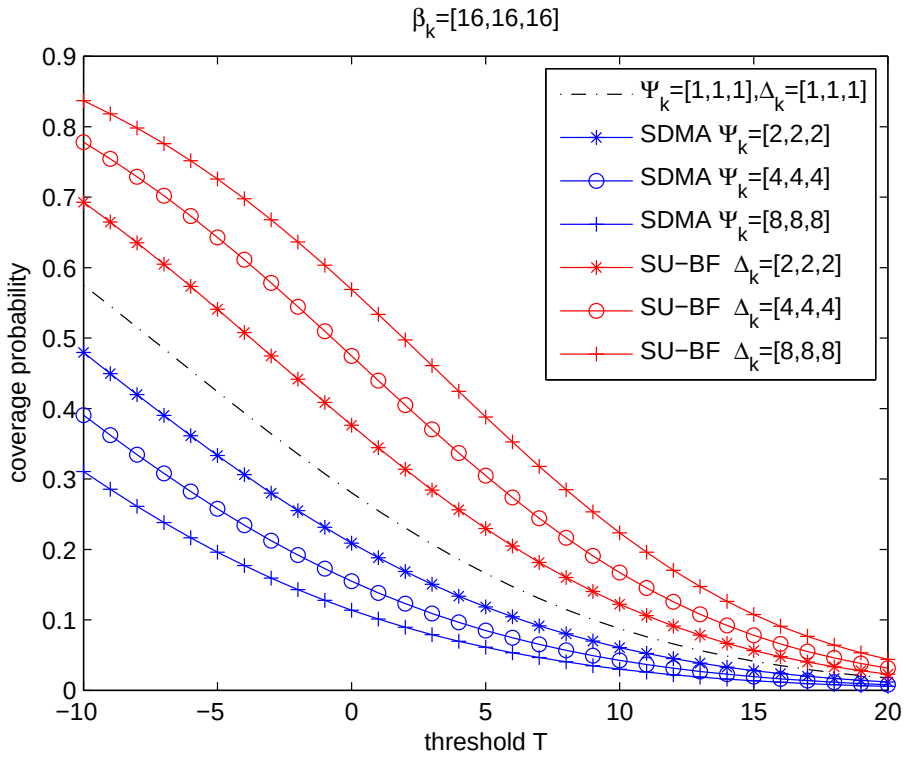

Figure 4-2: Downlink first tier cell-edge user coverage probability for SFR with closed access

users to access every tier, if there are more than one tier that can satisfy the SIR threshold, cell-interior users select the tier with the highest SIR to access. Therefore, the typical user is a cell-edge user just when its $SIR_1 < T_1$ and $SIR_2 < T_2$. The cell-edge user's coverage probability, which is conditioned on the SIR_1 and SIR_2, so the first tier cell-edge user's coverage probability will be a conditional probability, denoted as

$$\mathbb{P}(SIR_{edge} > T \,|\, SIR_1 < T_1, SIR_2 < T_2). \tag{4.7}$$

As we can see from (4.7), it is more complicated than that in the closed access case. It should be noted that although only coverage probability of the first tier cell-edge user is derived in theorems 4.3.1 and 4.3.2, the conclusion can be extended to that of the second tier cell-edge user. Furthermore, Denoting the coverage probability of the first and second tier cell-edge user as $\hat{P}_1$ and $\hat{P}_2$, respectively. Due to the independence between each tier, the two coverage probabilities are independent, too. Therefore,

according to the basic of probability theory, the cell-edge user's coverage probability under open access equals

$$1-(1-\hat{P}_1)(1-\hat{P}_2). \tag{4.8}$$

4.3.1 Coverage with Strict FFR

First we consider the strict FFR case. In this case, the cell-edge users will be allocated reserved subbands, thereby experience new fading power $\hat{g}_{1y_1}$ and only intra-tier interference thinned with D_1. (4.7) can be further expressed as

$$\mathbb{P}\Big(\frac{D_1 P_1 \hat{h}_{1x_1} x_1^{-\alpha}}{\hat{I}_1} > T \,\Big|\, SIR_1 < T_1, SIR_2 < T_2\Big) \tag{4.9}$$

and evaluate it, we can get

Theorem 4.3.1. *(strict FFR, open access, edge user, MIMO channel): The coverage probability of the first tier cell-edge user in the MIMO HetNets with the strict FFR and open access is* $P_{FFR,op} =$

$$\frac{\int_0^\infty\int_0^\infty \rho(1,\lambda)\,\rho(2,\lambda)\Big(\sum\limits_{i=0}^{\Delta_1-1}\frac{1}{i!}\Big[\Big(-\hat{s}'\Big)^i\frac{\delta^i}{\delta\Big(\hat{s}'\Big)^i}\,\mathrm{f}_3(\hat{s}',1)\Big]\Big)}{\int_0^\infty\int_0^\infty \rho(1,\lambda)\,\rho(2,\lambda)\,\mathrm{f}_{3\mathrm{d}}(s,s',s_2')\mathrm{d}x_1\mathrm{d}x_2} \cdot\Big(\mathrm{f}_{3\mathrm{d}}(s,s',s_2')\Big)\mathrm{d}x_1\mathrm{d}x_2 \tag{4.10}$$

where $s=\frac{T_1 x_1^\alpha}{P_1}$, $s'=\frac{x_1^\alpha}{P_1}$, $s_2'=\frac{P_2}{T_2}x_2^{-\alpha}$, $\hat{s}'=\frac{T x_1^\alpha}{P_1 D_1}$,

$$\mathrm{f}_3(x,k)=\exp\big(-x^{\frac{2}{\alpha}}\lambda_k P_k^{\frac{2}{\alpha}}\mathrm{C}\big(\alpha,\Psi_k\big)\big) \tag{4.11}$$

$$\begin{aligned}\mathrm{f}_{3\mathrm{d}}(s,s',s_2') = \; -\sum_{i=0}^{\Delta_1-1}\frac{1}{i!}\Bigg[\big(-s\big)^i\frac{\delta^i}{\delta\big(s\big)^i}\big(\mathrm{f}_3(s,1)\cdot\mathrm{f}_3(s,2)\\ \cdot\frac{1}{\big(1+sP_2x_2^{-\alpha}\big)^{\Delta_2}}\big)\Bigg]+\mathrm{f}_{3\mathrm{d}\_2}(s',s_2')\end{aligned} \tag{4.12}$$

where $n=\Delta_2-1$, *and*

$\mathrm{f}_{3\mathrm{d}\_2}(s', s_2') =$

$$\sum_{i=0}^{\Delta_1-1} \frac{1}{i!}\Bigg[(-s')^i \frac{\delta^i}{\delta(s')^i}\Bigg(1 + \frac{1}{\Gamma(\Delta_2)} \sum_{m=0}^{n} \frac{n!}{(n-m)!} \cdot (s_2')^{m-n} \left(\frac{1}{(1+s's_2')^{m+1}} - 1\right) \cdot (-1)^{n-m} \frac{\delta^{n-m}}{\delta(\frac{1}{s_2'})^{n-m}}\Big(\mathrm{f}_3(\tfrac{1}{s_2'}, 1)\ \mathrm{f}_3(\tfrac{1}{s_2'}, 2)\Big)\Bigg)\Bigg]. \tag{4.13}$$

Proof: see the appendix B.3

Comparing to the closed access case, the derivations are more complicated, and have double integrals. In fact, the number of tiers is the number of integrals. Nevertheless, it is expected that most practical deployments would not have more than about three tiers even in dense environments, which makes this analysis practical through the use of numerical evaluation of the integrals [30].

4.3.2 Coverage with SFR

Comparing to strict FFR, in the case of SFR, the transmit power will be increased to βP and the cell-edge users experience cross-tier interference. Taking these factors into account, and (4.7) can be further expressed as

$$\mathbb{P}\left(\frac{\beta_1 P_1 \hat{h}_{1x_1} x_1^{-\alpha}}{\eta_1 \hat{I}_1 + \eta_2 \hat{I}_2} > T \,\middle|\, SIR_1 < T_1, SIR_2 < T_2\right) \tag{4.14}$$

and evaluate above formula, we can conclude

Theorem 4.3.2. *(SFR, open access, edge user, MIMO channel): The coverage probability of the first tier cell-edge user in the MIMO HetNets with the SFR and open access is* $P_{SFR,op} =$

$$\frac{\int_0^\infty\int_0^\infty \rho(1,\lambda)\,\rho(2,\lambda)\big(\mathrm{f}_4(\hat{s})\big) \cdot \big(\mathrm{f}_{3\mathrm{d}}(s, s', s_2')\big)\mathrm{d}x_1\mathrm{d}x_2}{\int_0^\infty\int_0^\infty \rho(1,\lambda)\,\rho(2,\lambda)\,\mathrm{f}_{3\mathrm{d}}(s, s', s_2')\mathrm{d}x_1\mathrm{d}x_2} \tag{4.15}$$

where $\hat{s} = \frac{Tx_1^{\alpha}}{\beta_1 P_1}$, s, s' *and* s_2' *are the same as theorem 4.3.1,* $\mathrm{f}_4(\hat{s}) =$

$$\sum_{i=0}^{\Delta_1-1} \frac{1}{i!}\Big[\big(-\hat{s}\big)^i \frac{\delta^i}{\delta\big(\hat{s}\big)^i}\Big(\exp\big(-\hat{s}^{\frac{2}{\alpha}}\lambda_1\big(\eta_1 P_1\big)^{\frac{2}{\alpha}}\mathrm{C}\big(\alpha,\Psi_1\big)\big) \cdot \exp\big(-\hat{s}^{\frac{2}{\alpha}}\lambda_2\big(\eta_2 P_2\big)^{\frac{2}{\alpha}}\mathrm{C}\big(\alpha,\Psi_2\big)\big)\Big)\Big]. \tag{4.16}$$

Proof: see the appendix B.4

Since both SFR and strict FFR use the same method to partition cell-edge user, some parts of the theorem 4.3.2 result are the same as those of the theorem 4.3.1.

4.3.3 Numerical Results of Open Access

For open access case, we consider two tier interference-limited network and the related simulation parameters are the same as closed access. In this simulation, we first use the theorems 4.3.1 and 4.3.2 to calculate cell-edge user's coverage probability of each tier, and then according to (4.8), calculate the cell-edge user's under open access.

Fig. 4-3 shows cell-edge user's coverage probability with strict FFR. From the figure, we can see that the results are similar to that in the closed access. For full SDMA the probability decreases with the increase of the number of antennas M_k. This is because according to the fundamental theory of SDMA, increasing M_k means increasing the interference received by users, which results in the decrease of coverage probability. For SU-BF Δ_k can be seen as the number of transmit antennas, thus it is very easy to understand the average probability increases with the increase of Δ_k.

Fig. 4-4 shows the result of cell-edge user's coverage probability with SFR under open access. Under SFR, the coverage probability is also similar to that of strict FFR for the same reason of strict FFR. However, due to introducing the extra transmit power, which results in increasing the interference, the coverage probability is lower than that of strict FFR. It should be noted that although the coverage probability of the strict FFR is higher than that of the SFR, we can not say that strict FFR is better, because comparing them needs to take account that more frequency is available for

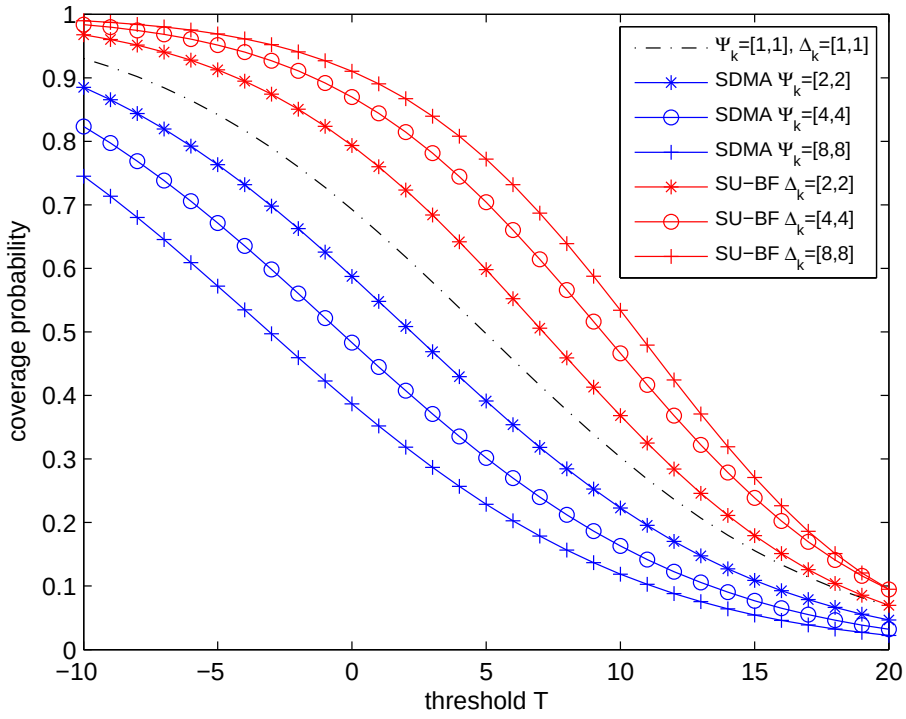

Figure 4-3: Downlink first tier cell-edge user coverage probability for open access with strict FFR

SFR since each BS fully utilizes the whole frequency.

It should be noted that since the users have more tiers to access, the coverage probabilities of open access is much higher than that of closed access, as shown if we compare Figs. 4-1 and 4-2 to Figs. 4-3 and 4-4.

4.4 System Design Implication

In this section we discuss the influence of main HetNets' parameters on the coverage probability of cell-edge user, and present several applications of the above conclusions, which illustrates how they can be used to help design MIMO HetNets utilizing FFR.

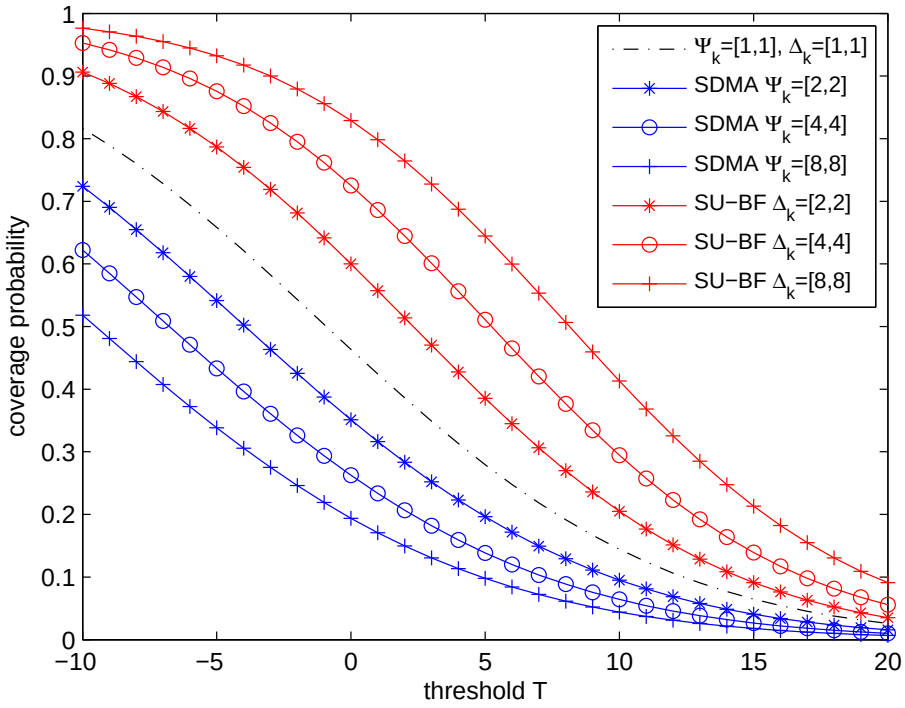

Figure 4-4: Downlink first tier cell-edge user coverage probability for open access with SFR

4.4.1 Average Cell-edge User Rate

In modern cellular networks, besides coverage probability, average rate is also very important metric and can be derived from the SIR statistics. As we know, [14] firstly illustrates how to use the above coverage probability results to derive the average rate expressions in one tier networks modeled by PPP. Although based on one tier networks, the method of [14] also applies to the K tiers networks modeled by PPP.

The average rate of the typical user is $\bar{\tau} = \mathbb{E}[\ln(1 + \mathrm{SIR})]$, which normalizes bandwidth and is given in terms of nats/Hz. The expectation is taken over both SIR, which including PPP, fading distribution and whole logarithm term. Since x_k follows the exponentail distribution, as we mentioned in Section 4.1.1, the expectation for the PPP can be easily evaluated by the definition of expectation. Using the fact that $\tau = \ln(1 + \mathrm{SIR})$ is a positive random variable, $\mathbb{E}[\tau] = \int_{t>0} P(\tau > t)\mathrm{d}t$, and considering the SIR of cell-edge user is conditional just as theorem 4.2.1-4.3.2, thus

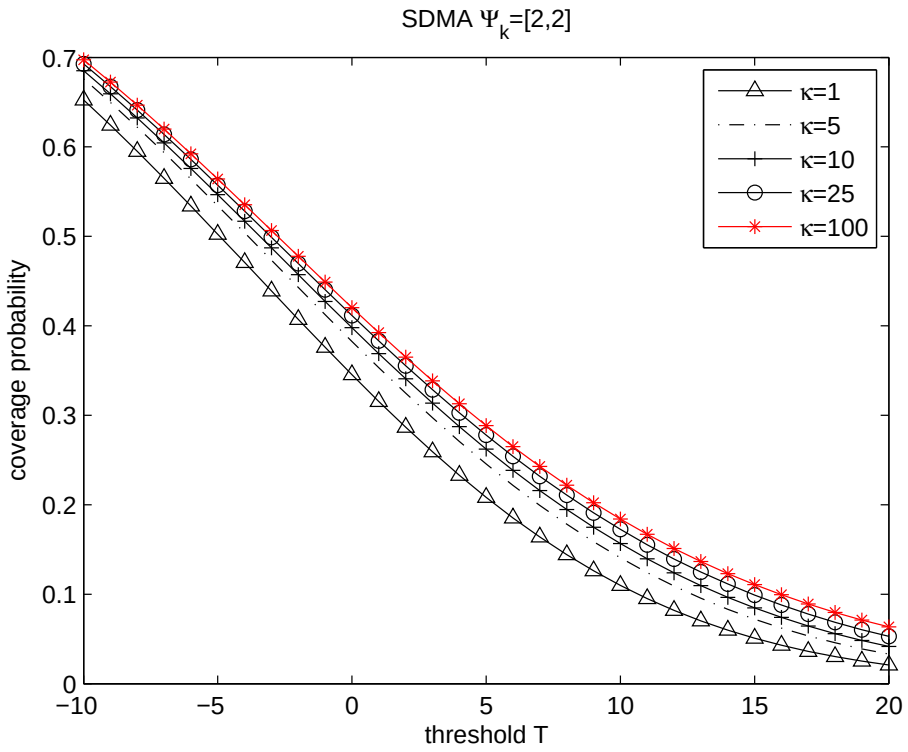

Figure 4-5: Downlink coverage probability of first tier cell-edge user for strict FFR with closed access as a function of the tier density ratio κ

we have $\bar{\tau} = \mathbb{E}[\ln(1 + \mathrm{SIR})] =$

$$\int_0^\infty \int_0^\infty \rho(k,\lambda)\mathbb{P}\Big[\ln(1+SIR_{edge}) > t \,|\, SIR_k < T_k)\Big]\mathrm{d}x_k\mathrm{d}t$$
$$= \int_0^\infty \int_0^\infty \rho(k,\lambda)\mathbb{P}\Big[SIR_{edge} > e^t - 1 \,|\, SIR_k < T_k)\Big]\mathrm{d}x_k\mathrm{d}t. \tag{4.17}$$

where $\rho(k,\lambda)$ is given in (4.3). As we can see from the above expression, the average rate of cell-edge user can be evaluated by substituting $e^t - 1$ for the threshold T of the results of the theorem 4.2.1-4.3.2 and computing additional integrals.

4.4.2 BSs' Density

Now we discuss the effects of the density of BSs on the coverage probability. We assume a two tiers SDMA HetNets, and focus on first tier cell-edge users. For the sake of convenience, we define $\kappa = \lambda_2/\lambda_1$, and change κ only by changing λ_2.

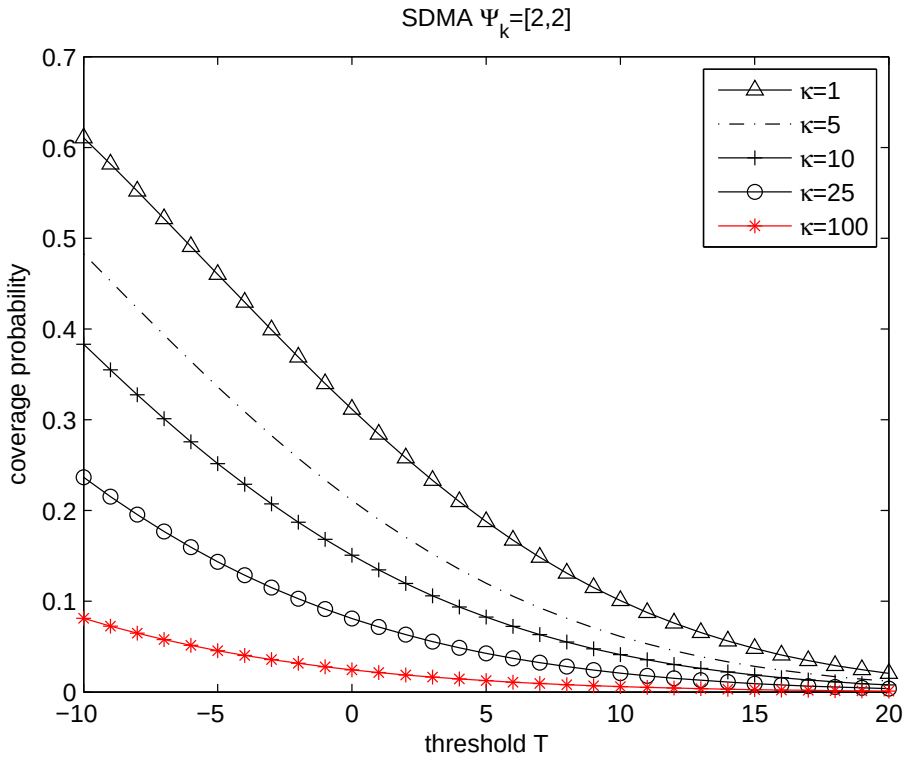

Figure 4-6: Downlink coverage probability of first tier cell-edge user for SFR with closed access as a function of the tier density ratio κ

Fig. 4-5 and Fig. 4-6 show the relationship between the coverage probability of first cell-edge users and κ under both strict FFR and SFR case, respectively. Fig. 4-5 shows that increasing λ_2 increases the coverage probability of first tier cell-edge users. This is because as the interference caused by increasing λ_2 increase, considering the closed access constraint, more and more first tier users become cell-edge users, and under strict FFR, reserved subbands are allocated to cell-edge users, which can greatly reduce interference, thus increase the coverage probability. It should be noted that, as the the number of cell-edge users increase, larger reserved subbands will be needed, which decreases the overall sum rate, due to the reduction of frequency reuse efficiency. Under SFR, we can see from Fig. 4-6, the results are contrary to those of strict FFR. This is because SFR does not reduce the interference of cell-edge users, thus the increase of interference directly impacts on the first cell-edge users, thereby decreases their coverage probability.

For open access, we can get very similar results to that of closed access under both strict FFR and SFR. However it should be noted that the results of open access just reflect the coverage probability of first tier rather than all tiers. Since open access allows users to access to any tier, we need to do further work about it in future.

4.4.3 Closed Access FFR Thresholds

For thresholds under closed access, from the expressions of theorem 4.2.1 and 4.2.2, we can know the coverage probability only depends on the threshold of the tier the cell-edge users access to. Fig. 4-7 shows the effects of T_1 on the coverage probability of first cell-edge users under both strict FFR and SFR, here we also assume a two tiers SDMA HetNets. As T_1 increases we see in Fig. 4-7, the coverage probability increases for both strict FFR and SFR. The reason is that increasing T_1 makes more and more users become cell-edge users, thereby increases the coverage probability.

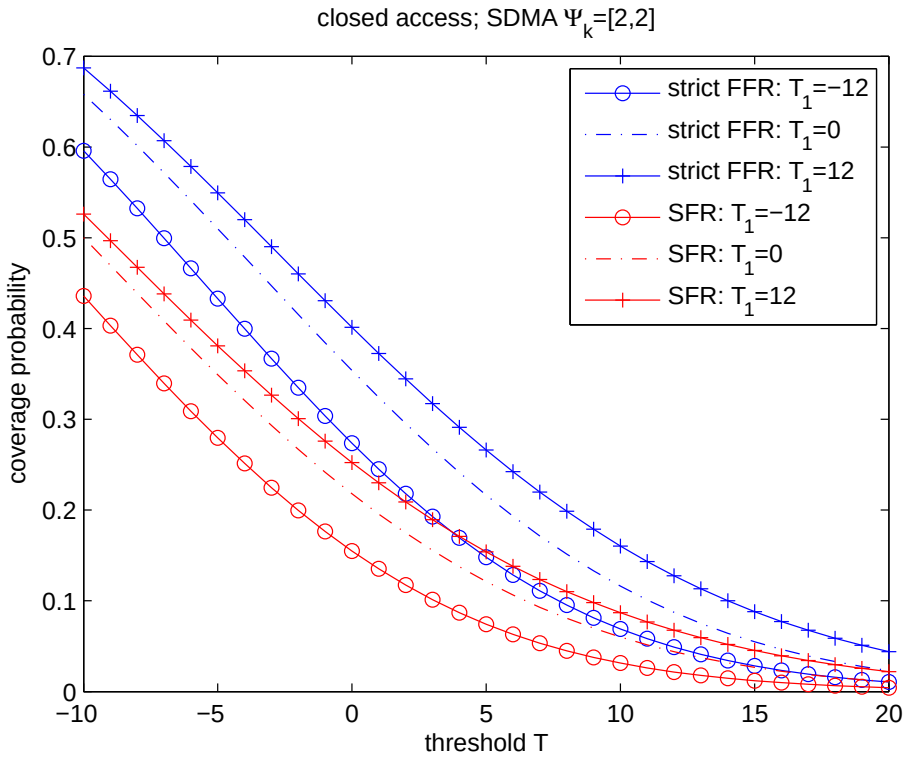

Figure 4-7: Downlink coverage probability of first tier cell-edge user for closed access as a function of T_1

4.4.4 Power Increase Factor β

Fig. 4-8 and Fig. 4-9 show the relationship between β_k and the coverage probability under closed and open access, respectively. For both access cases, from the figures we can see that increasing β_k can increase the coverage probability. The bigger β_k is, the higher the probability is, however it should be noted that the improvement of coverage probability becomes smaller and smaller, and the coverage probability approaches a limited value rather than 1, even in the case of $\beta_k = \infty$.

4.5 Conclusion

We use PPP to model the locations of BSs, and proposes a framework to analyze the downlink coverage probability of the MIMO HetNets utilizing the FFR technique. We give a tractable expression of the typical user coverage probability under both

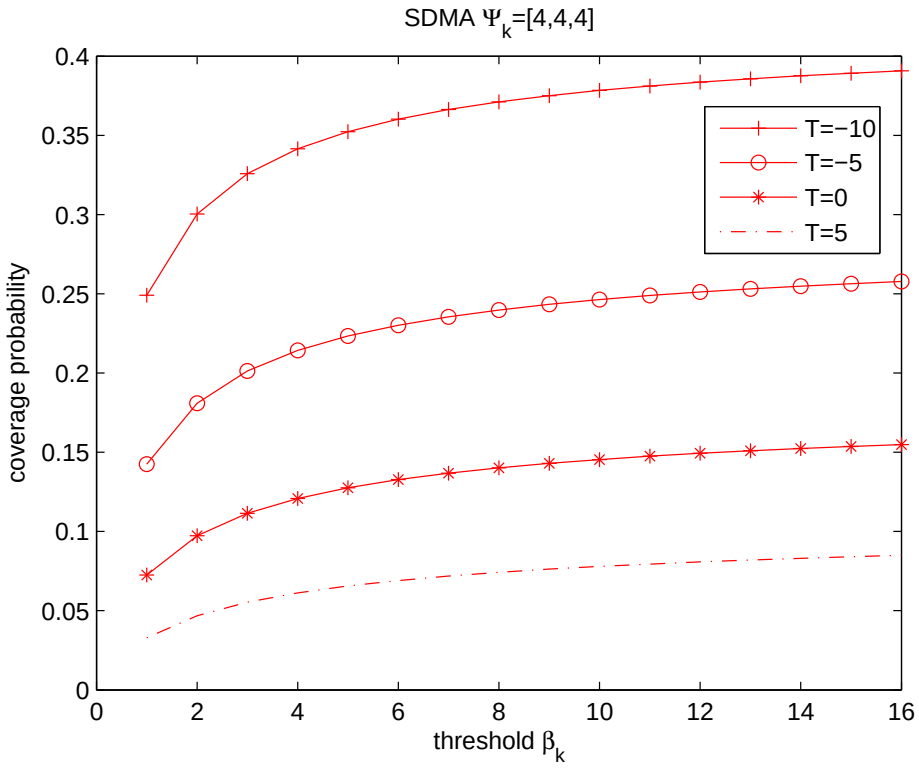

Figure 4-8: Relation between β_k and the coverage probability of the first tier cell-edge user for SFR with closed access

closed and open access cases, which can be easily extended to develop average cell-edge user rate expressions. We show the numerical results of different FFR and access cases under the full SDMA and SU-BF, and discuss the effects of main parameters on the coverage probability. We also illustrate how to use the coverage probability results to derive the average rate expressions. These analyses can assist system designers in designing networks, and evaluating new algorithm related to MIMO HetNets. It should be noted that this analysis is for downlink networks, without mentioning uplink case. Considering the importance of uplink case, we will analyze it in our future work.

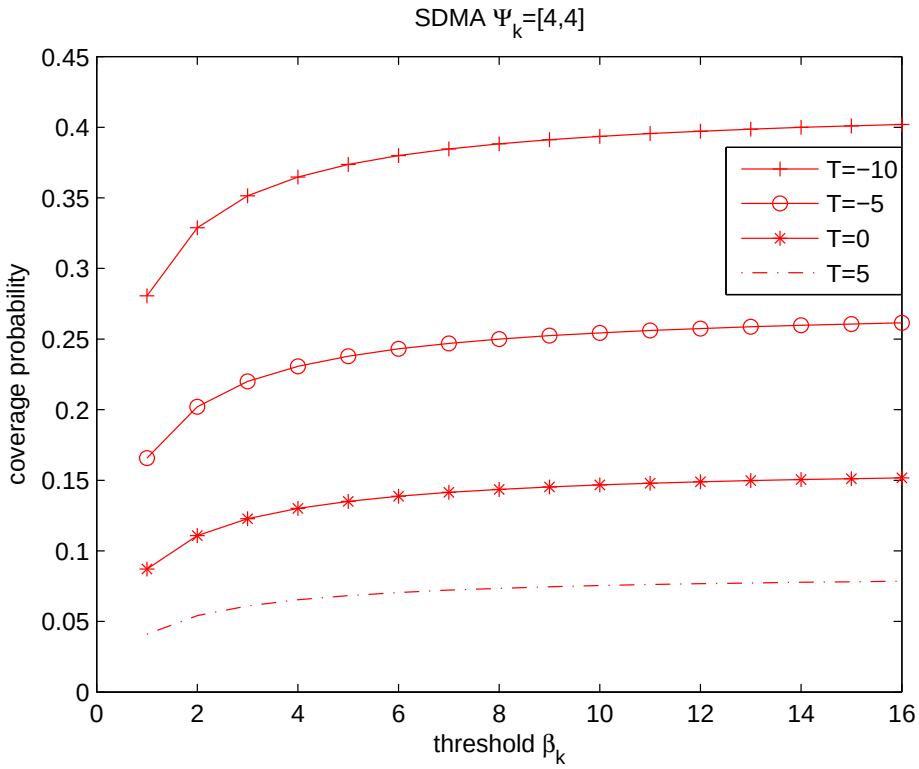

Figure 4-9: Relation between β_k and the coverage probability of the first tier cell-edge user for SFR with open access

Chapter 5

A Probabilistic Approach for Using Poisson Point Process to Model one tier Cellular Networks

Chapters 3 and 4 analyzes cellular networks based on PGFL, (introduced in Section 2.1.1). Although using the PGFL can derive tractable analysis results, the main drawback of PGFL is only valid to Rayleigh channel. Due to the drawback, the channel of PPP model restricts to fast fading, which greatly limits the application of the PPP model. In chapter, utilizing the conclusion of deterministic model, we develop a probabilistic approach of analyzing cellular networks based on PPP, which successfully breaks through the channel limitation, maintains the generality of the PPP model. Considering path loss, shadow, and fast fading impact, we derive the expressions of coverage probability at a given distance of the serving BS. The expressions can be calculated easier than the expression derived by the traditional method, and even get the closed form expression considering the path loss and fast fading channel. The simulations show that the expressions accords with that of the deterministic model and form the lower and upper bounds of the coverage probability.

5.1 System model

5.1.1 Cellular Networks Model

We focus on the downlink cellular networks and consider the path loss, shadowing, and fast fading effects. As Fig. 5-1 shows, we assume that the cellular network covers a circle area with the radius R. We use PPP Φ with intensity β to model the BSs' locations within the area. Let r_0 and r_i denote the distance between the user and the closest BS, and that between the user and the i_{th} BS, respectively. Without loss of generality, the analysis is conducted on a typical user located at the center, who is only served by the closest BS. Fig 5-2 shows the traditional hexagonal model of a cellular network, where A and a denote the side length of the hexagon that represents the entire network area and that of the hexagon of each cell, respectively. Compared to Fig 5-1, the difference between the hexagonal model and the proposed model are shown explicitly. The further parameters relationships between the two models will be addressed in Section 5.3.

5.1.2 SIR Calculation

By considering path loss, shadowing, and fast fading effects, the signal power received by the typical user is denoted as:

$$S = P_0 r_0 X_0 Y_0, \tag{5.1}$$

where P_0 denotes the transmit power of serving BS, X_0, Y_0 represent the fast fading and shadowing impact of direct link, respectively.

The interference power received by the typical user can be written as:

$$I = \sum_{i=1}^{n-1} P_i r_i X_i Y_i, \tag{5.2}$$

where P_i denotes the transmit power of the i_{th} interferer, X_i, Y_i represent the fast fading and shadowing impacts of i_{th} interference link, respectively. n and $n-1$ denote

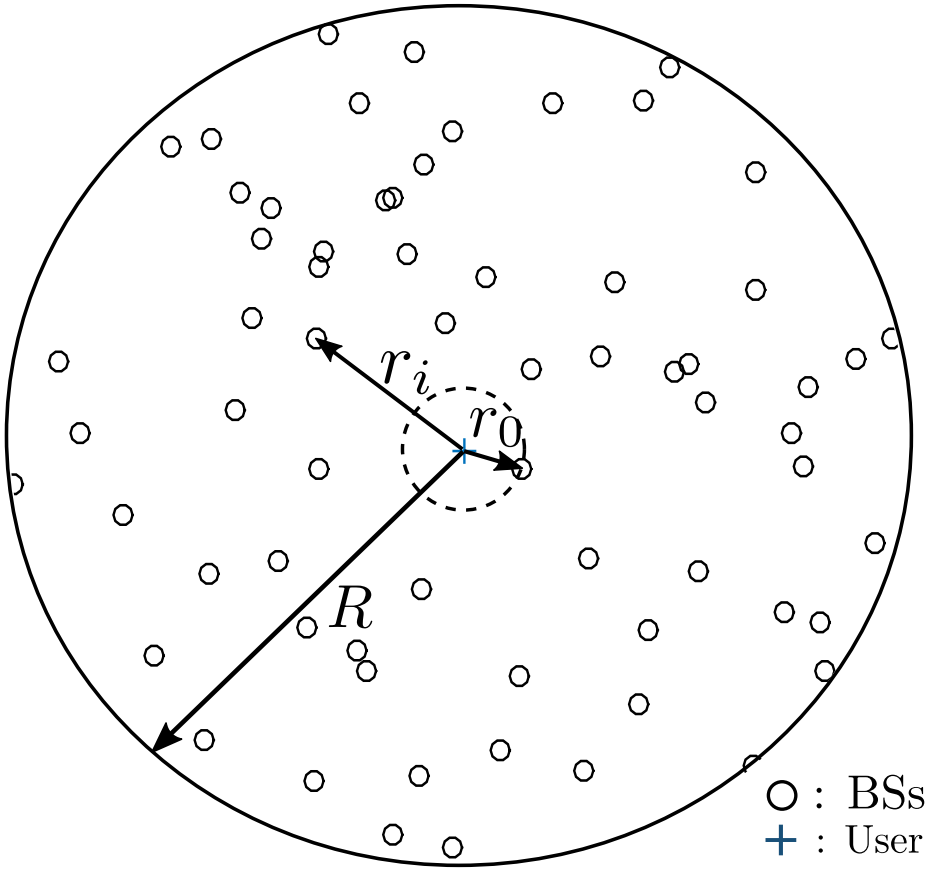

Figure 5-1: A typical realization of the proposed approach for distribution of base stations

the number of BSs and interference BSs, respectively.

Here both X_0 and X_i are random variables (RV) representing the Rayleigh fading effects, whose PDF is $P_X(x) = e^{-x}$. X_i and Y_i are lognormal RVs characterizing shadowing with zero mean and standard deviation σ [70].

Then, the SIR can now be obtained:

$$SIR = \frac{S}{I}. \tag{5.3}$$

5.2 Coverage probability

Here, we define the coverage probability as the probability that the SIR received is greater than a given threshold T, which is given as $\mathbb{P}(SIR > T)$.

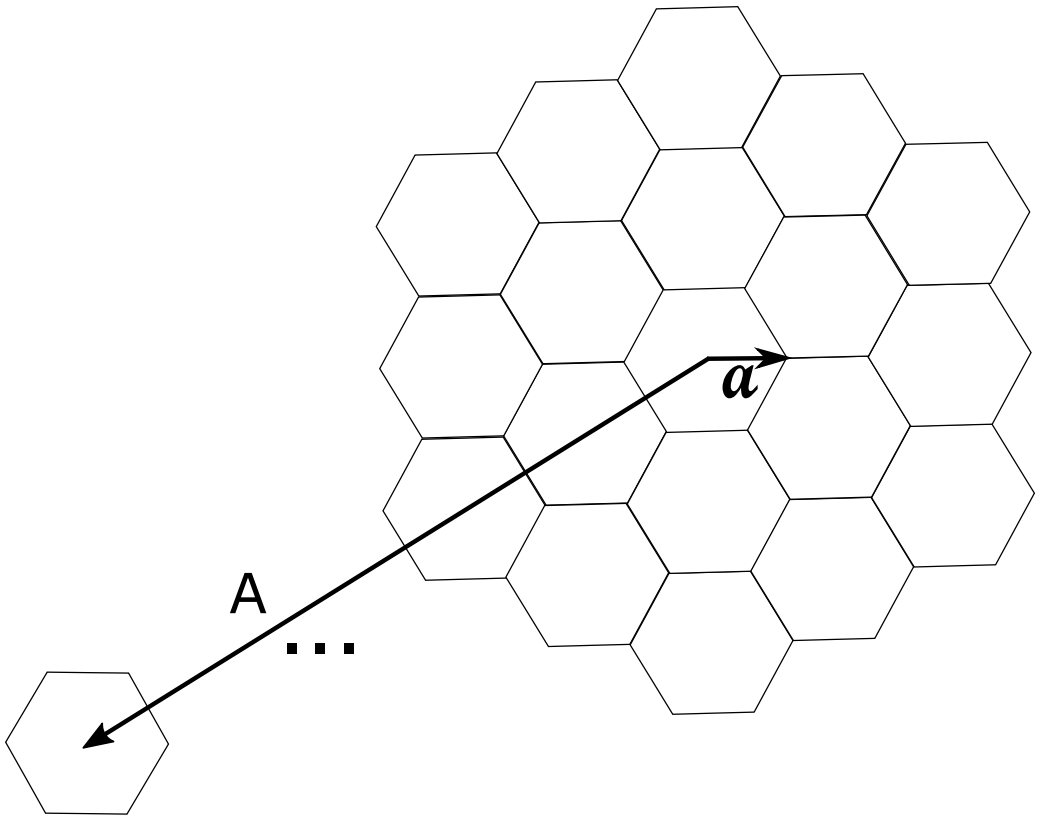

Figure 5-2: Hexagonal network and main parameters

5.2.1 Path Loss and Fast Fading Impact

Assuming interferers transmit data with same power $P_i = P_c$, and considering path loss and fast fading impact, the SIR is given by:

$$SIR = \frac{P_0 r_0^{-\eta} X_0}{\sum_{i=1}^{n-1} P_c r_i^{-\eta} X_i} = \frac{S}{I}, \tag{5.4}$$

where S and I are two independent RVs. The PDF of the signal power S is given by [71]:

$$f_S(x) = \frac{1}{r_0^{-\eta}} e^{\frac{x}{r_0^{-\eta}}}. \tag{5.5}$$

The authors of [70] approximate the interference PDF using the central limit theorem for causal functions [10] by a Gamma distribution. The PDF of I is given

by (for details, please refer to [70]):

$$f_I(x) = \frac{y^{\nu-1}}{\Gamma(\nu)\lambda^{\nu}} e^{\frac{y}{\lambda}}, \tag{5.6}$$

where $\nu = \frac{\mathbb{E}[I]^2}{\mathrm{var}(I)}$ and $\lambda = \frac{\mathrm{var}(I)}{\mathbb{E}[I]}$, $var(\cdot)$ denotes variance. Since $\mathbb{E}[X_i] = 1$ and $\mathrm{var}(X_i) = 1$, then the mean and the variance of I is given by:

$$\mathbb{E}[I] = \sum_{i=1}^{n-1} P_c r_i^{-\eta} \mathbb{E}[X_i] = \sum_{i=1}^{n-1} P_c r_i^{-\eta} \tag{5.7}$$

and

$$\mathrm{var}(I) = \sum_{i=1}^{n-1} P_c^2 r_i^{-\eta} \mathrm{var}(X_i) = \sum_{i=1}^{n-1} P_c^2 r_i^{-\eta}. \tag{5.8}$$

Then ν and λ are expressed as:

$$\nu = \frac{\left(\sum_{i=1}^{n-1} r_i^{-\eta}\right)^2}{\sum_{i=1}^{n-1} r_i^{-2\eta}} \tag{5.9}$$

and

$$\lambda = P_C \frac{\sum_{i=1}^{n-1} r_i^{-2\eta}}{\sum_{i=1}^{n-1} r_i^{-\eta}}. \tag{5.10}$$

Finally, the coverage probability can be derived as:

$$\begin{aligned} \mathbb{P}(SIR > T) &= \int_0^{\infty} \mathbb{P}(S > IT | I = y) f_I(y) d_y \\ &= \frac{1}{\left(\frac{\lambda T}{r_0^{-\eta} P_0} + 1\right)^{\nu}}. \end{aligned} \tag{5.11}$$

Since ν and λ are the functions of the distances from BSs to the typical user, and there are no restrictions to the distribution followed by BSs, the formula (5.11) based on the deterministic model is also applicable to the PPP model. Then the problem is how to calculate ν and λ under the PPP model. Assuming that the cellular networks

are deployed in a circle area with the radius R, according to the properties of PPP, we can derive the PDF of the distances r from BSs to the user at origin as:

$$f_r(r) = \frac{2r}{R^2}. \tag{5.12}$$

Referring to [72], the probability that r is greater than r_0 is:

$$\mathbb{P}(r > r_0) = e^{-\beta\pi r_0^2}. \tag{5.13}$$

Considering the distance from the serving BS r_0, the PDF of the distances from the interferers r_i can be written as:

$$\mathbb{P}(r_i | r > r_0) = \frac{\mathbb{P}(r_i, r > r_0)}{\mathbb{P}(r > r_0)} = \frac{2r_i e^{\beta\pi r_0^2}}{R^2 - r_0^2}. \tag{5.14}$$

Now we go back to the numerator of (5.9). Let $\sum_{i=1}^{n-1} r_i^{-\eta} = \sum_{i=1}^{n-1} x_i = \hat{X}$, where $x_i = r_i^{-\eta}\ \forall i = \{1, 2, \cdots, n-1\}$ is a sequence of independent and identically distributed (i.i.d.) random variables drawn from distributions of expected values and finite variances. Then $\hat{X}$ meets the central limit theorem, which means when $n \to \infty$

$$\frac{\hat{X} - (n-1)\mu_x}{\sqrt{(n-1)}\sigma_x} \backsim \Phi(0, 1), \tag{5.15}$$

where $\Phi(0, 1)$ denotes the normal distribution with mean 0 and variance 1. Then the expectation $\mu_{\hat{X}}$ and variance $\sigma_{\hat{X}}^2$ of $\hat{X}$ can be written as:

$$\mu_{\hat{X}} = (n-1)\mu_{x_i}, \tag{5.16}$$

and

$$\sigma_{\hat{X}}^2 = (n-1)\sigma_{x_i}^2. \tag{5.17}$$

According to the definition of variance, the expectation of $\hat{X}^2$.

$$\mathbb{E}[\hat{X}^2] = \mu_{\hat{X}^2} = \sigma^2_{\hat{X}} + \mu^2_{\hat{X}} = (n-1)\sigma^2_{x_i} + (n-1)^2\mu^2_{x_i}. \tag{5.18}$$

Now going back to the denominator of (5.9), similarly, assuming $\sum_{i=1}^{n-1} r_i^{-2\eta} = \sum_{i=1}^{n-1} y_i = \hat{Y}$ when $n \to \infty$

$$\frac{\hat{Y} - (n-1)\mu_{y_i}}{\sqrt{(n-1)}\sigma_{y_i}} \backsim \Phi(0,1), \tag{5.19}$$

then $\mathbb{E}[\hat{Y}] = \mu_{\hat{Y}} = (n-1)\mu_{y_i}$.

Conditioned on n, the numerator $\mu_{\hat{X}^2}$ and the denominator $\mu_{\hat{X}}$ of (5.9) are independent. Plug $\mu_{\hat{X}^2}$ and $\mu_{\hat{Y}}$ back to (5.9), then:

$$\mathbb{E}_\nu[\nu|n] = \frac{(n-1)\sigma^2_{x_i} + (n-1)^2\mu^2_{x_i}}{(n-1)\mu_{y_i}} = \frac{\sigma^2_{x_i} + (n-1)\mu^2_{x_i}}{\mu_{y_i}}. \tag{5.20}$$

According to the definition of PPP, where n follows a Poission distribution, which PDF is

$$\mathbb{P}(n) = f(n;\beta) = \frac{\beta^n e^{-\beta}}{n!}. \tag{5.21}$$

Then (5.9) equals

$$\begin{aligned}
\mathbb{E}_\nu[\nu] =& \sum_{n=0}^{\infty} \mathbb{E}_\nu[(\nu|n)]\mathbb{P}(n) = \sum_{n=0}^{\infty} \frac{\sigma_{x_i}^2 + (n-1)\mu_{x_i}^2}{\mu_{y_i}} \frac{\beta^n e^{-\beta}}{n!} \\
=& \frac{\sigma_{x_i}^2}{\mu_y} \sum_{n=0}^{\infty} \frac{\beta^n e^{-\beta}}{n!} - \frac{\mu_{x_i}^2}{\mu_{y_i}} \sum_{n=0}^{\infty} \frac{\beta^n e^{-\beta}}{n!} \\
&+ \frac{\mu_{x_i}^2}{\mu_{y_i}} \sum_{n=0}^{\infty} n \frac{\beta^n e^{-\beta}}{n!} \\
=& \frac{\sigma_{x_i}^2}{\mu_{y_i}} \beta - \frac{\mu_{x_i}^2}{\mu_{y_i}} \beta + \frac{\mu_{x_i}^2}{\mu_{y_i}} \sum_{n=1}^{\infty} n \frac{\beta^n e^{-\beta}}{n!} \\
=& \frac{\sigma_{x_i}^2}{\mu_{y_i}} \beta - \frac{\mu_{x_i}^2}{\mu_{y_i}} \beta + \frac{\mu_{x_i}^2 \beta}{\mu_{y_i}} \sum_{n=1}^{\infty} \frac{\beta^{(n-1)} e^{-\beta}}{(n-1)!} \\
=& \frac{\sigma_{x_i}^2}{\mu_{y_i}} \beta - \frac{\mu_{x_i}^2}{\mu_{y_i}} \beta + \frac{\mu_{x_i}^2 \beta}{\mu_{y_i}} \sum_{n=0}^{\infty} \frac{\beta^n e^{-\beta}}{n!} \\
=& \frac{\sigma_{x_i}^2}{\mu_{y_i}} \beta - \frac{\mu_{x_i}^2}{\mu_{y_i}} \beta + \frac{\mu_{x_i}^2}{\mu_{y_i}} \beta^2 \\
=& \frac{\mu_{x_i^2}}{\mu_{y_i}} \beta + \frac{\mu_{x_i}^2}{\mu_{y_i}} (\beta^2 - 2\beta).
\end{aligned} \tag{5.22}$$

The expectation of (5.10) can be similarly and more easily derived as:

$$\mathbb{E}[\lambda] = \frac{(n-1)\mu_{y_i}}{(n-1)\mu_{x_i}} = \frac{\mu_{y_i}}{\mu_{x_i}}. \tag{5.23}$$

Since $x_i = r_i^{-\eta}$ and $y_i = r_i^{-2\eta}$, based on the PDF of r_i (5.14), the PDFs of x_i and y_i can be derived as:

$$f(x_i|r > r_0) = \frac{2e^{\beta\pi r_0^2}}{\eta(R^2 - r_0^2)} x_i^{\frac{-2-\eta}{\eta}}, \tag{5.24}$$

$$f(y_i|r > r_0) = \frac{e^{\beta\pi r_0^2}}{\eta(R^2 - r_0^2)} y_i^{\frac{-1-\eta}{\eta}}. \tag{5.25}$$

Therefore,

$$\mu_{x_i} = \int_{R^{-\eta}}^{r_0^{-\eta}} x_i f(x_i|r > r_0) d_{x_i}$$
$$= \frac{2e^{\beta\pi r_0^2}}{(R^2 - r_0^2)(\eta - 2)} \Big(r_0^{2-\eta} - R^{2-\eta} \Big), \tag{5.26}$$

$$\mu_{y_i} = \int_{R^{-2\eta}}^{r_0^{-2\eta}} y_i f(y_i|r > r_0) d_{y_i}$$
$$= \frac{e^{\beta\pi r_0^2}}{(R^2 - r_0^2)(\eta - 1)} \Big(r_0^{2-2\eta} - R^{2-2\eta} \Big), \tag{5.27}$$

$$\mu_{x_i^2} = \int_{R^{-\eta}}^{r_0^{-\eta}} x_i^2 f(x_i|r > r_0) d_{x_i}$$
$$= \frac{e^{\beta\pi r_0^2}}{(R^2 - r_0^2)(\eta - 1)} \Big(r_0^{2-2\eta} - R^{2-2\eta} \Big). \tag{5.28}$$

Plugging μ_x, μ_y, and μ_{x^2} back in (5.22) and (5.23), we can get the values of ν and λ. Finally, plugging ν and λ back to (5.11), then we can get the coverage probability.

5.2.2 Path Loss, Shadowing and Fast Fading Impact

Assuming that interferers transmit data with the same power $P_i = P_c$, and considering the path loss, shadowing, and fast fading channel, we can write S and I in the expression $SIR = S/I$, as follows:

$$S = P_0 r_0^{-\eta} X_0 Y_0, \;\; I = \sum_{i=1}^{n-1} P_i r_i^{-\eta} X_i Y_i. \tag{5.29}$$

For readers' convenience, referring to [70], we briefly introduce the process of derivation again. Approximating the interference PDF using the central limit theorem for causal functions, we need to compute $\nu = \frac{\mathbb{E}[I]^2}{\mathrm{var}(I)}$ and $\lambda = \frac{\mathrm{var}(I)}{\mathbb{E}[I]}$. Since X_i and Y_i are independent, and recall that Y_i follows a log-normal distribution with logarithmic

mean 0 and standard deviation σ. Then

$$\mathbb{E}[I] = \sum_{i=1}^{n-1} P_c r_i^{-\eta} \mathbb{E}[X_i]\mathbb{E}[Y_i] = e^{\frac{\sigma^2}{2}} \sum_{i=1}^{n-1} P_c r_i^{-\eta} \tag{5.30}$$

and

$$\begin{aligned} \mathrm{var}(I) &= \sum_{i=1}^{n-1} P_c^2 r_i^{-\eta} \Big(\mathbb{E}[X_i^2]\mathbb{E}[Y_i^2] - \mathbb{E}[X_i]^2 \mathbb{E}[Y_i]^2 \Big). \\ &= \Big(2e^{2\sigma^2} - e^{\sigma^2} \Big) \sum_{i=1}^{n-1} P_c^2 r_i^{-\eta}. \end{aligned} \tag{5.31}$$

Now, ν_s and λ_s can be calculated as:

$$\nu_s = \frac{1}{2e^{\sigma^2} - 1} \nu,$$

and

$$\lambda_s = e^{\frac{\sigma^2}{2}} \Big(2e^{\sigma^2} - 1 \Big) \lambda.$$

Finally, the average coverage probability can be derived as [70]:

$$\begin{aligned} \mathbb{P}(SIR > T) &= \int P(S > IT | Y_0) f_Y(y) d_y \\ &= \int P\Big(r_0^{-\eta} X_0 > \frac{IT}{y} \Big) f_Y(y) d_y \\ &= \int_0^{\infty} \frac{1}{\Big(\frac{P_c \lambda_s T}{P_0 r_0^{-\eta} x} + 1 \Big)^{\nu_s}} \frac{1}{x\sigma\sqrt{2\pi}} \exp\Big(- \frac{\ln(x)^2}{2\sigma^2} \Big) d_x. \end{aligned} \tag{5.32}$$

5.3 Simulation

In this section we simulate the coverage probabilities of the proposed model, considering both the channel scenarios mentioned, and compare with that of the hexagonal model. The parameters are as: the intensity of PPP $\beta = 2$, the radius of area $R = 15$ km, path loss exponent $\eta = 3$, $P_c = 10$ dB, for the shadow channel $\sigma = 3$. Correspondingly the side length of the hexagon of networks area and the side lengh of the hexagon of each cellular can be calculated as $A = \sqrt{\frac{\pi}{2.6}} R$, $a = (2.6 * \beta)^{\frac{1}{2}}$,

respectively.

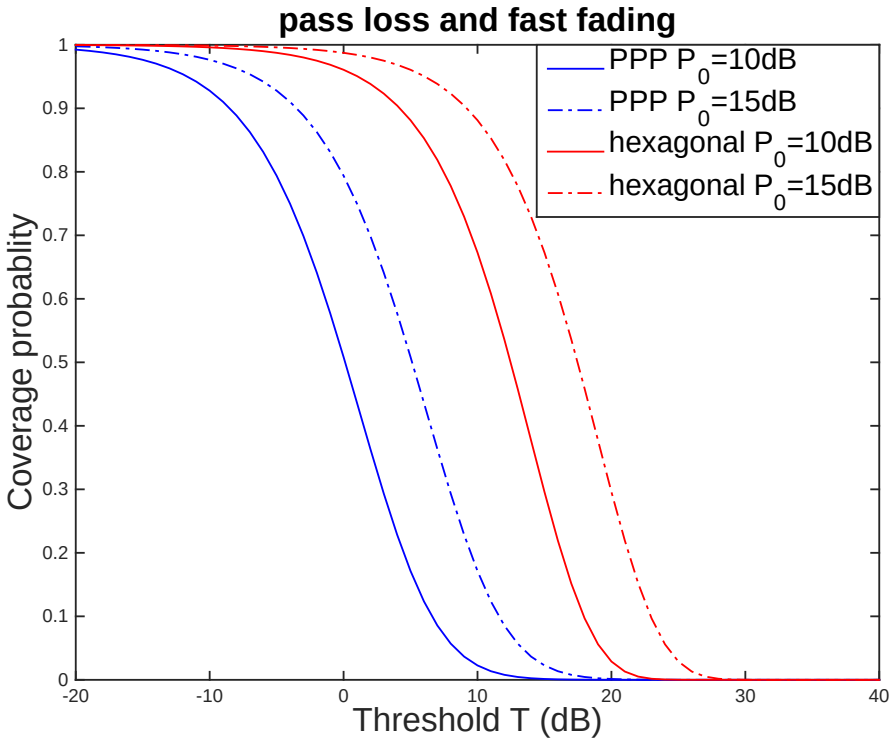

Figure 5-3: The coverage probability with path loss and fast fading impact

The simulation result of considering path loss and fast fading impact is shown in Fig. 5-3. From the figure, the shape of the coverage probability of the PPP model accords with that of the hexagonal model. As the increase of threshold, the coverages of both model decrease to 0. Theoretically, the coverage probabilities of the PPP model and the hexagonal model are the lower and upper bounds of the practical coverage probability. Here the impact of serving BS's transmit power also appears in the figure. Obviously, a higher serving BS transmitting power increase the coverage probability as expected.

The simulation result of considering the path loss, shadowing, and fast fading impact is shown in Fig. 5-4, which demonstrates the similar conclusion as that of considering path loss and fast fading impact. As the increase of the threshold, the coverage probabilities of both the models decrease to 0, too. The higher transmit power surely results in the higher coverage probability. In Fig. 5-5, we show what

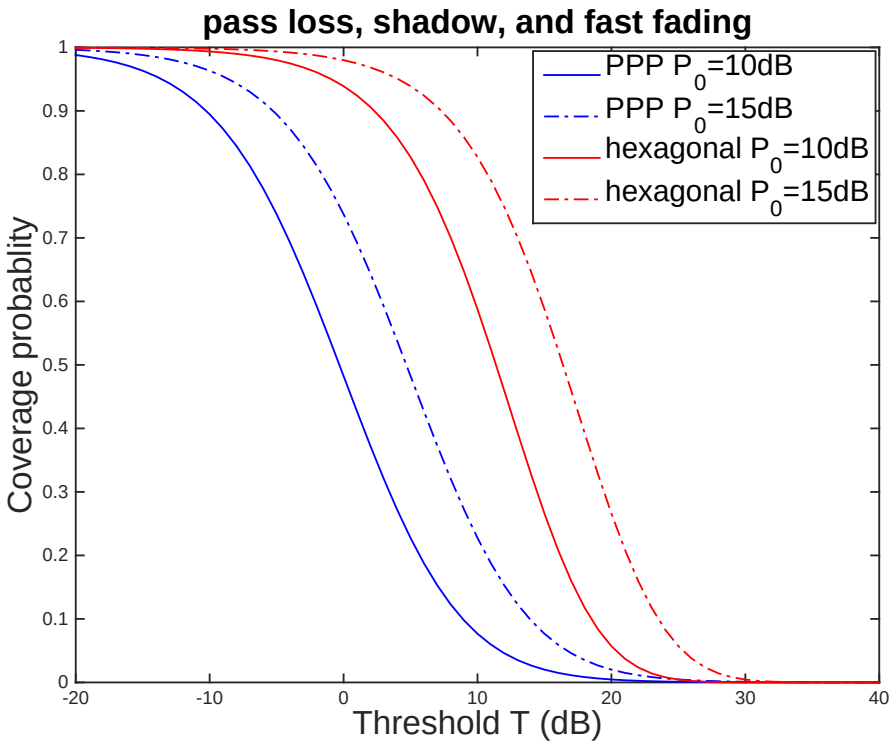

Figure 5-4: The coverage probability with path loss, shadow and fast fading impact

impact the standard derivation σ has on the coverage probability of both the PPP and hexagonal models. We can see from the figure, the coverage probability of low $\sigma = 3$ fits well with that of hexagonal model. For $\sigma = 5$, compared to the hexagonal model, the coverage probability is not quite accurate for the high threshold region, but remains accurate for the low threshold region. This is because both the derivation of [70] and this paper use the central limit theorem for approximations. Therefore, it is clear that the highest is σ, the highest is the error induced by the approximations.

5.4 Conclusion

We have proposed a novel way of analyzing cellular networks based on Poisson point process, and derive simple formulas of the coverage probabilities, while considering path loss, shadowing and fast fading impacts. Traditional analyses are based on PGFL of PPP, which restrict the channel to fast fading. The new approach is based on basic theory of probability and statistics, does not rely on PGFL, therefore,

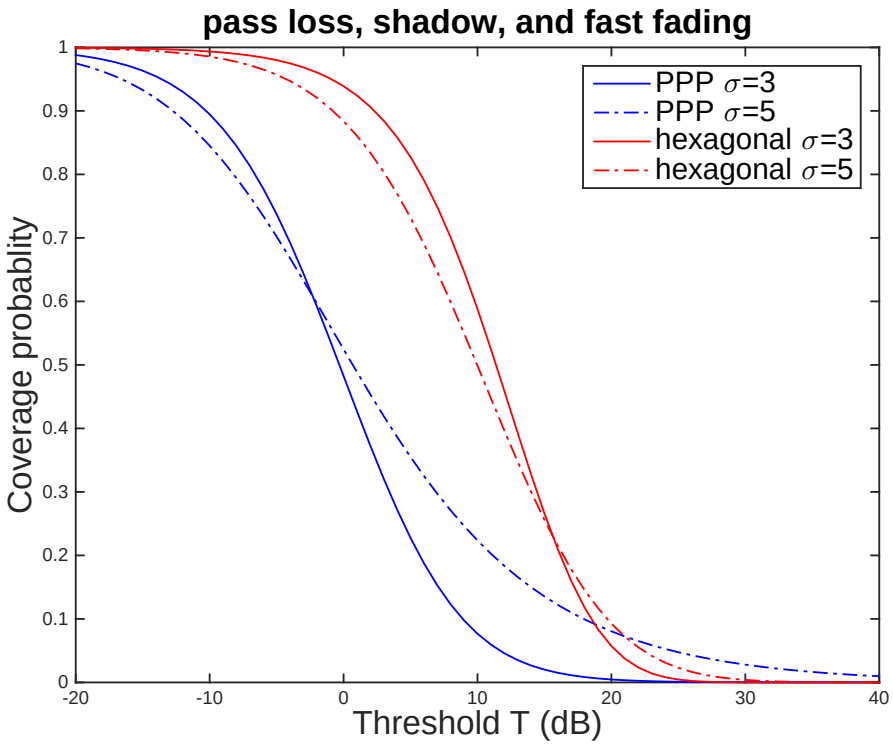

Figure 5-5: The impact of σ

it releases the restriction of channel. The expressions of the coverage probability in [70] are the function of only the distances from BSs, and the distances do not restrict to a special distribution. Therefore, the main idea of this paper is that using PPP to model the BSs' locations and substitute some expression depending on the distances with statistical values. Assuming that the network area is a circle, we derive the PDF of the distances from the BSs to the user. Based on this PDF, and combining the conclusions of deterministic model of cellular networks, the average value of the expressions depending on the distances can be calculated, then the expressions of the coverage probability are obtained.

First, considering the path loss and fast fading impacts, the closed form formula of the coverage probability at a given distance of the serving BS is obtained. We then consider path loss, shadowing, and fast fading and give an analytical expression of the outage probability at a given distance of the serving BS. Since the expression depends only on the distances from interferers, which allows further integrations much

more easily than with existing formulas derived in a traditional way of utilizing PPP. Finally, the simulation results verified the feasibility and correctness of the proposed method. This method releases the channel restriction of the traditional PPP model, surely promotes and broadens the applications of PPP in analysis of cellular network.

Chapter 6

Conclusions and Future Work

6.1 Conclusions

This dissertation has discussed a study on Stochastic Geometry Based Modeling and Analysis of Cellular Networks. The objectives, background, related works, contribution of this research are addressed in Chapter 1. In Chapter 2, the fundamentals of SG and necessary related content are presented. Three typical PPs, PPP, HCPP, PCP, and related properties are introduced.

In Chapter 3, we use PPP to model BSs' locations, and propose a framework to analyze the downlink coverage probability of HetNets utilizing the FFR technique. We give tractable expressions of typical users' coverage probability under both closed and open access cases, which can be furthermore simplified to a close form in interference-limited networks. Through analysis, some useful propositions and interesting observations are proposed: the coverage probability of edge user is independent of channel parameter μ; The coverage probability of edge user with FFR under open access scheme equals the sum of the coverage probability of each single tier under closed access scheme; In one tier network with FFR, both for SFR and strict FFR, density of BSs and transmit power do not affect coverage probability of both edge and interior users. We give the numerical results of coverage probability, and discuss the effects of main parameters on it. These analysis can assist system designers in designing networks, and evaluating new algorithm about HetNets utilizing

FFR.

Chapter 4 uses PPP to model the locations of BSs, and proposes a framework to analyze the downlink coverage probability of the MIMO HetNets utilizing the FFR technique. We give a tractable expression of the typical user coverage probability under both closed and open access cases, which can be easily extended to develop average cell-edge user rate expressions. We show the numerical results of different FFR and access cases under the full SDMA and SU-BF, and discuss the effects of main parameters on the coverage probability. We also illustrate how to use the coverage probability results to derive the average rate expressions. These analyses can assist system designers in designing networks, and evaluating new algorithm related to MIMO HetNets. It should be noted that this analysis is for downlink networks, without mentioning uplink case. Considering the importance of uplink case, we will analyze it in our future work.

In Chapter 5, we propose a novel way of analyzing cellular networks based on Poisson point process, and derive simple formulas of the coverage probabilities, while considering path loss, shadowing and fast fading impacts. Traditional analyses are based on PGFL of PPP, which restrict the channel to fast fading. The new approach is based on basic theory of probability and statistics, does not rely on PGFL, therefore, it releases the restriction of channel. The expressions of the coverage probability in [70] are the function of only the distances from BSs, and the distances do not restrict to a special distribution. Therefore, the main idea of this paper is that using PPP to model the BSs' locations and substitute some expression depending on the distances with statistical values. Assuming that the network area is a circle, we derive the PDF of the distances from the BSs to the user. Based on this PDF, and combining the conclusions of deterministic model of cellular networks, the average value of the expressions depending on the distances can be calculated, then the expressions of the coverage probability are obtained. First, considering the path loss and fast fading impacts, the closed form formula of the coverage probability at a given distance of the serving BS is obtained. We then consider path loss, shadowing, and fast fading and give an analytical expression of the outage probability at a given distance of

the serving BS. Since the expression depends only on the distances from interference BSs, which allows further integrations much more easily than with existing formulas derived in a traditional way of utilizing PPP. Finally, the simulation results verified the feasibility and correctness of the proposed method. This method releases the channel restriction of the traditional PPP model, surely promotes and broadens the applications of PPP in analysis of cellular network.

6.2 Future Work

The work carried out in this thesis could be completed by several extensions, especially, Chapter 5 is a starting point for other interesting research initiatives. As mentioned in Chapter 5, although the proposed approach can release the restriction of channel, obtain easier expressions of coverage probability, there are still some defects. First one is that due to using the central limit theorem (CLT) for approximation, the big standard derivation of shadowing channel results in the distortion of the coverage probability. Second one is that the CLT also requires high density of the BS, therefore, the low density of BSs impacts the accuracy of the coverage probability.

Furthermore, the proposed model just analyzes a simple scenario of cellular networks, actually, the more complex scenario should be considered. Therefore, the future works are that overcoming the shortcomings and extending the results to other scenarios of the cellular networks.

- Developing the model of one tier cellular networks, which can verify the feasibility and correctness of the new approach.

- Calculating interference with Fenton-Wilkinson approach instead of the CLT, which can overcome the first shortcoming above.

  Fenton-Wilkinson approach approximates a sum of log-normal random variables by a log-normal random variable and approximates fast fading coefficients in interference terms by their average value.

- Modeling (heterogeneous) cellular networks in terms of uniform distribution, which can overcome the second shortcoming above.

  Since uniform distribution is the simplest distribution, using it to model the BSs allows us to calculate the sum of average distances form BSs more accurately than approximating the sum with CLT.

- Extending the results above to multi tiers (heterogeneous) cellular networks.

- Developing the model of sector cellular networks, which is most important and practical situation, however, has not done yet.

Appendix A

Appedices of Chapter 3

A.1 Proof of theorem 3.2.1

In fact, the proof is the procedure of evaluating (3.3), for your reading convenience, we rewrite it here.

$$\sum_{k=1}^{K} \frac{\mathbb{P}\left(\frac{\beta_k P_k \hat{g}_k r_k^{-\alpha}}{\sum_{n=1}^{K} \eta_n \hat{I}_n + \sigma^2} > \hat{T}_k \,,\, \prod_{j=1}^{K} \frac{P_j g_j r_j^{-\alpha}}{\sum_{m=1}^{K} \eta_m I_m + \sigma^2} < T_j \right)}{\mathbb{P}\left(\prod_{j=1}^{K} \frac{P_j g_j r_j^{-\alpha}}{\sum_{m=1}^{K} \eta_m I_m + \sigma^2} < T_j \right)}. \tag{A.1}$$

Due to the independence of each tier, we can calculate the probabilities of each tier respectively. For k_{th} tier, we first focus on the denominator of (A.1). Conditioning

on r_j, it can be evaluated as

$$\begin{aligned}
& \mathbb{E}_{I_m}\Big[\prod_{j=1}^{K}\mathbb{P}\Big(\frac{P_j g_j r_j^{-\alpha}}{\sum_{m=1}^{K}\eta_m I_m+\sigma^2}<T_j\Big)\Big] \\
= \;& \mathbb{E}_{I_m}\Big[\prod_{j=1}^{K}\mathbb{P}\Big(g_j<\frac{T_j r_j^{\alpha}}{P_j}\Big(\sum_{m=1}^{K}\eta_m I_m+\sigma^2\Big)\Big)\Big] \\
= \;& \prod_{j=1}^{K}\mathbb{E}_{I_m}\Big[1-e^{-\frac{\mu T_j r_j^{\alpha}}{P_j}\left(\sum_{m=1}^{K}\eta_m I_m+\sigma^2\right)}\Big] \\
\overset{a}{=} \;& \prod_{j=1}^{K}\Big(1-e^{-s_j\sigma^2}\cdot\mathbb{E}_{I_m}\Big[e^{-\sum_{m=1}^{K}s_j\eta_m I_m}\Big]\Big),
\end{aligned} \tag{A.2}$$

where a defines $s_j=\frac{\mu T_j r_j^{\alpha}}{P_j}$.

The expectation of (A.2) equals

$$\begin{aligned}
& \mathbb{E}_{I_m}\big[e^{-\sum_{m=1}^{K}s_j\eta_m I_m}\big]=\prod_{m=1}^{K}\mathbb{E}_{I_m}\big[e^{-s_j\eta_m I_m}\big] \\
= \;& \prod_{m=1}^{K}\mathbb{E}_{G_m,\Phi_m}\big[e^{-s_j\sum_{R_{my}\in\Phi_m}\eta_m P_m G_m R_{my}^{-\alpha}}\big] \\
= \;& \prod_{m=1}^{K}\mathbb{E}_{\Phi_m}\Big[\prod_{y\in\Phi_m}\mathbb{E}_{G_m}[e^{-s_j\eta_m P_m G_m R_{my}^{-\alpha}}]\Big],
\end{aligned} \tag{A.3}$$

where G_m means the m_{th} interference link, R_{my} means the distance from m_{th} tier interference BSs to the typical edge user.

Eq. (A.3) has already been evaluated by the proof of theorem A.1 of [15], referring

to it, we can derive

$$
\begin{aligned}
& \prod_{m=1}^{K} \mathbb{E}_{\Phi_m}\Big[\prod_{y\in\Phi_m} \mathbb{E}_{G_m}[e^{-s_j\eta_m P_m G_m R_{my}^{-\alpha}}]\Big] \\
\overset{a}{=} & \prod_{m=1}^{K} \mathbb{E}_{\Phi_m}\Big[\prod_{y\in\Phi_m} \frac{\mu}{\mu + s_j\eta_m P_m R_{my}^{-\alpha}}\Big] \\
\overset{b}{=} & \prod_{m=1}^{K} \exp\Big(-\lambda_j \int_0^\infty \Big(1 - \frac{\mu}{\mu + s_j\eta_m P_m R_{my}^{-\alpha}}\Big)\mathrm{d}R_{my}\Big) \\
\overset{c}{=} & \prod_{m=1}^{K} \exp\Big(-2\pi\lambda_j (s_j\mu^{-1}\eta_m P_m)^{\frac{2}{\alpha}} \int_0^\infty r \int_0^\infty \mathrm{e}^{-t(1+r^\alpha)}\mathrm{d}t\mathrm{d}r\Big) \\
\overset{d}{=} & \exp\Big(-(s_j\mu^{-1})^{\frac{2}{\alpha}} C(\alpha) \sum_{m=1}^{K} \lambda_m (\eta_m P_m)^{\frac{2}{\alpha}}\Big),
\end{aligned} \tag{A.4}
$$

where $C(\alpha) = \frac{2\pi^2 \csc(\frac{2\pi}{\alpha})}{\alpha}$, $s_j = \frac{\mu T_j r_j^\alpha}{P_j}$. a follows from the Rayleigh fading assumption, b follows from probability generating functional (PGFL) of PPP [59], c results from algebraic manipulation after converting from Cartesian to polar coordinates, and d uses some properties of Gamma function. Plug (A.4) back into (A.2), and deconditon on r_k, we can get the result of the denominator of (A.1).

Now focus on numerator. Conditioning on r_k, the two terms of numerator of (A.1) are independent, and the second term is the same as denominator, so we just need to evaluate the first term, which equals

$$
\begin{aligned}
\mathbb{P}\big(\hat{S}INR_k > \hat{T}_k\big) &= \mathbb{P}\bigg(\frac{\beta_k P_k g_k r_k^{-\alpha}}{\sum\limits_{n=1}^{K} \eta_n I_n + \sigma^2} > \hat{T}_k\bigg) \\
&= \mathbb{P}\bigg(g_k > \frac{\hat{T}_k r_k^{\alpha}}{P_k \beta_k}\Big(\sum_{n=1}^{K} \eta_n I_n + \sigma^2\Big)\bigg) \\
&= \mathbb{E}_{I_n}\bigg[\exp\Big(-\frac{\mu \hat{T}_k r_k^{\alpha}}{P_k \beta_k}\Big(\sum_{n=1}^{K} \eta_n I_n + \sigma^2\Big)\Big)\bigg] \\
&\overset{a}{=} e^{-\hat{s}_k \sigma^2} \cdot \mathbb{E}_{I_n}\bigg[\exp\big(-\sum_{n=1}^{K} \hat{s}_k \eta_n I_n\big)\bigg] \\
&\overset{b}{=} \exp\bigg(-(\hat{s_k}\mu^{-1})^{\frac{2}{\alpha}} C(\alpha) \sum_{n=1}^{K} \lambda_n (\eta_n P_n)^{\frac{2}{\alpha}}\bigg)
\end{aligned} \tag{A.5}
$$

where a defines $\hat{s}_k = \frac{\mu \hat{T}_k r_k^{\alpha}}{P_k \beta_k}$, b refers to (A.3) and (A.4).

Now plug the result of denominator and numerator back into (A.1) and decondition on r_k, we can get theorem 3.2.1. It should be noted that after deconditioning on r_k, the term $\prod\limits_{j \neq k}^{K} \frac{P_j g_j r_j^{-\alpha}}{\sum_{m=1}^{K} \eta_m I_m + \sigma^2} < T_j$ contained by both denominator and numerator can be simplified out.

A.2 Proof of corollary 3.2.2

The proof of corollary just easily follows from theorem 3.2.1 with $\sigma^2 = 0$. For k_{th} tier, let $\sigma^2 = 0$, the numerator of (3.4) can be simplified and evaluated as

$$
\begin{aligned}
&\int_0^{\infty} \rho(k,\lambda) f_{SFR}(\hat{s}_k) \cdot \Big(1 - f_{SFR}(s_k)\Big) \mathrm{d}r_k \\
=\ &\int_0^{\infty} \rho(k,\lambda) f_{SFR}(\hat{s}_k) \mathrm{d}r_k - \int_0^{\infty} \rho(k,\lambda) f_{SFR}(\hat{s}_k) \cdot f_{SFR}(s_k) \mathrm{d}r_k \\
\overset{a}{=}\ &\int_0^{\infty} 2\pi\lambda_k r_k e^{-(\pi\lambda_k + (\frac{\hat{T}_k}{\beta_k})^{\frac{2}{\alpha}} \bar{\theta}) r_k^2} \mathrm{d}r_k - \int_0^{\infty} 2\pi\lambda_k r_k e^{-(\pi\lambda_k + (\frac{\hat{T}_k}{\beta_k})^{\frac{2}{\alpha}} \bar{\theta} + T_k^{\frac{2}{\alpha}} \bar{\theta}) r_k^2} \mathrm{d}r_k \\
=\ &\pi\lambda_k \cdot \frac{T_k^{\frac{2}{\alpha}} \bar{\theta}}{\big(\pi\lambda_k + (\frac{\hat{T}_k}{\beta_k})^{\frac{2}{\alpha}} \bar{\theta}\big)\big(\pi\lambda_k + (\frac{\hat{T}_k}{\beta_k})^{\frac{2}{\alpha}} \bar{\theta} + T_k^{\frac{2}{\alpha}} \bar{\theta}\big)},
\end{aligned} \tag{A.6}
$$

where a defines $\bar{\theta} = P_k^{-\frac{2}{\alpha}} C(\alpha) \sum_{m=1}^{K} \lambda_m (\eta_m P_m)^{\frac{2}{\alpha}}$.

Similarly, the denominator equals

$$\frac{T_k^{\frac{2}{\alpha}} \bar{\theta}}{\left(\pi \lambda_k + T_k^{\frac{2}{\alpha}} \bar{\theta}\right)}. \tag{A.7}$$

Now plug (A.6), (A.7) back to (3.4), after simplifying and defining $\theta = \lambda_k^{-1} \bar{\theta}$, we get corollary 3.2.2.

A.3 Proof of theorem 3.2.3

Comparing (3.3) and (3.9), the denominator and the second term of numerator are almost same. Therefore using the same method of (A.4) and (A.5), conditioning on r_j, the denominator and the second term of numerator of (3.9) equals $\left(1 - \mathrm{e}^{-s_k \sigma^2} f_{sFFR}(s_k)\right)$.

The first term of the numerator of (3.9) is simpler than that of the numerator of (3.3). Referring to (A.5) and conditioning on r_j, it equals $f_{edge}(\hat{s}_k)$.

Now plug the result of denominator and numerator back into (3.9) and decondition on r_j, we can get theorem 3.2.3.

Appendix B

Appedices of Chapter 4

B.1 Proof of the Theorem 4.2.1

Under this case, the users are allowed to access only one certain tier, thereby we consider the user, whose $SIR_k < T_k$, as cell-edge user. The coverage probability of the cell-edge user (4.1) can be further expressed as

$$\begin{aligned}
&\mathbb{P}\big(\frac{D_k P_k \hat{h}_{kx_k}\|x_k\|^{-\alpha}}{\hat{I}_k} > T \,\Big|\, \frac{P_k h_{kx_k}\|x_k\|^{-\alpha}}{\sum_{k=1}^{K} I_k} < T_k\big) \\
&\quad \stackrel{a}{=} \frac{\mathbb{P}\big(\frac{D_k P_k \hat{h}_{kx_k}\|x_k\|^{-\alpha}}{\hat{I}_k} > T, \frac{P_k h_{kx_k}\|x_k\|^{-\alpha}}{\sum_{k=1}^{K} I_k} < T_k\big)}{\mathbb{P}\big(\frac{P_k h_{kx_k}\|x_k\|^{-\alpha}}{\sum_{k=1}^{K} I_k} < T_k\big)}
\end{aligned} \tag{B.1}$$

where (a) means using Baye's rule, D_k means thinning the interference. (hereinafter for convenience of notation, we express $\|x_k\|$ as x_k). Conditioning on x_k, which is the distance to the nearest k_{th} tier BS, the two terms of numerator are independent, so

we can evaluate them respectively. The first term of numerator of (B.1) equals,

$$
\begin{aligned}
& \mathbb{E}_{\hat{I}_k}\big[\mathbb{P}\big(\hat{h}_{kx_k} > \frac{Tx_k^{\alpha}\hat{I}_k}{P_k D_k}\big)\big] \\
\overset{a}{=} \; & \mathbb{E}_{\hat{I}_k}\big[e^{-\frac{Tx_k^{\alpha}\hat{I}_k}{P_k D_k}} \sum_{i=0}^{\Delta_k-1} \frac{\big(\frac{Tx_k^{\alpha}\hat{I}_k}{P_k D_k}\big)^i}{i!}\big] \\
\overset{b}{=} \; & \mathbb{E}_{\hat{I}_k}\big[e^{-\hat{s}_{1x_k}\hat{I}_k} \sum_{i=0}^{\Delta_k-1} \frac{\big(\hat{s}_{1x_k}\hat{I}_k\big)^i}{i!}\big] \\
= \; & \sum_{i=0}^{\Delta_k-1} \frac{1}{i!}\mathbb{E}_{\hat{I}_k}\big[e^{-\hat{s}_{1x_k}\hat{I}_k}\big(\hat{s}_{1x_k}\hat{I}_k\big)^i\big] \\
\overset{c}{=} \; & \sum_{i=0}^{\Delta_k-1} \frac{1}{i!}\big[\big(-\hat{s}_{1x_k}\big)^i \frac{\delta^i}{\delta\big(\hat{s}_{1x_k}\big)^i}\mathcal{L}_{\hat{I}_k}\big(\hat{s}_{1x_k}\big)\big]
\end{aligned}
\tag{B.2}
$$

where referring to the formula (16)(17) of [33] , (a) follows $\hat{h}_{kx_k} \sim \Gamma(\Delta_k, 1)$, (b) defines $\hat{s}_{1x_k} = \frac{Tx_k^{\alpha}}{P_k D_k}$, (c) uses the property of Laplace transform (LT).

There is a lemma in [33] to detail how to evaluate the LT term of (B.2), for convenience of reading, we rewrite part of it here.

$$
\begin{aligned}
& \mathcal{L}_{\hat{I}_k}\big(\hat{s}_{1x_k}\big) = \mathbb{E}_{Z_k}\big[e^{-\hat{s}_{1x_k}\sum_{y_k\in Z_k} P_k\hat{g}_{ky_k}y_k^{-\alpha}}\big] \\
= \; & \mathbb{E}_{Z_k}\big[\Pi_{y_k\in Z_k} e^{-\hat{s}_{1x_k}P_k\hat{g}_{ky_k}y_k^{-\alpha}}\big] \\
= \; & \mathbb{E}_{Z_k}\big[\Pi_{y_k\in Z_k}\mathcal{L}_{\hat{g}_{ky_k}}\big(\hat{s}_{1x_k}P_k y_k^{-\alpha}\big)\big] \\
\overset{a}{=} \; & \exp\big(-\lambda_k\int_{R^2} 1-\mathcal{L}_{\hat{g}_{ky_k}}\big(\hat{s}_{1x_k}P_k y_k^{-\alpha}\big)\mathrm{d}y_k\big) \\
\overset{b}{=} \; & \exp\big(-\lambda_k\int_{R^2}\Big(1-\frac{1}{\big(1+\hat{s}_{1x_k}P_k y_k^{-\alpha}\big)^{\Psi_k}}\Big)\mathrm{d}y_k\big) \\
= \; & \exp\big(-\lambda_k\int_{R^2}\frac{\big(1+\hat{s}_{1x_k}P_k y_k^{-\alpha}\big)^{\Psi_k}-1}{\big(1+\hat{s}_{1x_k}P_k y_k^{-\alpha}\big)^{\Psi_k}}\mathrm{d}y_k\big) \\
\overset{c}{=} \; & \exp\big(-\lambda_k\int_{R^2}\frac{\sum_{m=1}^{\Psi_k}\binom{\Psi_k}{m}\big(\hat{s}_{1x_k}P_k y_k^{-\alpha}\big)^m}{\big(1+\hat{s}_{1x_k}P_k y_k^{-\alpha}\big)^{\Psi_k}}\mathrm{d}y_k\big) \\
\overset{d}{=} \; & \exp\big(-\hat{s}_{1x_k}^{\frac{2}{\alpha}}\lambda_k P_k^{\frac{2}{\alpha}}\mathrm{C}\big(\alpha,\Psi_k\big)\big)
\end{aligned}
\tag{B.3}
$$

where $\mathrm{C}(\alpha, \Psi_j)$ is given in (4.4). (a) follows the probability generating functional

(PGFL) of PPP [59], (b) follows the LT of the $g_{ky_k} \sim \Gamma(\Psi_k, 1)$, (c) follows from Binomial theorem, and (d) follows from converting to cartesian to polar coordinates followed by substituting $\big(1 + r^{-\alpha}\big)^{-1} \rightarrow t$ to convert the integral into Euler's Beta function $\int_0^1 t^{x-1}\big(1-t\big)^{y-1}\mathrm{d}t$ [33]. Plugging (B.3) back into (B.2), we can get the result of first term of numerator of (B.1), which is $f_1(\hat{s}_{1x_k})$.

Conditioning on the x_k, the second term of numerator and the denominator are the same, and they equal

$$1 - \mathbb{E}_{Z_k}\Bigg[\mathbb{P}\big(h_{kx_k} > \frac{T_k x_k^{\alpha}}{P_k}\sum_{k=1}^{K} I_k\big)\Bigg]. \tag{B.4}$$

Referring to (B.2), (B.4) equals

$$1 - \sum_{i=0}^{\Delta_k - 1} \frac{1}{i!}\big[\big(-s_{1x_k}\big)^i \frac{\delta^i}{\delta\big(s_{1x_k}\big)^i}\mathcal{L}_{I'_k}\big(s_{1x_k}\big)\big] \tag{B.5}$$

where we define $s_{1x_k} = \frac{T_k x_k^{\alpha}}{P_k}$, $I'_k = \sum_{k=1}^{K} I_k$. Due to being similar to (B.3), and referring to lemma 1 of [33], the LT term of (B.5) equals

$$\begin{aligned}\mathbb{E}_{I'_k}\big[e^{s_{1x_k} I'_k}\big] &= \mathbb{E}_{Z_k}\big[e^{s_{1x_k}\sum_{k=1}^{K}\sum_{y_k \in Z_k} P_k g_{ky_k} y_k^{-\alpha}}\big] \\ &= \exp\big(-s_{1x_k}^{\frac{2}{\alpha}} \sum_{k=1}^{K} \lambda_k P_k^{\frac{2}{\alpha}} \mathrm{C}\big(\alpha, \Psi_k\big)\big).\end{aligned} \tag{B.6}$$

Plugging (B.6) back to (B.5), we can get the result of (B.4), $(1-f'_1(\hat{s}_{1x_k}))$. Therefore, the numerator and denominator of (B.1), equal $f_1(\hat{s}_{1x_k})(1-f'_1(s_{1x_k}))$ and $(1-f'_1(s_{1x_k}))$, respectively. Now substituting for each term of (B.1), and conditioning on x_k, the result of (B.1) is $\frac{f_1(\hat{s}_{1x_k})(1-f'_1(s_{1x_k}))}{(1-f'_1(s_{1x_k}))}$. After deconditioning on x_k, we get the result of theorem 1.

B.2 Proof of the Theorem 4.2.2

Comparing to strict FFR, SFR increases transmit power and experiences inter-tier interference. Consider these two differences, the probability $P_{SFR,cl} =$

$$\mathbb{P}\Bigg(\frac{\beta_k P_k \hat{h}_{kx_k}\|x_k\|^{-\alpha}}{\sum\limits_{k=1}^{K}\eta_k\hat{I}_k} > T \,\Bigg|\, \frac{P_k h_{kx_k}\|x_k\|^{-\alpha}}{\sum\limits_{k=1}^{K}\eta_k I_k} < T_k\Bigg)$$
$$= \frac{\mathbb{P}\Bigg(\frac{\beta_k P_k \hat{h}_{kx_k}\|x_k\|^{-\alpha}}{\sum\limits_{k=1}^{K}\eta_k\hat{I}_k} > T\,,\, \frac{P_k h_{kx_k}\|x_k\|^{-\alpha}}{\sum\limits_{k=1}^{K}\eta_k I_k} < T_k\Bigg)}{\mathbb{P}\Bigg(\frac{P_k h_{kx_k}\|x_k\|^{-\alpha}}{\sum\limits_{k=1}^{K}\eta_k I_k} < T_k\Bigg)}. \tag{B.7}$$

Referring to (B.2) and conditioning on x_k, the first term of numerator equals

$$\begin{aligned}
&\mathbb{E}_{\hat{I}_k}\big[\mathbb{P}\big(\hat{h}_{kx_k} > \frac{Tx_k^{\alpha}}{\beta_k P_k}\sum_{k=1}^{K}\eta_k\hat{I}_k\big)\big] \\
=\ &\mathbb{E}_{\hat{I}_k}\big[e^{-\frac{Tx_k^{\alpha}}{\beta_k P_k}\sum_{k=1}^{K}\eta_k\hat{I}_k}\sum_{i=0}^{\Delta_k-1}\frac{\big(\frac{Tx_k^{\alpha}}{\beta_k P_k}\sum_{k=1}^{K}\eta_k\hat{I}_k\big)^i}{i!}\big] \\
\overset{a}{=}\ &\sum_{i=0}^{\Delta_k-1}\frac{1}{i!}\mathbb{E}_{\hat{I}'_k}\big[e^{-\hat{s}_{2x_k}\hat{I}'_k}\big(\hat{s}_{2x_k}\hat{I}'_k\big)^i\big] \\
=\ &\sum_{i=0}^{\Delta_k-1}\frac{1}{i!}\big[\big(-\hat{s}_{2x_k}\big)^i\frac{\delta^i}{\delta\big(\hat{s}_{2x_k}\big)^i}\mathcal{L}_{\hat{I}'_{x_k}}\big(\hat{s}_{2x_k}\big)\big]
\end{aligned} \tag{B.8}$$

where (a) defines $\hat{s}_{2x_k} = \frac{Tx_k^{\alpha}}{\beta_k P_k}$ and $\hat{I}'_k = \sum_{k=1}^{K}\eta_k\hat{I}_k$, and Referring to (B.3), the LT of above can be evaluated as

$$\begin{aligned}
\mathcal{L}_{\hat{I}'_k}\big(\hat{s}_{2x_k}\big) &= \mathbb{E}_{Z_k}\big[e^{-\hat{s}_{2x_k}}\sum_{y_k\in Z_k}\eta_k P_k\hat{g}_{ky_k}y_k^{-\alpha}\big] \\
&= \mathbb{E}_{Z_k}\big[\Pi_{y_k\in Z_k}e^{-\hat{s}_{2x_k}\eta_k P_k\hat{g}_{ky_k}y_k^{-\alpha}}\big] \\
&= \mathbb{E}_{Z_k}\big[\Pi_{y_k\in Z_k}\mathcal{L}_{\hat{g}_{ky_k}}\big(\hat{s}_{2x_k}\eta_k P_k y_k^{-\alpha}\big)\big] \\
&= \exp\big(-\hat{s}_{2x_k}^{\frac{2}{\alpha}}\sum_{k=1}^{K}\lambda_k\big(\eta_k P_k\big)^{\frac{2}{\alpha}}\mathrm{C}\big(\alpha,\Psi_k\big)\big).
\end{aligned} \tag{B.9}$$

Pluging (B.9) to (B.8), then we can get the result of first term of numerator, which is $f_2(\hat{s}_{2x_k})$. Conditioning on x_k, the procedure of calculating second term of numerator and the denominator are the same. Imitating the method of (B.8) and (B.9), we can get the result of second term and denominator

$$\begin{aligned} & 1-\mathbb{P}\big(\frac{P_k h_{kx_k}\|x_k\|^{-\alpha}}{\sum_{k=1}^{K}\eta_k I_k} > T_k\big) \\ \overset{a}{=} \; & 1-\sum_{i=0}^{\Delta_k-1}\frac{1}{i!}\big[\big(-s_{2x_k}\big)^i\frac{\delta^i}{\delta\big(s_{2x_k}\big)^i}\mathcal{L}_{I'_{x_k}}\big(s_{2x_k}\big)\big] \end{aligned} \tag{B.10}$$

where (a) defines $s_{2x_k}=\frac{T_k x_k^{\alpha}}{P_k}$ and $I'_k=\sum_{j=1}^{K}I_k$, and the LT term equals

$$\mathcal{L}_{I'_k}\big(s_{2x_k}\big)=\exp\big(-s_{2x_k}^{\frac{2}{\alpha}}\sum_{j=1}^{K}\lambda_j\big(\eta_j P_j\big)^{\frac{2}{\alpha}}\mathrm{C}\big(\alpha,\Psi_j\big)\big). \tag{B.11}$$

Pluging (B.11) back to (B.10), then we get the result of second term and denominator of (B.7), which are $(1-f_2(s_{2x_k}))$. Now substituting for each term of (B.7) with $f_2(\hat{s}_{2x_k})$ and $(1-f_2(s_{2x_k}))$, and conditioning on x_k, the result of (B.7) is $\frac{f_2(\hat{s}_{2x_k})(1-f_2(s_{2x_k}))}{(1-f_2(s_{2x_k}))}$. After deconditioning on x_k, we get the result of theorem 2.

B.3 Proof of the Theorem 4.3.1

Different from closed access, open access allows users to access each tier, thereby the cell-edge user is the user whose $SIR_1 < T_1$ and $SIR_2 < T_2$. The coverage probability of cell-edge user (4.7) can be further expressed as

$$\begin{aligned} & \mathbb{P}\big(\frac{D_1 P_1 \hat{h}_{1x_1} x_1^{-\alpha}}{\hat{I}_1} > T \,\big|\, SIR_1 < T_1, SIR_2 < T_2\big) \\ \overset{a}{=} \; & \frac{\mathbb{P}\Big(\frac{D_1 P_1 \hat{h}_{1x_1} x_1^{-\alpha}}{\hat{I}_1} > T, (SIR_1 < T_1, SIR_2 < T_2)\Big)}{\mathbb{P}\big(SIR_1 < T_1, SIR_2 < T_2\big)} \end{aligned} \tag{B.12}$$

where (a) follows the Bayes' rule.

Conditioning on x_1 and x_2, each part of (B.12) is independent, so we focus on the

denominator first.

$$\begin{aligned}
& \mathbb{P}\big(SIR_1 < T_1, SIR_2 < T_2\big) \\
= \;& \mathbb{P}\bigg(\frac{P_1 h_{1x_1} x_1^{-\alpha}}{I_1 + I_2 + P_2 h_{2x_2} x_2^{-\alpha}} < T_1 \\
& , \frac{P_2 h_{2x_2} x_2^{-\alpha}}{I_1 + I_2 + P_1 h_{1x_1} x_1^{-\alpha}} < T_2\bigg) \\
\overset{a}{=} \;& \mathbb{P}\bigg(\frac{x_1^\alpha}{P_1}\big(\frac{P_2}{T_2} h_{2x_2} x_2^{-\alpha} - \bar{I}\big) < h_{1x_1} \\
& < \frac{T_1 x_1^\alpha}{P_1}\big(P_2 h_{2x_2} x_2^{-\alpha} + \bar{I}\big) \,\big|\, h_{2x_2}\bigg)
\end{aligned} \tag{B.13}$$

where (a) condition on h_{2x_2} and $\bar{I} = I_1 + I_2$. Since h_{1x_1} follows $\Gamma(\Delta_1, 1)$, using the CCDF of the Gamma distribution, (B.13) equals

$$\begin{aligned}
& \mathbb{E}_{h_{2x_2}, \bar{I}}\bigg[1 - e^{-\frac{T_1 x_1^\alpha}{P_1}\left(P_2 h_{2x_2} x_2^{-\alpha} + \bar{I}\right)} \sum_{i=0}^{\Delta_1 - 1} \\
& \frac{\big(\frac{T_1 x_1^\alpha}{P_1}\big(P_2 h_{2x_2} x_2^{-\alpha} + \bar{I}\big)\big)^i}{i!} - \Big(1 - e^{-\frac{x_1^\alpha}{P_1}\left(\frac{P_2}{T_2} h_{2x_2} x_2^{-\alpha} - \bar{I}\right)^+} \\
& \sum_{i=0}^{\Delta_1 - 1} \frac{\big(\frac{x_1^\alpha}{P_1}\big(\frac{P_2}{T_2} h_{2x_2} x_2^{-\alpha} - \bar{I}\big)^+\big)^i}{i!}\Big)\bigg]
\end{aligned} \tag{B.14}$$

where

$$\big(x\big)^+ = \begin{cases} x, & x > 0 \\ 0, & x \leq 0 \end{cases}$$

Define $s = \frac{T_1 x_1^\alpha}{P_1}$, $\bar{I}' = \bar{I} + P_2 h_{2x_2} x_2^{-\alpha}$, and the first term of (B.14) equals

$$\mathbb{E}_{\bar{I}'}\bigg[e^{-s\bar{I}'} \sum_{i=0}^{\Delta_1 - 1} \frac{\big(s\bar{I}'\big)}{i!}\bigg] \;=\; \sum_{i=0}^{\Delta_1 - 1} \frac{1}{i!}\bigg[\big(-s\big)^i \frac{\delta^i}{\delta\big(s\big)^i} \mathcal{L}_{\bar{I}'}\big(s\big)\bigg]. \tag{B.15}$$

The LT in (B.15) equals

$$\begin{aligned}&\mathbb{E}_{\bar{I}'}\left[e^{-s\bar{I}'}\right]=\mathbb{E}_{\bar{I},h_{2x_2}}\left[e^{-s\left(\bar{I}+P_2h_{2x_2}x_2^{-\alpha}\right)}\right]\\=&\mathbb{E}_{g_{1y_1}}\left[\Pi_{y\in Z_1/x_1}e^{-sP_1g_{1y_1}y_1^{-\alpha}}\right]\cdot\\&\mathbb{E}_{g_{2y_2}}\left[\Pi_{y\in Z_2/x_2}e^{-sP_2g_{2y_2}y_2^{-\alpha}}\right]\cdot\mathbb{E}_{h_{2x_2}}\left[e^{-sP_2h_{2x_2}x_2^{-\alpha}}\right].\end{aligned}\tag{B.16}$$

Referring to (B.2), we can evaluate the first two terms of (B.16). Using the conclusion of the LT of the Gamma distribution, the third term of (B.16) equals

$$\mathcal{L}_{h_{2x_2}}\left(sP_2x_2^{-\alpha}\right)=\frac{1}{\left(1+sP_2x_2^{-\alpha}\right)^{\Delta_2}}.\tag{B.17}$$

Now plugging (B.16), (B.17) back into (B.15) and then we can get the result of (B.15).

Define $s'=\frac{x_1^\alpha}{P_1}$, $\bar{I}''=\left(\frac{P_2}{T_2}h_{2x_2}x_2^{-\alpha}-\bar{I}\right)^+$, and the second term of (B.14) equals

$$\begin{aligned}&\mathbb{E}_{\bar{I}''}\left[e^{-s'\bar{I}''}\sum_{i=0}^{\Delta_1-1}\frac{\left(s'\bar{I}''\right)^i}{i!}\right]\\&=\sum_{i=0}^{\Delta_1-1}\frac{1}{i!}\left[\left(-s'\right)^i\frac{\delta^i}{\delta\left(s'\right)^i}\mathcal{L}_{\bar{I}''}\left(s'\right)\right].\end{aligned}\tag{B.18}$$

Defining $s_2'=\frac{P_2}{T_2}x_2^{-\alpha}$, $n=\Delta_2-1$, and using the definition of expectation to evaluate the expectation of g_2, which follows the Gamma distribution, the LT of (B.18)

$$\begin{aligned}&\mathcal{L}_{\bar{I}''}\left(s'\right)=\mathbb{E}_{\bar{I}''}\left[e^{-s'\bar{I}''}\right]=\mathbb{E}_{\bar{I},h_{2x_2}}\left[e^{-s'\left(s_2'h_{2x_2}-\bar{I}\right)^+}\right]\\\overset{a}{=}\;&\mathbb{E}_{\bar{I}}\left[\int_0^{\frac{\bar{I}}{s_2'}}\frac{1}{\Gamma(\Delta_2)}h_{2x_2}^ne^{-h_{2x_2}}\mathrm{d}_{h_{2x_2}}\right.\\&\left.+\int_{\frac{\bar{I}}{s_2'}}^{\infty}\frac{1}{\Gamma(\Delta_2)}h_{2x_2}^ne^{-h_{2x_2}}e^{-s's_2'h_{2x_2}}e^{s'\bar{I}}\mathrm{d}_{h_{2x_2}}\right].\end{aligned}\tag{B.19}$$

Evaluating (B.19), collecting terms and simplifying gives

$$1+\frac{1}{\Gamma(\Delta_2)}\sum_{m=0}^{n}\frac{n!}{(n-m)!}\,(s_2')^{m-n}\ \cdot \\ \left(\frac{1}{(1+s's_2')^{m+1}}-1\right)\mathbb{E}_{\bar{I}}\big[e^{-\frac{1}{s_2'}\bar{I}^{n-m}}\big]. \tag{B.20}$$

According to the LT property, the last part of the (B.20) equals

$$\mathbb{E}_{\bar{I}}\big[e^{-\frac{1}{s_2'}\bar{I}^{n-m}}\big]=(-1)^{n-m}\frac{\delta^{n-m}}{\delta(\frac{1}{s_2'})^{n-m}}\mathcal{L}_{\bar{I}}\left(\frac{1}{s_2'}\right).$$

The LT term of above formula is the same as the part of (B.16), so it can be derived by directly using the result of (B.16). Now plugging the result of (B.18) and (B.15) back into (B.13), then we can get the result of (B.13).

Now we focus on the numerator of (B.12). Comparing it to the denominator, the second term is the same as denominator, so we just need to calculate the first term. the first term of (B.12) is similar to the first term of (B.1) numerator, so referring to (B.2), the first term of (B.12) can be evaluated as

$$\mathbb{P}\big(\frac{D_1P_1\hat{h}_{1x_1}x_1^{-\alpha}}{\hat{I}_1}>T\big)\overset{a}{=}\sum_{i=0}^{\Delta_1-1}\frac{1}{i!}\big[\big(-\hat{s}'\big)^i\frac{\delta^i}{\delta\big(\hat{s}'\big)^i}\mathcal{L}_{\hat{I}_1}\big(\hat{s}'\big)\big] \tag{B.21}$$

where (a) defines $\hat{s}'=\frac{Tx_1^{\alpha}}{P_1D_1}$, $\hat{I}_1=\sum_{y\in Z_1/x_1}P_1\hat{g}_{1y_1}y_1^{-\alpha}$. The Laplace transform of (B.21) equals

$$\begin{aligned}\mathcal{L}_{\hat{I}_1}\big(\hat{s}'\big) &= \mathbb{E}_{\hat{g}_{1y_1}}\big[e^{-\hat{s}'\sum_{y\in Z_1/x_1}P_1\hat{g}_{1y_1}y_1^{-\alpha}}\big]\\ &= \exp\big(-\hat{s}'^{\frac{2}{\alpha}}\lambda_1P_1^{\frac{2}{\alpha}}\mathrm{C}'\big(\alpha,\Psi_1\big)\big).\end{aligned} \tag{B.22}$$

Now plugging (B.13) and (B.21) back into (B.12) and decontitioning on x_1 and x_2, we get the result of theorem 4.3.1.

B.4 Proof of the Theorem 4.3.2

Referring to theorem 4.2.2 and theorem 4.3.1, the coverage probability in the case of SFR and open access can be expressed as

$$\begin{aligned} & \mathbb{P}\Big(\frac{\beta_1 P_1 \hat{h}_{1x_1} x_1^{-\alpha}}{\eta_1 \hat{I}_1 + \eta_2 \hat{I}_2} > T \,\Big|\, SIR_1 < T_1, SIR_2 < T_2\Big) \\ = \; & \frac{\mathbb{P}\Big(\frac{\beta_1 P_1 \hat{h}_{1x_1} x_1^{-\alpha}}{\eta_1 \hat{I}_1 + \eta_2 \hat{I}_2} > T, \big(SIR_1 < T_1, SIR_2 < T_2\big)\Big)}{\mathbb{P}\big(SIR_1 < T_1, SIR_2 < T_2\big)}. \end{aligned} \tag{B.23}$$

Here conditioning on x_1 and x_2, the first term and second term of the numerator of (B.23) are independent. The denominator and second term of the numerator of (B.23) are the same as (B.13), so we just need to calculate the first term of numerator. Define $\hat{s} = \frac{T x_1^{\alpha}}{\beta_1 P_1}$, $\hat{I}_{12} = \eta_1 \hat{I}_1 + \eta_2 \hat{I}_2$, and using the method of theorem 4.2.2, the first term of the numerator of (B.23) equals

$$\mathbb{P}\big(\frac{\beta_1 P_1 \hat{h}_{1x_1} x_1^{-\alpha}}{\eta_1 \hat{I}_1 + \eta_2 \hat{I}_2} > T\big) = \sum_{i=0}^{\Delta_1 - 1} \frac{1}{i!} \big[\big(-\hat{s}\big)^i \frac{\delta^i}{\delta\big(\hat{s}\big)^i} \mathcal{L}_{\hat{I}_{12}}\big(\hat{s}\big)\big] \tag{B.24}$$

where

$$\begin{aligned} \mathcal{L}_{\hat{I}_{12}}\big(\hat{s}\big) = & \exp\big(-\hat{s}^{\frac{2}{\alpha}} \lambda_1 \big(\eta_1 P_1\big)^{\frac{2}{\alpha}} \mathrm{C}\big(\alpha, \Psi_1\big)\big) \\ & \cdot \exp\big(-\hat{s}^{\frac{2}{\alpha}} \lambda_2 \big(\eta_2 P_2\big)^{\frac{2}{\alpha}} \mathrm{C}\big(\alpha, \Psi_2\big)\big). \end{aligned} \tag{B.25}$$

Plugging the result of (B.25) and (B.13) back into (B.23), and deconditioning on x_1 and x_2, we have the result of theorem 4.3.2.

Bibliography

[1] S. Yang and L. Hanzo, "Fifty years of mimo detection: The road to large-scale mimos," *IEEE Communications Surveys Tutorials*, vol. 17, no. 4, pp. 1941–1988, Fourthquarter 2015.

[2] X. Zhou, B. Bai, and W. Chen, "Invited paper: Antenna selection in energy efficient mimo systems: A survey," *China Communications*, vol. 12, no. 9, pp. 162–173, 2015.

[3] K. Zheng, L. Zhao, J. Mei, B. Shao, W. Xiang, and L. Hanzo, "Survey of large-scale mimo systems," *IEEE Communications Surveys Tutorials*, vol. 17, no. 3, pp. 1738–1760, thirdquarter 2015.

[4] G. T. . v9.0.0, "Evolved universal terrestrial radio access (e-utra); further advancements for e-utra physical layer aspects (release 9)," *Sophia-Antipolis, France*, 2010.

[5] "Part 16: Air interface for fixed and mobile broadband wireless access systems v draft amendment to ieee standard for local and metropolitan area networksadvanced air interface," *e, IEEE P802.16m/D4, IEEE Std. 802.16*, 2010.

[6] S. H. Lu, L. C. Wang, T. T. Chiang, and C. H. Chou, "Cooperative hierarchical cellular systems in lte-a networks," *IEEE Systems Journal*, vol. 9, no. 3, pp. 766–774, Sept 2015.

[7] V. Mhatre and C. Rosenberg, "Homogeneous vs heterogeneous clustered sensor

networks: a comparative study," in *Communications, 2004 IEEE International Conference on*, vol. 6, June 2004, pp. 3646–3651 Vol.6.

[8] A. A. M. Saleh, A. Rustako, and R. Roman, "Distributed antennas for indoor radio communications," *IEEE Transactions on Communications*, vol. 35, no. 12, pp. 1245–1251, December 1987.

[9] J. Zhang and J. G. Andrews, "Distributed antenna systems with randomness," *IEEE Transactions on Wireless Communications*, vol. 7, no. 9, pp. 3636–3646, September 2008.

[10] V. Chandrasekhar, J. G. Andrews, and A. Gatherer, "Femtocell networks: a survey," *IEEE Communications Magazine*, vol. 46, no. 9, pp. 59–67, September 2008.

[11] L. Kleinrock and J. Silvester, "Optimum transmission radii for packet radio networks or why six is a magic number," in *NTC '78; National Telecommunications Conference, Volume 1*, vol. 1, 1978, pp. 4.3.1–4.3.5.

[12] R. Nelson and L. Kleinrock, "The spatial capacity of a slotted ALOHA multihop packet radio network with capture," *IEEE Transactions on Communications*, vol. 32, pp. 684–694, Jun. 1984.

[13] R. Mathar and J. Mattfeldt, "Optimal transmission ranges for mobile communication in linear multihop packet radio networks," *Wireless Networks*, vol. 2, no. 4, pp. 329–342, 1996. [Online]. Available: http://dx.doi.org/10.1007/BF01262051

[14] J. G. Andrews, F. Baccelli, and R. K. Ganti, "A tractable approach to coverage and rate in cellular networks," *CoRR*, vol. abs/1009.0516, 2010. [Online]. Available: http://arxiv.org/abs/1009.0516

[15] H. S. Dhillon, R. K. Ganti, F. Baccelli, and J. G. Andrews, "Modeling and analysis of k-tier downlink heterogeneous cellular networks," *IEEE Journal on Selected Areas in Communications*, vol. 30, no. 3, pp. 550–560, April 2012.

[16] F. B. H. S. Dhillon, R. K. Ganti and J. G. Andrews, "Coverage and ergodic rate in k-tier downlink heterogeneous cellular networks," in *Communication, Control, and Computing (Allerton), 2011 49th Annual Allerton Conference on*, Sept 2011, pp. 1627–1632.

[17] S. Singh, H. S. Dhillon, and J. G. Andrews, "Offloading in heterogeneous networks: Modeling, analysis, and design insights," *IEEE Transactions on Wireless Communications*, vol. 12, no. 5, pp. 2484–2497, May 2013.

[18] H. S. Dhillon, R. K. Ganti, and J. G. Andrews, "Load-aware modeling and analysis of heterogeneous cellular networks," *IEEE Transactions on Wireless Communications*, vol. 12, no. 4, pp. 1666–1677, April 2013.

[19] H. S. Jo, Y. J. Sang, P. Xia, and J. G. Andrews, "Outage probability for heterogeneous cellular networks with biased cell association," in *Global Telecommunications Conference (GLOBECOM 2011), 2011 IEEE*, Dec 2011, pp. 1–5.

[20] H. S. Jo and Y. J. Sang and P. Xia and J. G. Andrews, "Heterogeneous cellular networks with flexible cell association: A comprehensive downlink sinr analysis," *IEEE Transactions on Wireless Communications*, vol. 11, no. 10, pp. 3484–3495, October 2012.

[21] D. Cao, S. Zhou, and Z. Niu, "Optimal base station density for energy-efficient heterogeneous cellular networks," in *2012 IEEE International Conference on Communications (ICC)*, June 2012, pp. 4379–4383.

[22] M. D. Renzo, A. Guidotti, and G. E. Corazza, "Average rate of downlink heterogeneous cellular networks over generalized fading channels: A stochastic geometry approach," *IEEE Transactions on Communications*, vol. 61, no. 7, pp. 3050–3071, July 2013.

[23] P. Madhusudhanan, J. G. Restrepo, Y. Liu, T. X. Brown, and K. R. Baker, "Downlink performance analysis for a generalized shotgun cellular system," *IEEE*

Transactions on Wireless Communications, vol. 13, no. 12, pp. 6684–6696, Dec 2014.

[24] T. Bai and R. W. Heath, "Location-specific coverage in heterogeneous networks," *IEEE Signal Processing Letters*, vol. 20, no. 9, pp. 873–876, Sept 2013.

[25] S. Mukherjee, "Distribution of downlink sinr in heterogeneous cellular networks," *IEEE Journal on Selected Areas in Communications*, vol. 30, no. 3, pp. 575–585, April 2012.

[26] Y. J. Chun, M. O. Hasna, and A. Ghrayeb, "Modeling heterogeneous cellular networks interference using poisson cluster processes," *IEEE Journal on Selected Areas in Communications*, vol. 33, no. 10, pp. 2182–2195, Oct 2015.

[27] R. W. Heath, M. Kountouris, and T. Bai, "Modeling heterogeneous network interference using poisson point processes," *IEEE Transactions on Signal Processing*, vol. 61, no. 16, pp. 4114–4126, Aug 2013.

[28] H. ElSawy, E. Hossain, and M. Haenggi, "Stochastic geometry for modeling, analysis, and design of multi-tier and cognitive cellular wireless networks: A survey," *IEEE Communications Surveys Tutorials*, vol. 15, no. 3, pp. 996–1019, Third 2013.

[29] Y. Zhong and W. Zhang, "Downlink analysis of multi-channel hybrid access two-tier networks," in *2012 IEEE International Conference on Communications (ICC)*, June 2012, pp. 2479–2484.

[30] A. G. T. D. Novlan, R. K. Ganti and J. G. Andrews, "Analytical evaluation of fractional frequency reuse for heterogeneous cellular networks," *IEEE Transactions on Communications*, vol. 60, no. 7, pp. 2029–2039, July 2012.

[31] T. D. Novlan, R. K. Ganti, A. Ghosh, and J. G. Andrews, "Analytical evaluation of fractional frequency reuse for ofdma cellular networks," *IEEE Transactions on Wireless Communications*, vol. 10, no. 12, pp. 4294–4305, December 2011.

[32] L. C. Wang and C. J. Yeh, "3-cell network mimo architectures with sectorization and fractional frequency reuse," *IEEE Journal on Selected Areas in Communications*, vol. 29, no. 6, pp. 1185–1199, June 2011.

[33] H. S. Dhillon, M. Kountouris, and J. G. Andrews, "Downlink coverage probability in mimo hetnets," in *2012 Conference Record of the Forty Sixth Asilomar Conference on Signals, Systems and Computers (ASILOMAR)*, Nov 2012, pp. 683–687.

[34] H. S. Dhillon and M. Kountouris and J. G. Andrews, "Downlink mimo hetnets: Modeling, ordering results and performance analysis," *IEEE Transactions on Wireless Communications*, vol. 12, no. 10, pp. 5208–5222, October 2013.

[35] C. B. P. Howard Huang and S. Venkatesan, *MIMO Communication for Cellular Networks*. Springer, 2012.

[36] A. K. Gupta, H. S. Dhillon, S. Vishwanath, and J. G. Andrews, "Downlink multi-antenna heterogeneous cellular network with load balancing," *IEEE Transactions on Communications*, vol. 62, no. 11, pp. 4052–4067, Nov 2014.

[37] R. Tanbourgi, H. S. Dhillon, and F. K. Jondral, "Analysis of joint transmit–receive diversity in downlink mimo heterogeneous cellular networks," *IEEE Transactions on Wireless Communications*, vol. 14, no. 12, pp. 6695–6709, Dec 2015.

[38] R. Tanbourgi, H. S. Dhillon, J. G. Andrews, and F. K. Jondral, "Effect of spatial interference correlation on the performance of maximum ratio combining," *IEEE Transactions on Wireless Communications*, vol. 13, no. 6, pp. 3307–3316, June 2014.

[39] M. D. Renzo and W. Lu, "Stochastic geometry modeling and performance evaluation of mimo cellular networks using the equivalent-in-distribution (eid)-based approach," *IEEE Transactions on Communications*, vol. 63, no. 3, pp. 977–996, March 2015.

[40] R. Tanbourgi, H. S. Dhillon, J. G. Andrews, and F. K. Jondral, "Dual-branch mrc receivers under spatial interference correlation and nakagami fading," *IEEE Transactions on Communications*, vol. 62, no. 6, pp. 1830–1844, June 2014.

[41] M. D. Renzo and P. Guan, "A mathematical framework to the computation of the error probability of downlink mimo cellular networks by using stochastic geometry," *IEEE Transactions on Communications*, vol. 62, no. 8, pp. 2860–2879, Aug 2014.

[42] C. Li, J. Zhang, and K. B. Letaief, "Performance analysis of sdma in multicell wireless networks," in *2013 IEEE Global Communications Conference (GLOBECOM)*, Dec 2013, pp. 3867–3872.

[43] N. Lee, D. Morales-Jimenez, A. Lozano, and R. W. Heath, "Spectral efficiency of dynamic coordinated beamforming: A stochastic geometry approach," *IEEE Transactions on Wireless Communications*, vol. 14, no. 1, pp. 230–241, Jan 2015.

[44] Y. Lin and W. Yu, "Downlink spectral efficiency of distributed antenna systems under a stochastic model," *IEEE Transactions on Wireless Communications*, vol. 13, no. 12, pp. 6891–6902, Dec 2014.

[45] H. Zhuang and T. Ohtsuki, "A model based on poisson point process for analyzing mimo heterogeneous networks utilizing fractional frequency reuse," *IEEE Transactions on Wireless Communications*, vol. 13, no. 12, pp. 6839–6850, Dec 2014.

[46] A. Adhikary, H. S. Dhillon, and G. Caire, "Massive-mimo meets hetnet: Interference coordination through spatial blanking," *IEEE Journal on Selected Areas in Communications*, vol. 33, no. 6, pp. 1171–1186, June 2015.

[47] H. ElSawy and E. Hossain, "Two-tier hetnets with cognitive femtocells: Downlink performance modeling and analysis in a multichannel environment," *IEEE Transactions on Mobile Computing*, vol. 13, no. 3, pp. 649–663, March 2014.

[48] H. ElSawy and E. Hossain, "On cognitive small cells in two-tier heterogeneous networks," in *Modeling Optimization in Mobile, Ad Hoc Wireless Networks (WiOpt), 2013 11th International Symposium on*, May 2013, pp. 75–82.

[49] H. Elsawy, E. Hossain, and D. I. Kim, "Hetnets with cognitive small cells: user offloading and distributed channel access techniques," *IEEE Communications Magazine*, vol. 51, no. 6, pp. 28–36, June 2013.

[50] H. S. Dhillon, T. D. Novlan, and J. G. Andrews, "Coverage probability of uplink cellular networks," in *Global Communications Conference (GLOBECOM), 2012 IEEE*, Dec 2012, pp. 2179–2184.

[51] T. D. Novlan, H. S. Dhillon, and J. G. Andrews, "Analytical modeling of uplink cellular networks," *IEEE Transactions on Wireless Communications*, vol. 12, no. 6, pp. 2669–2679, June 2013.

[52] H. ElSawy and E. Hossain, "On stochastic geometry modeling of cellular uplink transmission with truncated channel inversion power control," *IEEE Transactions on Wireless Communications*, vol. 13, no. 8, pp. 4454–4469, Aug 2014.

[53] L. H. Afify, H. ElSawy, T. Y. Al-Naffouri, and M. S. Alouini, "Error performance analysis in k-tier uplink cellular networks using a stochastic geometric approach," in *2015 IEEE International Conference on Communication Workshop (ICCW)*, June 2015, pp. 87–93.

[54] S. Singh, X. Zhang, and J. G. Andrews, "Joint rate and sinr coverage analysis for decoupled uplink-downlink biased cell associations in hetnets," *IEEE Transactions on Wireless Communications*, vol. 14, no. 10, pp. 5360–5373, Oct 2015.

[55] A. AlAmmouri, H. ElSawy, and M. S. Alouini, "Load-aware modeling for uplink cellular networks in a multi-channel environment," in *2014 IEEE 25th Annual International Symposium on Personal, Indoor, and Mobile Radio Communication (PIMRC)*, Sept 2014, pp. 1591–1596.

[56] H. Y. Lee, Y. J. Sang, and K. S. Kim, "On the uplink sir distributions in heterogeneous cellular networks," *IEEE Communications Letters*, vol. 18, no. 12, pp. 2145–2148, Dec 2014.

[57] Z. Zeinalpour-Yazdi and S. Jalali, "Outage analysis of uplink two-tier networks," *IEEE Transactions on Communications*, vol. 62, no. 9, pp. 3351–3362, Sept 2014.

[58] T. Kobayashi and N. Miyoshi, "Uplink cellular network models with ginibre deployed base stations," in *Teletraffic Congress (ITC), 2014 26th International*, Sept 2014, pp. 1–7.

[59] W. K. D. Stoyan and J. Mecke, *Stochastic Geometry and Its Applications*. 2nd edition. John Wiley and Sons, 1996.

[60] F. Baccelli and B. Blaszczyszyn, *Stochastic Geometry and Wireless Networks: Volume I Theory*. Foundations and Trends®in Networking, 2010, vol. 1.

[61] H. ElSawy, A. Sultan-Salem, M.-S. Alouini, and M. Z. Win, "Modeling and Analysis of Cellular Networks using Stochastic Geometry: A Tutorial," *ArXiv e-prints*, Apr. 2016.

[62] N. Himayat, S. Talwar, A. Rao, and R. Soni, "Interference management for 4g cellular standards [wimax/lte update]," *IEEE Communications Magazine*, vol. 48, no. 8, pp. 86–92, August 2010.

[63] T. Novlan, J. G. Andrews, I. Sohn, R. K. Ganti, and A. Ghosh, "Comparison of fractional frequency reuse approaches in the ofdma cellular downlink," in *Global Telecommunications Conference (GLOBECOM 2010), 2010 IEEE*, Dec 2010, pp. 1–5.

[64] K. Doppler, C. Wijting, and K. Valkealahti, "Interference aware scheduling for soft frequency reuse," in *Vehicular Technology Conference, 2009. VTC Spring 2009. IEEE 69th*, April 2009, pp. 1–5.

[65] M. Al-Shalash, F. Khafizov, and Z. Chao, "Interference constrained soft frequency reuse for uplink icic in lte networks," in *21st Annual IEEE International Symposium on Personal, Indoor and Mobile Radio Communications*, Sept 2010, pp. 1882–1887.

[66] F. Baccelli, B. Blaszczyszyn, and P. Muhlethaler, "Stochastic analysis of spatial and opportunistic aloha," *IEEE Journal on Selected Areas in Communications*, vol. 27, no. 7, pp. 1105–1119, September 2009.

[67] P. Xia, V. Chandrasekhar, and J. G. Andrews, "Open vs. closed access femtocells in the uplink," *IEEE Transactions on Wireless Communications*, vol. 9, no. 12, pp. 3798–3809, December 2010.

[68] V. Chandrasekhar, J. G. Andrews, and A. Gatherer, "Femtocell networks: a survey," *IEEE Communications Magazine*, vol. 46, no. 9, pp. 59–67, September 2008.

[69] G. Boudreau, J. Panicker, N. Guo, R. Chang, N. Wang, and S. Vrzic, "Interference coordination and cancellation for 4g networks," *IEEE Communications Magazine*, vol. 47, no. 4, pp. 74–81, April 2009.

[70] D. Ben Cheikh, J.-M. Kelif, M. Coupechoux, and P. Godlewski, "Sir distribution analysis in cellular networks considering the joint impact of path-loss, shadowing and fast fading," *EURASIP Journal on Wireless Communications and Networking*, vol. 2011, no. 1, pp. 1–10, 2011. [Online]. Available: http://dx.doi.org/10.1186/1687-1499-2011-137

[71] M. A. M.K. Simon, *Digital Communication Over Fading Channels*. 2nd edition. John Wiley and Sons, 2005.

[72] H. S. Dhillon, R. K. Ganti, and J. G. Andrews, "A tractable framework for coverage and outage in heterogeneous cellular networks," in *Information Theory and Applications Workshop (ITA), 2011*, Feb 2011, pp. 1–6.